THIRTY - FOURTH ANNUAL
GASEOUS ELECTRONICS CONFERENCE
October 20 - 23, 1981

AVCO EVERETT
RESEARCH LABORATORY, INC.

A Topical Conference of
The American Physical Society

Sponsored by:
Avco Everett Research Laboratory, Inc.
American Physical Society
Division of Electron
and Atomic Physics

P R O G R A M C H A N G E S

The paper:

BA-5 "Thermal Conductivity of O_2 in the Dissociation Regime"

Authors A.Kurtz and J. Mentel

will not be presented.

****

The paper:

LA-1 "Excitation of ArH* Luminescence by Electron Ion Recombination During the Afterflow"

Authors J. Shmulovich and S. Yatsiv

will not be presented.

****

The Chairperson for Session AA: ARCS I will be R.E. Voshall, Westinghouse R&D Center

mm

THIRTY - FOURTH ANNUAL
GASEOUS ELECTRONICS CONFERENCE
October 20 - 23, 1981

AVCO EVERETT
RESEARCH LABORATORY, INC.

A Topical Conference of
The American Physical Society

Sponsored by:
Avco Everett Research Laboratory, Inc.
American Physical Society
Division of Electron
and Atomic Physics

Address Correspondence to:

DR. M.J. BONESS
34th Gaseous Electronics Conference
Avco Everett Research Laboratory, Inc.
2385 Revere Beach Parkway
Everett, MA 02149
Telephone: 617-389-3000
TWX: 710 348 0470

To all registrants of the 34th G.E.C., Boston, Massachusetts

Enclosed you will find a list of the 289 registered participants at the 34th G.E.C. Additional copies of the book of abstracts are available from the above address at $8/copy. Please make checks payable to 34th G.E.C.

Next year the meeting will be hosted by the University of Texas at Dallas. The meeting dates will be Oct 19-22, 1982. Relevant addresses are:

Chairman	Secretary
Lawson P. Harris	Carl B. Collins
General Research Corp.	Mail Station NB1
R & D Division	Univ. of Texas at Dallas
P. O. Box 8	Box 688
Schenectady NY 12301	Richardson TX 75080
(518) 385-8106	(214) 690-2864

On behalf of the Conference Committee I would like to thank you for attending this meeting. We hope that you found it an enjoyable and stimulating experience.

Sincerely,

John Boness

JB:sh

John Boness
Secretary 34th G.E.C.

34th ANNUAL GASEOUS ELECTRONICS CONFERENCE
Boston Park Plaza Hotel
Boston, Massachusetts
20-23 October 1981

LIST OF PARTICIPANTS

ADLER-GOLDEN, Steven M.	Spectral Sciences, Inc., 99 S. Bedford St., Burlington MA 01803
ALLIS, William P.	Room 30-231, Massachusetts Institute of Technology, Cambridge MA 02139
AMME, Robert C.	Department of Physics, University of Denver, Denver CO 80208
ANDERSON, L. W.	Physics Department, University of Wisconsin, 1150 University Ave., Madison WI 53706
ANDERSON, Richard J.	Department of Physics, University of Arkansas, Fayetteville AR 72701
ASARO, Catherine A.	Harvard College Observatory, 60 Garden St., Cambridge MA 02138
AUSTAD, Helge	Canrad Hanovia, Inc., 100 Chestnut St., Newark NJ 07105
BAILEY, Thomas L.	Department of Physics, University of Florida, Gainesville FL 32601
BAILEY, William F.	A.F. Institute of Technology, 7012 Hubbard Dr., Dayton OH 45424
BARDSLEY, J. Norman	Physics Department, University of Pittsburgh, Pittsburgh PA 15260
BARRETO, Ernesto	Suny-Albany ES 324, 1400 Washington Ave., Albany NY 12222
BENEDICT, Lt. Col. R.	DARPA/DEO, 1400 Wilson Blvd., Arlington VA 22209
BENENSON, David M.	SUNYAB, 53 Andover Lane, Williamsville NY 14221
BERGMAN, Rolf S.	General Electric, Nela Park, Cleveland OH 44112
BERNECKI, Thomas F.	SUNYAB, 195 Halstead, Sloan NY 14212
BEZUK, Steve J.	University of Minnesota, Ctr. of Plasma Chem., 328 Space Sci. Ctr., Minneapolis MN 55108
BHASAVANICH, Don	Westinghouse R&D, 1310 Beulah Rd., Pittsburgh PA 15235
BHATTACHARYA, Ashok K.	General Electric Co., Lamp Business Group, Nela Park, Cleveland OH 44112
BIBLARZ, Oscar	Naval Postgraduate School, Code 67B; Aeronautics, Monterey CA 93940
BIENSTOCK, Sergio	Harvard-Smithsonian Ctr. for Astrophysics, 60 Garden St., Cambridge MA 02138
BIGIO, Irving	Los Alamos National Lab., MS-535, Los Alamos NM 87545
BIONDI, Manfred A.	Department of Physics & Astronomy, University of Pittsburgh, Pittsburgh PA 15260
BISCHEL, William K.	SRI International, 333 Ravenswood Avenue PS091, Menlo Park CA 94025
BLETZINGER, Peter	Plasma Physics Group, Wright-Patterson AFB, AFWAL/P00C-3, Wright-Patterson AFB OH 45433
BOHRINGER, Hans	NOAA Environmental Res. Lab., Aeronomy Laboratory, Boulder CO 80303
BONESS, John	Avco Everett Research Lab., Inc., 2385 Revere Beach Parkway, Everett MA 02149
BOODY, Fred	Princeton Plasma Physics Lab., P.O. Box 451, Princeton NJ 08544
BOXMAN, Raymond L.	College of Engineering, University of South Carolina, Columbia SC 29208
BRATES, Nanu	SUNYAB, 4232 Ridge Lea Rd., Amherst NY 14226
BROOKS, Howard L.	Physics & Astronomy Department, DePauw University, Greencastle IN 46135
BROWN, Robert T.	United Tech. Res. Ctr., Silver Lane, East Hartford CT 06108
BRUNET, Henry	Laboratories de Marcoussis, Division Lasers, 91 460-Marcoussis France
BUCKMAN, Stephen J.	Department of Physics, Schuster Lab., University of Manchester M139PL, Manchester U.K.
BUDINGER, A. Bowman	GTE Laboratories, 40 Sylvan Rd., Waltham MA 02254
BURKHARDT, Charles E.	University of Missouri-St. Louis, 4320 Walker, Normandy MO 63121

BURNHAM, Ralph	Naval Research Lab., Code 6540, Washington DC 20375
BYSZEWSKI, Wojciech W.	GTE Laboratories, Inc., 40 Sylvan Rd., Waltham MA 02254
CALEDONIA, George E.	Physical Sciences, Inc., 30 Commerce Way, Woburn MA 01801
CENTER, Bob	Mathematical Sciences NW, 2755 Northup Way, Bellevue WA 98004
CHAMPAGNE, Louis F.	Naval Research Lab., Washington DC 20375
CHANG, C. S.	Beers Associates, Inc., P.O. Box 2549, Reston VA 22090
CHANG, Robert S. F.	Naval Research Lab., Code 6540, Washington DC 20375
CHANIN, L. M.	Department of Electrical Engineering, University of Minnesota, Minneapolis MN 55455
CHANTRY, Peter J.	Westinghouse R&D Center, 1310 Beulah Rd., Pittsburgh PA 15235
CHEN, C. L.	Westinghouse R&D Center, 1310 Beulah Rd., Pittsburgh PA 15235
CHEN, Hao-Lin	Lawrence Livermore National Lab., Box 808, Livermore CA 94550
CHIEN, Yun-Ko	Westinghouse R&D Center, 1310 Beulah Rd., Pittsburgh PA 15235
CHILUKURI, Santaram	Department of Physics, Union College, Barbourville KY 40906
COLLINS, Carl B.	University of Texas at Dallas, P.O. Box 688, Richardson TX 75080
COPELAND, Drew A.	Rocketdyne, A Division of Rockwell International, 6633 Canoga Park Ave., Canoga CA 91362
COTT, Don	Mountain States Energy, Box 3767, Butte MT 59701
CUNNINGHAM, A. J.	University of Texas at Dallas, P.O. Box 688, Richardson TX 75080
DALGARNO, A.	Center for Astrophysics, 60 Garden St., Cambridge MA 02138
D'AUTEUIL, Raymond J.	Dynatrend Incorporated, 21 Cabot Rd., Woburn MA 01801
DAVIDOVITS, Paul	Department of Chemistry, Boston College, Chestnut Hill MA 02167
DAVIES, D. Ken	Westinghouse R&D Center, 1310 Beulah Rd., Pittsburgh PA 15235
DeJOSEPH, Charles A.	Plasma Physics Group, Wright-Patterson AFB, AFWAL/P00C-3, Wright-Patterson AFB OH 45433
DELCROIX, J. L.	Lab de Physique des Plasmas, Bat 212, Univ Paris Sud, Centre d'Orsay 91405, France
DELPECH, Jean F.	Univ Paris Sud, Bat 220, 91405 Orsay, France
DEMIRJIAN, Ara	Avco Everett Research Lab., Inc., 2385 Revere Beach Parkway, Everett MA 02149
DENES, Louis J.	Westinghouse R&D Center, 1310 Beulah Rd., Pittsburgh PA 15235
DeWITT, Robert N.	Naval Surface Weapons Center, Code F12, Dahlgren VA 22448
DeYOUNG, Russell	NASA Langley, 8 Luanita Lane, Newport News VA 23606
DICK, G. W.	Bell Laboratories, 2525 N 11th St., Reading PA 19604
DJEU, Nicholas	Naval Research Lab., Washington DC 20375
DOLLINGER, Richard E.	Dept. of Elec. Eng., State Univ. of New York at Buffalo, 4232 Ridge Lea Rd., Amherst NY 14226
DOUGLAS-HAMILTON, Diarmaid	Avco Everett Research Lab., Inc., 2385 Revere Beach Parkway, Everett MA 02149
DOWNES, Lawrence W.	Physics Department, Miami University, Oxford OH 45056
DROUET, Michel G.	Institut de Recherche, Hydro-Quebec, B.P. 1000, Varennes, Quebec J0L 2P0 Canada
DUKE, Gary L.	Plasma Physics Group, Wright-Patterson AFB, AFWAL/P00C-3, Wright-Patterson AFB OH 45433
DURRETT, Mike	Physics Department, Rice University, P.O. Box 1892, Houston TX 77001
DUZY, Carolyn	Avco Everett Research Lab., Inc., 2385 Revere Beach Parkway, Everett MA 02149
ECKSTROM, Donald J.	SRI International, 333 Ravenswood Ave., Menlo Park CA 94025
EDDY, Thomas L.	School of Mech. Eng., Georgia Tech., Atlanta GA 30332
EDIGER, Marwood	Gaseous Electronics Lab., University of Illinois, 607 E. Healey St., Champaign IL 61820

ENGEL, James W.	AFIT/EN WPAFB Ohio, 67 Emerald Ct., Satellite Beach FL 32937
ENGLISH, George	GTE Sylvania, Danvers MA 01923
ENINGER, Jan	Avco Everett Research Lab., Inc., 2385 Revere Beach Parkway, Everett MA 02149
ENRIGHT, Michael J.	GTE Laboratories, Dept. 306, 40 Sylvan Rd., Waltham MA 02254
EPLER, John	Gaseous Electronics Lab., University of Illinois, 607 E. Healey St., Champaign IL 61820
ERLANDSON, Alvin	Applied Physics Department, Cornell University, Ithaca NY 14853
ERNIE, Douglas W.	University of Minnesota, 123 Church St S.E., Minneapolis MN 55455
EWING, J. J.	Mathematical Sciences NW, 2755 Northup Way, Bellevue WA 98004
FAHEY, David W.	NOAA/ERL Aeronomy Lab., 325 S. Broadway, 1-3522, Boulder CO 80303
FANG, Ta-Ming	Boston University, 110 Cummington St., Boston MA 02165
FARRALL, George	General Electric Co., 1 River Rd., Schenedtady NY 12305
FERGUSON, Eldon	NOAA Research Lab, Rm 3522, Radio Bldg., Boulder CO 80302
FERNSLER, Richard	3804 Hillcrest Lane, Annandale VA 22003
FERREIRA, Carlos M.	Centro Electrodinamica, University of Lisbon, Av. Rovisco Pais, 1000 Lisbon Portugal
FEUERSANGER, Alfred E.	GTE Laboratories, 40 Sylvan St., Waltham MA 02154
FINN, Tom	W. J. Schafer Assoc., 6013 Clerken Well Ct., Burke VA 22015
FISHER, Charles	Mathematical Sciences NW, 2755 Northup Way, Bellevue WA 98004
FLAMM, Daniel L.	Bell Laboratories, Room 6E-216, Murray Hill NJ 07974
FLANNERY, M. Raymond	School of Physics, Georgia Tech., Atlanta GA 30332
FOHL, Timothy	GTE Products Corp., 681 South St., Carlisle MA 01741
FOLTZ, Greg	Oak Ridge National Laboratory, MS-202, Bldg-5500, P.O. Box X, Oak Ridge TN 37830
FOLTZ, Mary F.	196 N. Purdue #110, Oak Ridge TN 37830
FORESTIER, Bernard	I.M.F.M., 1 Rue Honnorat, Marseille 13003 France
FREUND, Robert S.	Bell Labs., Murray Hill NJ 07974
FULGHUM, Stephen F.	Avco Everett Research Lab., Inc., 2385 Revere Beach Parkway, Everett MA 02149
GALLAGHER, Alan	JILA, University of Colorado, Boulder CO 80309
GARSCADDEN, Alan	Plasma Physics Group, Wright-Patterson AFB, AFWAL/P00C-3, Wright-Patterson AFB OH 45433
GASTINEAU, John E.	Department of Physics, University of Wisconsin, 1150 University Ave., Madison WI 53703
GIBBS, George R.	GTE Laboratories, 40 Sylvan Rd., Waltham MA 02154
GILLIARD, Richard P.	General Electric Co., Lighting Res. & Tech. Serv. Operation, Nela Park #1310, Cleveland OH 44112
GOLDFARB, Victor	Avco Everett Research Lab., Inc., 2385 Revere Beach Parkway, Everett MA 02149
GREEN, B. D.	Physical Sciences Inc., 30 Commerce Way, Woburn MA 01801
GREENBERG, Kenneth	Gaseous Electronics Lab., University of Illinois, 607 E. Healey St., Champaign IL 61820
GRIPSHOVER, Ronald J.	Naval Surface Weapons Center, Code F12, Dahlgren VA 22448
GROSJEAN, Dennis F.	Systems Research Laboratories, Inc., 2800 Indian Ripple Rd., Dayton OH 45440-3696
GROSSE-WILDE, H.	Siemens AG, FL Plas, Werner-v. Siemens, 8520 Erlangen W. Germany
GUSTAFSON, John	GTE Laboratories, 40 Sylvan Rd., Waltham MA 02154
HAGLER, Marion	Department of Elec. Eng., Texas Tech. University, Lubbock TX 79409-4439
HAMMOND, John H.	W. J. Schafer Assoc., 3734 Prince William Dr., Fairfax VA 22031
HARRIS, L. P.	General Electric Corp. R&D, P.O. Box 8, Schenectady NY 12301

HATFIELD, Lynn L.	Physics Department, Texas Tech. University, P.O. Box 4180, Lubbock TX 79409
HAUCK, James P.	Rockwell International, 3370 Miraloma Ave., MS GE-57, Anaheim CA 92803
HAUGSJAA, Paul O.	GTE Laboratories, Inc., 40 Sylvan Rd., Waltham MA 02154
HECHTMAN, Chas.	Avco Systems Division, 201 Lowell St., Wilmington MA 01887
HELMY, E. M.	Physics Department, Delaware State College, Newark DE 19711
HENSON, Bob L.	Physics Department, University of Missouri-St. Louis, St. Louis MO 63121
HERMANN, Max	Avco Systems Division, 201 Lowell St., Wilmington MA 01887
HERZENBERG, Arvid	Applied Physics, Yale University, P.O. Box 2157 Yale Station, New Haven CT 06520
HINCHEN, John J.	United Technologies, Research Center, E. Hartford CT 06108
HIRSH, Merle N.	Plasma Resources, 28 Spier Ave., Rochester NY 14620
HOMSEY, Robert J.	G. E. Space Division, Goddard Building, King of Prussia PA
HONG, Siu-Ping	Bell Laboratories, 555 Union Blvd., Allentown PA 18103
HOUSTON, John	G.E. R&D Center, P.O. Box 8, Schenectady NY 12301
HUDSON, David F.	Naval Surface Weapons Center, Bldg-4 Rm-237, Silver Spring MD 20910
HUESTIS, David L.	SRI International, 333 Ravenswood Ave. PS091, Menlo Park CA 94025
HUTCHINSON, M. Henry R.	Blackett Laboratory, Imperial College, London SW7 U.K.
HUTCHINSON, Sheldon	Allied Corp., 3665 Benton St., #135, Santa Clara CA 95051
HYMAN, Howard A.	Avco Everett Research Lab., Inc., 2385 Revere Beach Parkway, Everett MA 02149
ICHIKAWA, Y.	York University, 10 San Romanoway, #109, Downsview, Ontario Canada
INGOLD, John H.	General Electric Co., Lamp Business Group, Cleveland OH 44112
ISLAM, M. Azadul	JILA, University of Colorado, Campus Box 440, Boulder CO 80309
JACOB, Jonah	Avco Everett Research Lab., Inc., 2385 Revere Beach Parkway, Everett MA 02149
JAECKS, Duane H.	Physics Department, University of Nebraska, Lincoln NB 68588
JANCAITIS, Kenneth S.	Lawrence Livermore National Laboratory, P.O. Box 5508, L-470, Livermore CA 94550
JOG, Vidya E.	Department of Physics, University of Pittsburgh, 100 Allen Hall, Pittsburgh PA 15260
JOHNSEN, Rainer	Department of Physics & Astronomy, University of Pittsburgh, Pittsburgh PA 15260
JOHNSON, Peter D.	G.E. R&D Center, Bldg-K-1 Rm-5831, Schenectady NY 12301
JOHNSON, Steve	GTE Lighting Products, 8 Marlboro Rd., Georgetown MA 01833
JOHNSON, Wayne L.	Advanced Crystal Sciences, San Jose CA 95125
JURENKA, Henry	ASRC SUNY at Albany, 1400 Washington Ave., Albany NY 12222
KAUFMAN, Yitzhak	The Hebrew University of Jerusalem, Racah Institute of Physics, Jerusalem Israel
KEEFE, William M.	GTE Sylvania, 100 Endicott St., Danvers MA 01923
KELLER, John H.	IBM, Department 52G, Bldg-300-49A, Hopewell Jct. NY 12533
KESSLER, Robert	Avco Everett Research Lab., Inc., 2385 Revere Beach Parkway, Everett MA 02149
KLIMEK, Dan	Avco Everett Research Lab., Inc., 2385 Revere Beach Parkway, Everett MA 02149
KLINE, Larry E.	Westinghouse R&D Center, 1310 Beulah Rd., Pittsburgh PA 15235
KRAUSS, Morris	National Bureau of Standards, Molecular Spectroscopy Div., Rm-B268 Bldg-221, Washington DC 20234
KREBS, Danny J.	Physics Department, University of Missouri-Rolla, Rolla MO 65401

KOLB, Charles E.	Aerodyne Research, Inc., Crosby Drive, Bedford MA 01730
KUNG, Robert T. V.	W. J. Schafer Associates, 10 Lakeside Office Pk., Wakefield MA 01810
KUNHARDT, Erich E.	Texas Tech. University, Lubbock TX 79409
KUSHAWAHA, V. S.	Department of Physics, University of Missouri, St. Louis MO 63121
LAGUSHENKO, Radomir	1817 Beacon Street, Brookline MA 02146
LAPATOVICH, Walter P.	GTE Laboratories, 40 Sylvan Rd., Waltham MA 02154
LAU, Y. C.	SUNY/AB, 4232 Ridge Lea, Amherst NY 14226
LAUDENSLAGER, Jim	JPL, 570 Las Rocas, Sierra Madre CA 91024
LEE, F. W.	University of Texas at Dallas, NB11, P.O. Box 688, Richardson TX 75080
Lee, Long C.	SRI International, 333 Ravenswood Ave. PS091, Menlo Park CA 94025
LEVATTER, Jeffrey I.	Helionetics, Inc., Laser Division, 3878 Ruffin Rd., Suite A, San Diego CA 92123
LEVENTHAL, Jacob J.	Department of Physics, University of Missouri, St. Louis, St. Louis MO 63121
LIN, Chun C.	Department of Physics, University of Wisconsin, Madison WI 53706
LISHAWA, C. Randal	Southern Research Institute, P.O. Box 3307-A, Birmingham AL 35255
LITTLEWOOD, I. M.	Department of Physics, University of Missouri-Rolla, Rolla MO 65401
LONG, William H., Jr.	Northrop Research & Technology Center, One Research Park, Palos Verdes Penninsula CA 90274
LORENTS, Donald C.	SRI International, 333 Ravenswood Ave. PS091, Menlo Park CA 94025
LU, Wen-lian	SUNYAB, 1 LeBrun Rd., Buffalo NY 14215
LUESSEN, Lawrence H.	Naval Surface Weapons Center, Code F12, Dahlgren VA 22448
LYNCH, Denis A., Jr.	General Electric Co., 8499 Darrow Road, Twinburg OH 44087
MACDONALD, Jeff	Physics Department, University of Pittsburgh, Pittsburgh PA 15235
MANDL, Alexander	Avco Everett Research Lab., Inc., 2385 Revere Beach Parkway, Everett MA 02149
MAROWSKY, G.	Max-Planck-Institute, Am Fassberg, D-3400 Gottingen, W. Germany
MARTINEZ-SANCHEZ, Manuel	Massachusetts Institute of Technology, Rm-37-371, Cambridge, MA 02138
MAUK, Peter	Physics Department, University of Delaware, Newark DE 19711
MAYA, Jakob	GTE Products Corp., 100 Endicott St., Danvers MA 01923
MCCLURE, Gordon W.	Sandia National Laboratories, 2324 Cutler Ave. N.E., Albuquerque NM 87106
MCGARVEY, John A.	Boeing Aerospace, P.O. Box 3999 M/S 8H-29, Seattle WA 98007
MCGEOCH, Malcolm W.	Avco Everett Research Lab., Inc., 2385 Revere Beach Parkway, Everett MA 02149
MICHELS, H. Harvey	Physics Department, United Technologies Research Center, E. Hartford CT 06108
MIDORIKAWA, Katsumi	Department of Elec. Eng., Keio University, 3-14-1 Hiyoshi, Kohoku-Ku, Yokohama 223, Japan
MILLER, John L.	Lawrence Livermore National Lab., MS L-467, P.O. Box 5508, Livermore CA 94550
MOISAN, Michel	Department de Physique, Universite de Montreal, BP 6128, Montreal H3C 3J7 Quebec
MORGAN, Wm. Lowell	Lawrence Livermore National Laboratory, Box 808 L-18, Livermore CA 94550
MUSCHLITZ, E. E., Jr.	Department of Chemistry, University of Florida, Gainesville FL 32611
NADEAU, Francois	National Research Council of Canada, 15 Briar Dale Ct., Derwood MD 20855
NEWITT, John H.	Image Technology, 103 Moody St., Waltham MA 02154
NIGHAN, William L.	United Technologies Research Center, MS 90, Silver Lane, E. Hartford CT 06108
NILSON, John A.	Lumonics Inc., lor Schneider Rd., Kanata, Ontario K2K 1Y3 Canada
NORCROSS, David W.	JILA, University of Colorado, Boulder CO 80309

NOVAK, Jaroslav	Institut de recherche d'Hydro-Quebec, 1800 Montee Ste-Julie, Varennes, Quebec J0L 2P0 Canada
OSKAM, H. J.	Department of Elec. Eng., University of Minnesota, 123 Church St. S.E., Minneapolis MN 55455
PAI, Robert	GTE, 40 Carriage Way, Danvers MA 01923
PALUMBO, Louis J.	Naval Research Lab., Code 6540, Washington DC 20375
PARTLOW, W. D.	Westinghouse R&D Center, 1310 Beulah Rd., Pittsburgh PA 15235
PAULSON, John F.	AFGL-LKB, Hanscom AFB MA 01731
PETROVIC, Dragan	Physics Department, Miami University, Oxford OH 45056
PFENDER, Emil	Departmentof Mech. Eng., University of Minnesota, 125 Mechanical Eng., Minneapolis MN 55455
PHELPS, A. V.	JILA/NBS, University of Colorado, Campus Box 440, Boulder CO 80309
PINSKER, Robert I.	Westinghouse R&D/M.I.T., 450 Memorial Dr., Rm-H217, Cambridge MA 02139
PIPER, Lawrance G.	Physical Sciences Inc., 30 Commerce Way, Woburn MA 01801
PITCHFORD, Leanne	Sandia National Labs., Division 4211, Albuquerque NM 87185
PLUMMER, Michael J.	Northrup Research & Technology Center, One Research Pk., Palos Verdes Penninsula CA 90274
POWELL, Howard T.	Lawrence Livermore National Laboratory, P.O. Box 5508, L-470, Livermore CA 94550
PROUD, Joseph M., Jr.	GTE Laboratories, 40 Sylvan Rd., Waltham MA 02254
REES, J. A.	Department of Electric Eng. & Electronics, University of Liverpool, Liverpool LG9 3BX U.K.
REISER, Paul A.	GTE Sylvania, 100 Endicott St., Danvers MA 01923
RICARD, A.	Plasma Phys. Lab., Paris-Sud Universite, 91-405 Orsay France
RISEBERG, L. A.	GTE Laboratories, Inc., 40 Sylvan Rd., Waltham MA 02254
ROBERTS, Victor	General Electric R&D Center, Bldg K1-4638, P.O. Box 8, Schenectady NY 12301
ROCCA, Jorge	Laser Lab-Eng. Res. Ctr., Colorado State University, Fort Collins CO 80523
ROGOFF, G. L.	Westinghouse R&D Center, 1310 Beulah Rd., Pittsburgh PA 15235
ROSSING, Barry	Westinghouse R&D Center, 1310 Beulah Rd., Pittsburgh PA 15235
ROTHWELL, Harold L.	GTE Sylvania, 100 Endicott St., Danvers MA 01923
SADOVNIK, Isaac	Avco Everett Research Lab., Inc., 2385 Revere Beach Parkway, Everett MA 02149
SAMUEL, Goldsmith	Department of Physics & Astromomy, Tel-Aviv University, Tel-Aviv Israel
SCHAEFER, Gerhard	Department of Elec. Eng., Texas Tech. University, Box 4439, Lubbock TX 79409
SCHEARER, L. D.	Physics Department, University of Missouri-Rolla, Rolla MO 65401
SCHIMITSCHEK, E.	Naval Ocean Systems Center, Code 811, San Diego CA 92152
SCHMIDT, Harold J.	University of Tennessee Space Institute, Tullahoma TN 37388
SCHOENBACH, Karl H.	Department of Elec. Eng., Texas Tech. University, Lubbock TX 79409
SCHULZ, Rose A.	Yale University, 37 Old Mill Rd., Woodbridge CT 06525
SCHWOERER, John	Massachusetts Institute of Technology, Rm 3-359, Cambridge, MA 02146
SHARPTON, Francis A.	Northwest Nazarene College, Nampa ID 83651
SHAW, David G.	General Electric, Capacitor Products Dept., John St., Hudson Falls NY 12839
SHELDON, John W.	Department of Physical Sciences, Florida International University, Miami FL 33199
SIERRA, R.	Los Alamos National Lab., MS 564, Los Alamos NM 87545
SIGMOND, R. Svein	Physics Department, Norwegian Inst. of Technology, Fysikkseksjonen, N-7034 Trondheim-NTH
SKAL, Michael	Canrad Hanovia, Inc., 100 Chestnut St., Newark NJ 07105

SLATER, Richard	Avco Everett Research Lab., Inc., 2385 Revere Beach Parkway, Everett MA 02149
SMILANSKI, Israel	Mathematical Sciences NW, 2755 Northup Way, Bellevue WA 98004
SPRINGER, Robert H.	General Electric Co., Lamp Business Group, Cleveland OH 44112
ST. JOHN, Robert M.	Department of Physics, University of Oklahoma, 440 W. Brooks, Norman OK 73019
STANTON, Alan C.	Aerodyne Research Inc., Bedford Research Park, Crosby Dr., Bedford MA 01730
STEVEFELT, J.	C.R.P.H.T.-C.N.R.S., 1, rue de Ecureuils, 45590 St. Cyr en Val France
STEWART, Charles N.	General Electric Co., Nela Park, Cleveland OH 44112
STICKLER, David B.	Avco Everett Research Lab., Inc., 2385 Revere Beach Parkway, Everett MA 02149
STOCKDALE, John A.	Oak Ridge National Lab., 11323 Berry Hill Dr., Knoxville TN 37921
STOCKTON, Marilyn	Sandia National Labs., Division 4252, P.O. Box 5800, Albuquerque NM 87185
STONE, David H.	Air Force Weapons Lab., 3230B A St., Kirtland AFB NM
STORMBERG, Peter	Philips Research Lab., Weisshaus Str., 5100 Aachen, W. Germany
SUHRE, Dennis	Westinghouse R&D Center, 1310 Beulah Rd. Pittsburgh PA 15235
SZABO, Andreas	Max-Planck-Inst. fur Aeronomie, Postfach 20, D-3411 Katlenburg-Lindau 3, W. Germany
TANG, Kenneth Y.	SRI International, 333 Ravenswood Ave. PS091, Menlo Park CA 94025
TANNEN, Peter D.	W. H. Schafer Associates, 8920 Matthew N.E., Albuquerque NM 87112
TASCH, Andrew	Union Carbide Corp., 1546 Cohassett Ave., Lakewood OH 44107
TAYLOR, Raymond L.	Research and Laser Technology, Inc., 30 Commerce Way, Woburn MA 01801
TAYLOR, Rod S.	National Research Council of Canada, Bldg M23-A, Montreal Rd., Ottawa, Ont., Canada
TEKULA, Milan	Avco Everett Research Lab., Inc., 2385 Revere Beach Parkway, Everett MA 02149
THOMASON, Michael	Los Alamos National Lab., MS 548, Los Alamos NM 87545
TOUZEAU, M.	Laboratoire de Physique des Plasmas, Universite Paris-Sud, 91405 Orsay, Cedex France
TOWNSEND, Paul	Physics Department, University of Delaware, Newark, DE 19711
TRAINOR, Daniel W.	Avco Everett Research Lab., Inc., 2385 Revere Beach Parkway, Everett MA 02149
TRENCHARD, H. A.	Westinghouse, 6909-40th Ave., Hyattesville MD 20782
TUMA, David T.	Electrical Engineering, Carnegie-Mellon University, Pittsburgh PA 15213
TURNER, Charles E.	Rockwell/Rocketdyne, 6633 Canoga Ave., Canoga Park CA 91304
TWIST, James R.	Universal Energy Systems, Inc., WPAFB, 3195 Plainfield Rd., Dayton OH 45432
UNKEL, William	Massachusetts Institute of Technology, Rm 3-342, 77 Mass. Ave., Cambridge MA 02139
VAN BRUNT, Richard J.	National Bureau of Standards, Bldg 220 Rm B344, Washington DC 20234
VAN DE WEYER, P.	Philips Research Labs., 5600 MD Eindhoven, The Netherlands
VERDEYEN, J. T.	Gaseous Electronics Lab., University of Illinois, 607 E. Healey St., Champaign IL 61820
VICTOR, G. A.	Harvard-Smithsonian Center for Astrophysics, 60 Garden St., Cambridge MA 02138
VON ROSENBERG, C. W., Jr.	Avco Everett Research Lab., Inc., 2385 Revere Beach Parkway, Everett MA 02149
VOSHALL, Roy E.	Westinghouse R&D Center, 1310 Beulah Rd., Pittsburgh PA 15235
VREHEN, Q. H. F.	Philips Research Labs, 5600 MD Eindhoven, The Netherlands
WANG, Eddy	Physics Department, University of Delaware, Newark DE 19711
WATSON, Alan	Elect. Eng. Dept., University of Windsor, Windsor, Ontario Canada

WAYMOUTH, John F.	GTE Sylvania Lighting Products, 100 Endicott St., Danvers MA 01923
WEEKS, Robert W.	Lumonics, Inc., 105 Schneider Rd., Kanata, Ontario K2K 1Y3 Canada
WELLS, William E.	Department of Physics, Miami University, 10 Culler Hall, Oxford OH 45056
WEXLER, Bernard	Naval Research Laboratory, Washington DC 20375
WHITE, Philip J.	GTE Sylvania, 100 Endicott St., Danvers MA 01923
WHITNEY, Kenneth	Naval Research Laboratory, Optical Sciences Div., Code 6509, Washington DC 20375
WHITTEN, Barbara	Lawrence Livermore National Lab., L-355, Box 808, Livermore CA 94550
WILLIAMS, Fraser	Department of Elect. Eng., Texas Tech. University, Lubbock TX 79407
WITTING, Harald L.	General Electric Co., Corp. Res. Division, K-1, EP32 Box 8, Schenectady NY 12301
WOO, S. B.	Physics Department, University of Delaware, Newark DE 19711
WORMHOUDT, Jody	Aerodyne Research, Inc., Bedford Research Park, Crosby Drive, Bedford MA 01730
WU, Richard L. C.	Brehm Lab., Wright State University, Dayton OH 45435
WYNER, Elliot	GTE Sylvania, 100 Endicott St., Danvers MA 01923
YOKOZAWA, Mihori	K-7-1 Micono, Sagamihana 228 Japan
YOS, Jerrold M.	Avco Systems Division, 201 Lowell St., Wilmington MA 01887
ZEDIKER, Mark	University of Illinois, 103 S. Goodwin, 102 Nuclear Eng. Lab, Urbana Il 61801
ZIPF, Edward C.	University of Pittsburgh, Pittsburgh PA 15238
ZNOTINS, Tom	Mathematical Sciences NW, 2755 Northup Way, Bellevue WA 98004
ZOLLWEG, Robert J.	Westinghouse R&D Center, 1310 Beulah Rd., Pittsburgh PA 15235

34th annual GASEOUS ELECTRONICS CONFERENCE

OCTOBER 20-23, 1981

BOSTON
MASSACHUSETTS

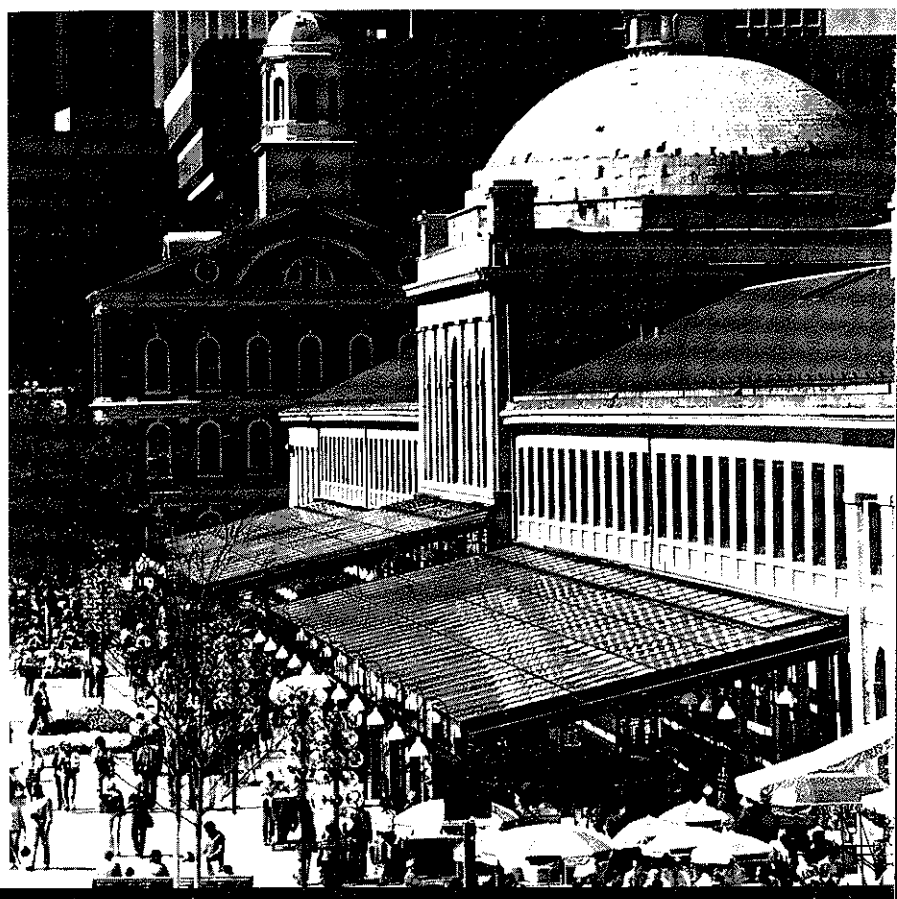

AVCO EVERETT RESEARCH LABORATORY, INC.

THIRTY-FOURTH ANNUAL
GASEOUS ELECTRONICS CONFERENCE

October 20-23, 1981

PROGRAM AND ABSTRACTS

SPONSORED BY:

Avco Everett Research Laboratory, Inc.

American Physical Society
Division of Electron and Atomic Physics

ASSISTED BY:

The Office of Naval Research and the National Science Foundation

A TOPICAL CONFERENCE OF THE AMERICAN PHYSICAL SOCIETY

ACKNOWLEDGMENT

THE EXECUTIVE COMMITTEE ACKNOWLEDGES FINANCIAL ASSISTANCE FROM THE OFFICE OF NAVAL RESEARCH AND THE NATIONAL SCIENCE FOUNDATION, AND THE GENEROUS SUPPORT OF THE FOLLOWING PATRONS:

AERODYNE RESEARCH, INC.

G.T.E. LABORATORIES, INC.

G.T.E. LIGHTING PRODUCTIONS BUSINESS

M.K.S. INSTRUMENTS, INC.

PHYSICAL SCIENCES, INC.

WE ARE INDEBTED TO THE LOCAL COMMITTEE FOR ITS WORK IN PLANNING AND ORGANIZING THIS MEETING. WE ALSO WISH TO THANK AVCO EVERETT RESEARCH LABORATORY, INC. (AERL) FOR HOSTING THIS CONFERENCE AND FOR THE MANY CONTRIBUTIONS PROVIDED BY INDIVIDUALS FROM SEVERAL DEPARTMENTS WITHIN THE LABORATORY FOR THEIR EFFORTS ON BEHALF OF THIS CONFERENCE.

CONTENTS

COVER

A portion of the Veil Nebula, an expanding, radiating gas cloud in the constellation cygnus, provides a backdrop to the Faneuil Hall Marketplace, the symbol of Boston's modern day resurgence.

DESIGNED BY JOSEPH SPATOLA, AVCO EVERETT RESEARCH LABORATORY, INC.

34th ANNUAL GASEOUS ELECTRONICS CONFERENCE PROGRAM

REGISTRATION AND MIXER (CASH BAR)
STANBRO HALL

OCTOBER 19, 1981

MONDAY EVENING 7:30 – 10:00 P.M.

BOSTON PARK PLAZA HOTEL
BOSTON, MASSACHUSETTS

AA: ARCS I 8:45 a.m.
Chairperson: R. J. Zollweg, Westinghouse R&D Center Room A

AA-I LONGITUDINAL ACOUSTIC RESONANCES IN HIGH PRESSURE MERCURY LAMPS
R. Schafer (7 min)

AA-2 TIME DEPENDENT BEHAVIOR OF HIGH PRESSURE MERCURY DISCHARGES
H. P. Stormberg (7 min)

AA-3 TIME RESOLVED SPECTROSCOPIC DIAGNOSTICS OF AC OPERATED HID ARCS
W. D. Partlow (7 min)

AA-4 COLLISIONAL BROADENING OF METAL ADDITIVE RESONANCE RADIATION IN HIGH PRESSURE METAL HALIDE ARCS
Harold L. Rothwell and William M. Keeffe (7 min)

AA-5 CHEMICAL REACTION STUDIES BY PLASMA DIAGNOSTICS AND MODELING OF A SCANDIUM IODIDE ARC
W. D. Partlow, R. W. Liebermann
R. J. Zollweg and L. N. Yannopoulos (7 min)

AA-6 EFFECTS OF LOW ENERGY ELECTRON IMPACT ON THE RADIATION CONVERSION EFFICIENCY OF HIGH POWER CESIUM NEON ARC LAMPS
C. S. Chang, and K. G. Whitney (7 min)

AA-7 INVESTIGATION AND MODEL CALCULATION OF THE INITIAL ARC IN A HIGH–PRESSURE MERCURY–VAPOUR LAMP
H. Grosse-Wilde (7 min)

AA-8 SATURATION OF THE ACOUSTIC WAVES PRODUCED BY PULSED ARCS
F. Nadeau and M. G. Drouet (7 min)

AA-9 HOT CATHODES IN HIGH PRESSURE DISCHARGE LAMPS
John F. Waymouth (7 min)

AB: GLOW DISCHARGES I 9:00 a.m.
Chairperson: A. J. Cunningham, University of Texas Room B

AB-1 DISCHARGE CHARACTERISTICS OF EXTERNALLY IONIZED METHANE
P. Bletzinger (7 min)

AB-2 DISCHARGE CHARACTERISTICS, OPTICAL EMISSION AND CONCENTRATION OF SPECIES IN Cl_2 PLASMA: THEIR SIGNIFICANCE FOR PLASMA ETCHING
D. L. Flamm and V. M. Donnelly (20 min)

AB-3 PROPERTIES OF THE POSITIVE COLUMN OF A GLOW DISCHARGE IN FLOWING HYDROGEN
H. Brunet, J. Rocca Serra and M. Mabru (20 min)

AB-4 EFFECTS OF EXCITATION MECHANISM ON LINEWIDTH PARAMETERS OF CONVENTIONAL VUV DISCHARGE LINE SOURCES
L. G. Piper and W. T. Rawlins (7 min)

AB-5 METASTABLE Ne ($^3P_{0,2}$) PRODUCTION IN A NEON GAS DISCHARGE
J. W. Sheldon and K. A. Hardy (7 min)

COFFEE BREAK 10:15 - 10:45 A.M.

BA: ARCS II 10:45 a.m.
Chairperson: E. Pfender, Univ. Minnesota Room A

BA-1 DISCHARGE SPECTROSCOPY BY THE OPTOGALVANIC EFFECT
R. Shuker, A. Ben-Amar and G. Erez (20 min)

BA-2 ARC–GAS FLOW INTERACTIONS USING DIFFERENTIAL INTERFEROMETRY
N. Brates, M.H. Sanwarwalla S. M. Mahajan and D. M. Benenson (7 min)

BA-3 ARC TEMPERATURES IN HIGH SPEED FLOW
T. F. Bernecki, Y. C. Lau and D. M. Benenson (7 min)

BA-4 HYDRODYNAMIC TRANSIENT IN A TIP–PLANE ARC CONFIGURATION
J. Converti and W. Unkel (7 min)

BA-5 THERMAL CONDUCTIVITY OF O_2 IN THE DISSOCIATION REGIME
A. Kurtz and J. Mentel (7 min)

BA-6 APPROXIMATE NON–LTE STATE DIAGRAMS FOR ATOMIC PLASMAS
T. L. Eddy (7 min)

BA-7 THERMAL CONSIDERATIONS FOR AN ELECTRIC ARC
T. –M. Fang (7 min)

BB: GLOW DISCHARGES II 10:45 a.m.
Chairperson: R. Anderson, Univ. Arkansas Room B

BB-1 POPULATION OF N_2 ($A^3\Sigma^+_u$, v) AND N (^4S_o) IN NITROGEN DC GLOW DISCHARGES
G. Cernogora, C.M. Ferreira, L. Hochard, and M. Touzeau (7 min)

BB-2 ELECTRON DISTRIBUTION FUNCTION AND CHARACTERISTICS OF ARGON GLOW DISCHARGES IN $10^{-2} < P < 1$ TORR
C.M. Ferreira (7 min)

BB-3 MASS SPECTRA FROM SILANE DISCHARGES
H. Chatham, R. Robertson, and A. Gallagher (7 min)

BB-4 EFFECT OF HYDROGEN ON DEIONIZATION PROCESSES IN Ne–A MIXTURES
A.K. Bhattacharya (7 min)

BB-5 EFFECTS OF WATER VAPOUR CONCENTRATION ON PLASMA PARAMETERS OF RARE GAS POSITIVE COLUMN PLASMAS
Y. Ichikawa, R.M. Hobson, T. Kaneda, and Jen-Shin Chang (7 min)

BB-6 GLOW DISCHARGES IN HELIUM-NEON LASER MIXTURES
J.A. Rees, V.K. Lakdawalla, S. Hunter, and J.L. Moruzzi (7 min)

LUNCH 12:15 – 1:30

CA: ELECTRON COLLISIONS

Chairperson: P. Davidovits, Boston College

1:30 a.m.
Room A

CA-1 USE OF LASER–INDUCED FLUORESCENCE TO STUDY ELECTRON EXCITATION AND COLLISIONAL EXCITATION TRANSFER OF ATOMS
M. H. Phillips, J. E. Gastineau, R. E. Miers, L. W. Anderson and C. C. Lin (20 min)

CA-2 EMISSION OF FREE–FREE RADIATION FROM ELECTRONS IN ARGON
C. Yamabe, and A. V. Phelps (7 min)

CA-3 ELECTRON IMPACT EXCITATION OF H_2, D_2 AND HD RESULTING IN VACUUM ULTRAVIOLET EMISSION
P. W. Erdman and E. C. Zipf (7 min)

CA-4 EXCITATION OF THE CO ($a^3\pi \rightarrow X^1\Sigma^+$) CAMERON BANDS BY ELECTRON IMPACT ON CO AND CO_2
P. W. Erdman and E. C. Zipf (7 min)

CA-5 ELECTRON EXCITATION OF THE XENON AND KRYPTON ATOMS
Francis A. Sharpton, John E. Gastineau, L. W. Anderson and Chun C. Lin (7 min)

CA-6 IONIZATION AND DISSOCIATIVE EXCITATION OF N_2 BY ELECTRON IMPACT ON THE METASTABLE N_2 ($A^3\Sigma_u^+$) STATE
M. R. Gorman and E. C. Zipf (7 min)

CA-7 KINETICS OF NH CREATED VIBRATIONALLY EXCITED IN ELECTRON–IRRADIATED N_2/H_2 MIXTURES
B. D. Green and G. E. Caledonia (7 min)

CB: XENON HALIDE LASERS

Chairperson: S.F. Fulghum, Avco Everett Research Lab., Inc.

1:30 p.m.
Room B

CB-1 INFLUENCE OF THE PULSE–FORMING–NETWORK UPON XeCL LASER DISCHARGE KINETICS
D. F. Grosjean (7 min)

CB-2 VIBRATIONAL EXCITATION OF HCl IN Ar/HCl, Ar/Xe/HCl AND Ne/Xe/HCl MIXTURES UNDER ELECTRON BEAM IRRADIATION
R. E. Center, J. H. Jacob, M. Rokni, and Z. Rozenberg (7 min)

CB-3 ION CHEMISTRY IN XeCL LASER MIXTURES
J. B. Laudenslager and V. G. Anicich (7 min)

CB-4 XeCL* – AND Xe_2CL^* –LASER KINETICS
G. Marowsky, F. K. Tittel, W. L. Wilson and G. P. Glass (7 min)

CB-5 TRANSIENT ABSORPTION OF PICOSECOND PULSES IN A 5J UV–PREIONIZED XeCL LASER
R. S. Taylor, P. B. Corkum and A. J. Alcock (7 min)

CB-6 SELF–SUSTAINED XeF LASER DISCHARGE CHARACTERISTICS
L. J. Denes and L.E. Kline (7 min)

CB-7 KINETICS OF DISCHARGE PUMPED XeF* LASERS
L. E. Kline and L. J. Denes (7 min)

CB-8 MULTILINE MODEL FOR XeF LASER PARAMETERS
D. A. Copeland, J. A. Blauer and C. E. Turner, Jr. (7 min)

CB-9 NF_2 RADICALS AS HALIDE DONORS FOR XeF LASING EXPERIMENTS
D.W. Trainor and J.H. Jacob (7 min)

COFFEE BREAK 3:00 – 3:30 P.M.

COFFEE BREAK 3:00 – 3:30 P.M.

OCTOBER 20, 1981 **TUESDAY AFTERNOON**

D: MERCURY BROMIDE LASERS
Chairperson: E.J. Schimitschek, Naval Ocean Systems Center

3:30 p.m.
Room B

D-1	KINETICS OF THE SUSTAINED DISCHARGE HgBr LASER M. McGeoch, J. Hsia, and D. Klimek	(20 min)
D-2	A 1.8 JOULE, X-RAY PREIONIZED HgBr LASER C.H. Fisher, I. Smilanski, T. DeHart, J.P. McDaniel and J.J. Ewing	(7 min)
D-3	A KINETIC MODEL FOR ELECTRIC DISCHARGE HgBr LASERS A.L. Pindroh, J.J. Ewing and C.H. Fisher	(7 min)
D-4	ELECTRON COLLISION PROCESSES IN $HgBr_2$ J.J. Hinchen, W.J. Wiegand and W.L. Nighan	(7 min)
D-5	ELECTRON ATTACHMENT AND FLUORESCENCE OF $HgBr_2$ – RARE GAS MIXTURES H.L. Brooks, K.J. Nygaard, L. Frost, J. Fletcher and E. Weigold	(7 min)
D-6	BOUND–BOUND AND BOUND–FREE FLUORESCENCE FROM HgBr ($B^2\Sigma^+$): THE ($B^2\Sigma^+ - X^2\Sigma^+$) AND ($B^2\Sigma^+ - A^2\pi$) TRANSITIONS W.P. Lapatovich, G.R. Gibbs, and J.M. Proud	(7 min)
D-7	PHOTODISSOCIATION OF HgBr, $X\Sigma_{1/2}$ M. Krauss and W.J. Stevens	(7 min)

DINNER 5:00 - 8:00 P.M.

E: WORKSHOP ON KINETIC PROCESSES IN BLUE–GREEN LASERS
Chairperson: W.L. Nighan, United Technologies Res. Center

8:00 p.m.
Room B

This workshop will focus on fundamental kinetic processes occuring in the 502 nm HgBr(B)/$HgBr_2$ dissociation laser, and in the 308 nm XeCl laser, the latter a prime candidate for wavelength conversion to the visible region of the spectrum. Attention in the formal portion of the workshop will be directed toward recent advances in understanding electron dissociative attachment to vibrationally excited HCl (the Cl donor in XeCl lasers), and electron impact dissociative excitation of $HgBr_2$. Ample time has been provided for general discussion of these topics as well as other subjects relevant to these lasers.

1. VIBRATIONAL EXCITATION AND DISSOCIATIVE ATTACHMENT OF HCl BY ELECTRON IMPACT – A. Herzenberg
2. DISSOCIATIVE EXCITATION OF $HgBr_2$ BY ELECTRONS – M. McGeoch
3. GENERAL DISCUSSION

FA: ARCS III 9:00 a.m.
Chairperson: D.K. Davies, Westinghouse R&D Center Room A

FA-1 EFFECT OF ELECTRODE TEMPERATURE ON DC BREAKDOWN IN VACUUM
D.B. Lowe, D.T. Tuma, and D.K. Davies (7 min)

FA-2 DEPENDENCY OF DIELECTRIC RECOVERY FIELD OF VACUUM GAPS ON di/dt AND RECOVERY VOLTAGE FREQUENCY
R.E. Voshall, and D. Bhasavanich (7 min)

FA-3 DENSITY POPULATION OF Zn I, Zn II EXCITED STATES IN MULTI-CATHODE-SPOT VACUUM ARCS
S. Goldsmith, Y. Bresler and R. L. Boxman (7 min)

FA-4 RETROGRADE MOTION OF ARC SPOTS ON COPPER CATHODES IN VACUUM
L.P. Harris (7 min)

FA-5 SURFACE MELTING OF VACUUM ARC CATHODES IN AREAS REMOTE FROM CATHODE SPOTS
P. Talarico, R. Dollinger, D. Dettman, A.S. Gilmour, Jr. and M. Nikolich (7 min)

FA-6 ELECTRICAL DISCHARGES ALONG THIN RIBBONS OF TITANIUM DEUTERIDE
G.W. McClure and J.A. Webb (7 min)

FA-7 INVESTIGATION OF CONSTRICTED METAL VAPOR ARC COLUMNS AT HIGH CURRENTS
D. Bhasavanich and Y.K. Chien (7 min)

FA-8 THE ANODE REGION IN A UNIFORM MULTI-CATHODE-SPOT VACUUM ARC
R.L. Boxman and S. Goldsmith (7 min)

FB: VISIBLE AND UV LASERS 8:45 a.m.
Chairperson: L.J. Denes, Westinghouse R&D Center Room B

FB-1 DISCHARGE EFFECTS ON A XeCl PUMPED S_2 HEAT PIPE LASER
K.E. Greenberg, K. Killeen, and J.T. Verdeyen (7 min)

FB-2 KINETICS AND LINE TUNABILITY OF THE DISCHARGE PUMPED IF LASER
M.L. Dlabal and J.G. Eden (7 min)

FB-3 LONG PULSE XeCl LASER PUMPED BY AN ELECTRON BEAM ASSISTED DISCHARGE
B. Fontaine, B. Forestier, and C. Perry (7 min)

FB-4 LONG PULSE X–RAY ASSISTED DISCHARGE XeCl LASER
B. Forestier, B. Fontaine, and M. Sentis (7 min)

FB-5 KrF^* SHORT PULSE STUDIES
A. Mandl, J.H. Parks, and D. Klimek (7 min)

FB-6 VIBRATIONAL RELAXATION AND LASER EXTRACTION IN KrF
W.L. Morgan, N. Winter, and K. Kulander (7 min)

FB-7 STUDY OF KrCl(B) AND Kr_2Cl EXCITED STATE KINETICS USING SYNCHROTRON RADIATION EXCITATION
M.G. Durrett, L. Houston, G.K. Walters, K.Y. Tang, D.C. Lorents and D.L. Huestis (7 min)

FB-8 ABSORPTION SPECTRA OF Ar_2F AND Kr_2F
H.T. Powell and K.S. Jancaitis (7 min)

FB-9 HEAVY PARTICLE, ELECTRON, AND RADIATIVE QUENCHING OF Ar_2F AND Kr_2F
K.S. Jancaitis and H.T. Powell (7 min)

COFFEE BREAK 10:15 - 10:45 A.M.

GA: ARCS IV
Chairperson: R. Kessler, Avco Everett Research Lab., Inc.
10:45 a.m.
Room A

GA-1 THE INFLUENCE OF THE SELF-MAGNETIC FIELD ON THE CURRENT FLOW IN AXI-SYMMETRIC TENSOR CONDUCTIVITY PLASMA
I. Israeli, R.L. Boxman, and S. Goldsmith (7 min)

GA-2 ELECTRODE ARCING PHENOMENA IN MHD GENERATORS
I. Sadovnik, A. Solbes, and M. Martinez-Sanchez (7 min)

GA-3 PLASMATRON SIMULATION OF MHD-CHANNEL CONDITONS
V. Goldfarb, V. Hruby, and R. Kessler (7 min)

GA-4 MHD CHANNEL PLASMA DIAGNOSTICS
A.M. Demirjian (7 min)

GA-5 ARC CHARACTERISTICS IN A SEEDED COMBUSTION PRODUCTS PLASMA
E. Harmon, W. Unkel, D.A. Kirby, and A.Y. Chang (7 min)

GB: ION REACTIONS I
Chairperson: J.B. Laudenslager, Jet Propulsion Laboratory, Caltech.
10:45 a.m.
Room B

GB-1 CHARGE EXCHANGE IN C^{++} / RARE GAS ATOM COLLISIONS
C.E. Burkhardt, and J.J. Leventhal (7 min)

GB-2 EMISSION SPECTRUM OF THE He^{+} + Ne RADIATIVE CHARGE-TRANSFER AND ASSOCIATION REACTIONS AT NEAR-THERMAL ENERGIES
Rainer Johnsen, and Manfred A. Biondi (7 min)

GB-3 NITROGEN ION ASSOCIATION REACTIONS
S.R. Alger, and J.A. Rees (7 min)

GB-4 BASIC MICROSCOPIC THEORY OF NEUTRALIZATION AND OF CHEMICAL REACTIONS IN DENSE GASES
M.R. Flannery (20 min)

GB-5 MOLECULAR DYNAMICS SIMULATION OF IONIC RECOMBINATION IN A PLASMA
W.L. Morgan, J.N. Bardsley, J. Lin, and B.L. Whitten (7 min)

GB-6 TWO AND THREE BODY RECOMBINATION IN RARE GAS FLUORIDES
B.L. Whitten, W.L. Morgan, and J.N. Bardsley (7 min)

LUNCH 12:00 - 1:30 P.M.

HA: ELECTRON CAPTURE 1:30 p.m.
Chairperson: F.C. Sharpton, Univ. of Wisconsin Room A

HA-1 ELECTRON ATTACHMENT TO HCl AND DCl IN EXCITED VIBRATIONAL OR ROTATIONAL STATES
J.N. Bardsley (7 min)

HA-2 REACTION KINETICS OF A HIGH PRESSURE HELIUM FAST DISCHARGE AFTERFLOW
J. Stevefelt, J.M. Pouvesle, and A. Bouchoule (7 min)

HA-3 NOBLE-GAS TRIMER IONS: DISSOCIATIVE RECOMBINATION OF Ne_3^+ IONS AND ELECTRONS
Jeffrey A. MacDonald, Manfred A. Biondi, and Rainer Johnsen (7 min)

HA-4 DISSOCIATIVE RECOMBINATION OF O_2^+
Steven L. Guberman (7 min)

HA-5 DISSOCIATIVE RECOMBINATION OF Hg_2^+ IONS AND ELECTRONS
Vidya E. Jog and Manfred A. Biondi (7 min)

HA-6 ELECTRON AFFINITIES OF MOLECULES – AN EMPIRICAL CORRELATION
P. Davidovits, A. Freedman, and G.W. Stewart (7 min)

HA-7 MEASUREMENTS OF ELECTRON DRIFT VELOCITY AND ATTACHMENT IN DRY AIR
D.K. Davies (7 min)

HB: NON–UNIFORM GLOWS & CORONA 1:30 p.m.
Chairperson: P. Bletzinger, Wright-Patterson Room B

HB-1 THE GLOW DISCHARGE CATHODE FALL
J.H. Ingold (7 min)

HB-2 ALTERNATING CURRENT CATHODE FALL CHARACTERISTICS FOR RARE GASES IN COLD CATHODE DISCHARGES
J. Maya and R. Lagushenko (7 min)

HB-3 ANALYSIS OF A 1-DIMENSIONAL STEADY STATE GLOW DISCHARGE
G.L. Duke and A. Garscadden (7 min)

HB-4 PLASMA BOUNDARY LAYER OVER A POSITIVE ELECTRODE
S.T. Van Brocklin and O. Biblarz (7 min)

HB-5 STABILITY OF SELF-SUSTAINED DISCHARGES IN ATTACHING GAS MIXTURES
L.J. Denes, P.J. Chantry, R.R. Mitchell, and L.E. Kline (7 min)

HB-6 PLASMA DENSITY PROFILES IN GAS DISCHARGES
J.P. Hauck (7 min)

HB-7 UNIPOLAR CURRENTS IN A LOW-PRESSURE Hg-Ar PLASMA
G.L. Rogoff, J.R. Lowry, and R.I. Pinsker (7 min)

HB-8 SPACE CHARGE MODEL FOR STEADY POINT-PLANE CORONAS
B.L. Henson (7 min)

HB-9 CORONAPHORESIS IN He AND N_2 CONTAINING Cs
D.H. Douglas-Hamilton and V. Goldfarb (7 min)

SESSION I: WORKSHOP ON CURRENT TRANSFER TO MHD ELECTRODES — **WEDNESDAY AFTERNOON**

Chairperson: C.E. Kolb, Aerodyne Research, Inc.

3:00 p.m.
Room B

A key aspect of successful open-cycle MHD technology involves current transport from the bulk flowing plasma to the channel electrodes. Prototype open-cycle MHD generators operate primarily in an arcing mode which can result in significant electrode damage. The workshop will explore recent modeling and experimental studies which characterize both arc and diffuse discharge current transport through the electrode boundary layer and investigate the effects of this transfer on heat flux to the electrodes, electrode erosion, and electro-chemical corrosion for test electrode materials.

The workshop will begin with a series of 15 minute reviews of key issues by invited speakers. These reviews will be followed by a discussion session open to all attendees. A summary of the problem by an invited speaker will close the session.

PROBLEM DEFINITION AND OVERVIEW – M. Martinez-Sanchez, Department of Aeronautics and Astronautics, M.I.T.

THEORETICAL UNDERSTANDING OF ARCING – W. Unkel, Department of Mechanical Engineering, M.I.T.

EXPERIMENTAL DATA ON ARCING PHENOMENA – I. Sadovnik, Avco Everett Research Laboratory, Inc.

EFFECTS OF SLAG ON CURRENT TRANSPORT – D. Stickler, Avco Everett Research Laboratory, Inc.

ELECTRODE CORROSION PHENOMENA – B. Rossing, Westinghouse Research and Development Center

WORKSHOP SUMMARY – D. Oliver, STD Research, Inc.

JA: ION REACTIONS II 8:45 a.m.
Chairperson: B.L. Whitten, Rice University Room A

JA-1 THEORETICAL STUDIES OF THE $O^+ + N_2$ ION-MOLECULE REACTION
H.H. Michels and R.H. Hobbs (20 min)

JA-2 SILICON-OXIDE NEGATIVE ION CHEMISTRY
F.C. Fehsenfeld, D.W. Fahey, and E.E. Ferguson (7 min)

JA-3 REACTIONS OF $O_2^- (H_2O)_n$, n = 0-4, IONS WITH O_3, NO, SO_2, AND CO_2
D.W. Fahey, F.C. Fehsenfeld, and E.E. Ferguson (7 min)

JA-4 THE HYDRATED NEGATIVE HYDROGEN ION
J.F. Paulson and M.J. Henchman (7 min)

JA-5 NEGATIVE ION REACTIONS WITH ACETONITRILE
J.F. Paulson and F. Dale (7 min)

JA-6 COLLISONAL STUDIES OF HIGH TEMPERATURE MOLECULAR NEGATIVE ION-NEUTRAL REACTIONS
R.L.C. Wu and T.O. Tiernan (7 min)

JA-7 FRAGMENTATION AND INTERNAL EXCITATION OF UF_6^- IONS IN COLLISIONS WITH NOBLE GAS ATOMS
J.A.D. Stockdale (7 min)

JB: DISTRIBUTION FUNCTIONS I 9:00 a.m.
Chairperson: W.L. Morgan, Lawrence Livermore Laboratory Room B

JB-1 ELECTRON SWARMS IN N_2 AT HIGH E/N
L.C. Pitchford and A.V. Phelps (20 min)

JB-2 DIFFUSION OF FAST ELECTRONS IN A MAGNETIC FIELD
M.S. Tekula and J.H. Jacob (7 min)

JB-3 TRANSPORT PROPERTIES OF CCl_2F_2 FROM THE BOLTZMANN EQUATION
J.P. Novak and M.M. Shoucri (7 min)

JB-4 VIBRATIONAL PUMPING MECHANISMS INFLUENCING DISSOCIATIVE ATTACHMENT OF HYDROGEN
J.W. Engel, W.F. Bailey and A. Garscadden (7 min)

JB-5 ELECTRON KINETICS OF SILANE GAS MIXTURES OF SEMI-CONDUCTOR PLASMA REACTOR INTEREST
A. Garscadden, G.L. Duke, and W.F. Bailey (7 min)

COFFEE BREAK 10:00 - 10:30 A.M.

SESSION K
Chairperson: A.V. Phelps, JILA/N.B.S. & Univ. Colorado

10:30 A.M.
Room B

PLENARY SESSION IN HONOR OF

PROFESSOR W.P. ALLIS

The Conference will honor Professor Allis' many contributions to the field of gaseous electronics through talks given by several of his friends and colleagues. (45 min)

K-1 THE NON-CONVERGENCE OF THE LEGENDRE EXPANSION OF THE ELECTRON VELOCITY DISTRIBUTION
W.P. Allis (20 min)

BUSINESS MEETING 11:45 – 12:15 P.M. Room B

LUNCH 12:15 – 1:30 P.M.

LA: VISIBLE & INFRARED LASERS 1:30 p.m.
Chairperson: M.J. Plummer, Northrop Research & Tech. Ctr. Room A

LA-1 EXCITATION OF ArH^* LUMINESCENCE BY ELECTRON ION RECOMBINATION DURING THE AFTERGLOW (7 min)
J. Shmulovich and S. Yatsiv

LA-2 KINETICS OF AN Ar-O_2 NUCLEAR-PUMPED PLASMA FOR AN O_2 ($^1\Delta$) - I_2 LASER
M.S. Zediker, T.R. Dooling, D. Burlet, and G.H. Miley (7 min)

LA-3 4.3μm CO_2 LASER PARAMETERIZATION
D.R. Suhre and L.H. Taylor (7 min)

LA-4 DISCHARGE PARAMETERS OF A MULTI-ATMOSPHERIC UV-PREIONIZED TE CO_2 LASER
K. Midorikawa, K. Nakamure, K. Wakabayashi, M. Obara, and T. Fujioka (7 min)

LA-5 ZnI, CdI AND CdBr PHOTO-DISSOCIATION LASERS: QUENCHING KINETICS AND B STATE RADIATIVE LIFETIMES
M.N. Ediger, A.W. McCown, and J. G. Eden (7 min)

LA-6 ELECTRON BEAM EXCITATION OF CW ION LASERS
J.J. Rocca, J. Meyer, Z. Yu, and G. J. Collins (7 min)

LB: DISTRIBUTION FUNCTIONS II 1:30 p.m.
Chairperson: L.C. Pitchford, Sandia National Labs Room B

LB-1 ELECTRON ENERGY DISTRIBUTION AND VIBRATIONAL POPULATION IN CO AND He-CO DISCHARGES
Y. Kaufman and Yu. M. Kagen (7 min)

LB-2 ELECTRON COLLISION CROSS SECTIONS FOR HCl DERIVED FROM SWARM MEASUREMENTS
D.K. Davies (7 min)

LB-3 ELECTRON DRIFT VELOCITIES IN CO_2 GAS LASER MIXTURES
M.C. Cornell, H.J. Brooks, and K.J. Nygaard (7 min)

LB-4 MONTE CARLO SIMULATION OF ELECTRON SWARMS USING AN IDEAL SOURCE
P.J. Chantry, G.L. Braglia (20 min)

LABORATORY TOUR 3:00 – 6:00 P.M.
AVCO EVERETT RESEARCH LABORATORY, INC. and AVCO EVERETT METALWORKING LASER MANUFACTURING AND APPLICATION FACILITIES (Bus Transportation)

SOCIAL HOUR 7:00 P.M. Room A

BANQUET 8:00 P.M. Georgian Room

guest speaker – Dr. J. HERBERT HOLLOMAN, Director, Center for Policy Alternatives, Massachusetts Institute of Technology "Reindustrialization – Why and What are the Alternatives"

MA: EXCITATION TRANSFER
Chairperson: G.L. Duke, Wright-Patterson
9:00 a.m.
Room A

MA-1 OBSERVATION OF SPONTANEOUS EMISSION FROM PENNING-LIKE COLLISIONS BETWEEN He(2^3S) AND NITROGEN
L.W. Downes, S.D. Marcum, D. Petrovic, and W.E. Wells (7 min)

MA-2 EXCITATION TRANSFER REACTIONS IN NEON AFTER-GLOWS AT 150°K
J. Clark and A.J. Cunningham (7 min)

MA-3 ELECTRONIC ENERGY TRANSFER BETWEEN METASTABLE ARGON ATOMS AND GROUND-STATE OXYGEN ATOMS
L.G. Piper, M.A.A. Clyne, and P.B. Monkhouse (7 min)

MA-4 RADIAL DISTRIBUTION OF EXCITED ATOMS IN AN Ar-O_2 SURFACE WAVE PRODUCED PLASMA
A. Ricard, M. Moisan, and D. Collobert (7 min)

MA-5 PRODUCT ROTATIONAL DISTRIBUTIONS IN ELECTRONIC ENERGY TRANSFER COLLISIONS OF Ar($^3P_{0,2}$) WITH N_2
C.R. Lishawa and E.E. Muschlitz, Jr. (7 min)

MA-6 LASER DOUBLE RESONANCE DETERMINATION OF RAPID VIBRATIONAL AND ROTATIONAL ENERGY TRANSFER RATES IN CO_2
M.D. Thomason and B.J. Feldmen (7 min)

MA-7 EXCITATION TRANSFER BETWEEN XENON METASTABLE ATOMS AND NITROGEN MOLECULES
M. Touzeau and J. Jolly (7 min)

MB: BREAKDOWN & CORONA
Chairperson: P.F. Williams, University of Texas
8:45 a.m.
Room B

MB-1 BREAKDOWN OF HELIUM AT A VERY HIGH E/N
D. Bhasavanich and A.B. Parker (7 min)

MB-2 DEVELOPMENT OF A SHORT PULSE DISCHARGE
W.W. Byszewski, M.J. Enright, and J.M. Proud (7 min)

MB-3 THE EFFECT OF ELECTRON BEAM INDUCED SPACE CHARGE ON BREAKDOWN OF N_2-SF_6 MIXTURES
T. Tzeng, E.E. Kunhardt, M. Kristiansen, and A.H. Guenther (7 min)

MB-4 STATISTICAL INVESTIGATIONS OF OVERVOLTAGE BREAKDOWN
E.E. Kunhardt and S.J. Levinson (7 min)

MB-5 A STUDY OF ELECTRON WAVES IN ELECTRICAL DISCHARGE CHANNELS
H. Jurenka and E. Barreto (7 min)

MB-6 LOW FREQUENCY AC(25-70 Hz) EFFECTS IN BREAKDOWN IN THE PRETEXT TOKAMAK
Jay F. Benesch, Roger D. Bengtson, L. Frommhold, and M.E. Oakes (7 min)

MB-7 INFLUENCE OF MOLECULAR ION FORMATION ON A CONTINUOUS OPTICAL DISCHARGE
A. Cybulski (7 min)

MB-8 MULTIPHOTON IONIZATION OF Xe AS A CHARGE SOURCE FOR ELECTRICAL BREAKDOWN
S.K. Dhali and P.F. Williams (7 min)

MB-9 EFFECTS OF MAGNETIC PRESSURE ON HIGH DENSITY Al AND C PLASMAS
R.J. Anderson, L.G. Gray, and R.H. Hughes (7 min)

COFFEE BREAK 10:15 - 10:30 A.M.

NA: PHOTON INTERACTIONS 10:30 a.m.
Chairperson: C. Duzy, Avco Everett Research Lab., Inc. Room A

NA-1 BRANCHING RATIOS IN THE EUV FOR SII AND SIII
M.D. Morrison and A.J. Cunningham (7 min)

NA-2 OPTICAL PROCESSES AFFECTING FLOW DISCHARGES
Martin Gundersen, Shekhar Guha, and Howard Cole (7 min)

NA-3 300 nm ABSORPTION BY Xe_2^* EXCIMER
K.Y. Tang, J.S. Dickinson, D.L. Huestis, and D.C. Lorents (7 min)

NA-4 ZERO CORE-CONTRIBUTION CALCULATION OF THE PHOTODETACHMENT CROSS SECTION OF NO_2^-
W.B. Clodius, R.M. Stehman, and S.B. Woo

NA-5 THE UNIQUENESS OF A FRANCK-CONDON ANALYSIS
P.W. Townsend, W.B. Clodius, and S.B. Woo (10 min)

NA-6 MEASUREMENT OF ABSOLUTE PHOTOIONIZATION CROSS SECTIONS FOR THE 7p EXCITED STATES OF CESIUM (7 min)
G.W. Foltz, M.G. Payne, and G.S. Hurst

NA-7 ELECTRON ATTACHMENT AND CHARGE RECOMBINATION FOLLOWING TWO-PHOTON-IONIZATION OF METHYLAMINES
Long C. Lee and William K. Bischel (7 min)

NA-8 A THEORETICAL INVESTIGATION OF THE PHOTODISSOCIATION OF POLYATOMIC MOLECULES
C.A. Asaro and A. Dalgarno (7 min)

NA-9 STATE-SELECTIVE PHOTOLYSIS OF CsKr and Cs_2Kr^*
C.B. Collins, F.W. Lee, H. Golnabi, F. Davanloo and P. Vicharelli; D. Popescu and I. Popescu (7 min)

NB: EXCITATION TRANSFER II & QUENCHING 10:45 a.m.
Chairperson: J. Stevefelt, University Orléans, France Room B

NB-1 COLLISIONAL RELAXATION OF ELECTRONICALLY EXCITED COPPER ATOMS
Hao–Lin Chen and Gaylen V. Erbert (7 min)

NB-2 COLLISIONAL DEACTIVATION OF THE Pb $6p^2\ ^3P_2$ and $^3P_1$ METASTABLES BY GROUND-STATE Pb ATOMS
C. Reiser, N. Djeu, and R. Burnham (7 min)

NB-3 COLLISIONAL PROCESSES IN A DENSE SODIUM VAPOR FOLLOWING RESONANT EXCITATION BY SHORT LASER PULSES
D.J. Krebs and L.D. Schearer (7 min)

NB-4 ASSOCIATIVE IONIZATION IN LASER EXCITED SODIUM VAPOR
V.S. Kushawaha, J.J. Leventhal (7 min)

NB-5 COLLISIONAL DEPOPULATION OF HIGH-RYDBERG Na s STATES BY ARGON
J. Boulmer, J.-F. Delpech, J.-C. Gauthier, and K.A. Safinya (7 min)

NB-6 EXPERIMENTAL DETERMINATION OF 6 ^3P-6 ^3P COLLISIONAL EXCITATION CROSS SECTIONS FOR LINE EMISSION IN THE POSITIVE COLUMN OF DC MERCURY DISCHARGES (7 min)
P. van de Weijer and R.M.M. Cremers

NB-7 PROTON-INDUCED DEACTIVATION OF METASTABLE IONS
S. Bienstock, T.G. Heil and A. Dalgarno (7 min)

ADJOURN 12:00 NOON

SESSION AA

8:45 A.M., TUESDAY, OCTOBER 20, 1981

ROOM A

ARCS 1

CHAIRPERSON: R.J. ZOLLWEG
WESTINGHOUSE R&D CENTER

AA-1 Longitudinal Acoustic Resonances in High Pressure Mercury Lamps - R. SCHÄFER, Philips GmbH Forschungslabor Aachen/Germany. --The influence of the fundamental longitudinal[1] and higher acoustic resonances on the arc temperature profiles and the wall temperature distribution of cylindrical high pressure mercury lamps has been investigated experimentally. It is found that the axial variations of these temperatures in the vicinity of a resonance depend on the acoustic resonance mode. This result can be explained by an additional axial heat flow caused by the standing pressure wave associated with the respective resonance. Based on the above considerations the shape of the visual arc instability correlated with a specific resonance mode can be understood.

[1]R. Schäfer and H.P. Stormberg, to be published.

AA-2 Time Dependent Behaviour of High Pressure Mercury Discharges - H.P. STORMBERG, Philips GmbH Forschungslabor Aachen/Germany. --A numerical model for the time dependent behaviour of cylindrical high pressure mercury discharges has been developed. The model allows the calculation of time dependent plasma parameters as temperature profiles T(r,t), arc conductance etc. for arbitrary supply voltage wave shapes and frequencies. The model is based on an expansion of the heat flux potential into a series of Bessel functions of zeroth order. The net emission coefficients, used as input parameters for the model, were determined as a function of lamp diameter, axis temperature and radial temperature profile by calculating the radiation transport of the mercury lines. The calculated time dependent lamp voltage, current and arc temperature profiles show good agreement with the respective experimental results.

AA-3 Time Resolved Spectroscopic Diagnostics of AC Operated HID Arcs W. D. PARTLOW Westinghouse R&D Center--We have measured the variation within the AC cycle of temperatures and additive pressures of mercury and metal halide arcs operated from 60Hz to 2000Hz. Radiance measurements on optically thin emission lines were time resolved with a boxcar integrator, and the temperatures and species densities were obtained using the Abel inversion technique. The mercury data were compared to a previously reported AC model of the mercury arc.[1] The model predicted the shape of the variation of the central temperature within the AC cycle but differed somewhat from the data in average value. We evaluated the metal halide data to assess the validity of comparing spectroscopic measurements of AC operated arcs to steady state models of arc composition. It was found that high frequency operation was advantageous for such comparisons. Axial cataphoretic effects are eliminated, and temperature fluctuations are reduced allowing accurate determination to be made from time averaged measurements.

[1]J.J. Lowke, R.J. Zollweg and R.W. Liebermann, J. Appl. Phys. 46, 650 (1975).

AA-4 Collisional Broadening of Metal Additive Resonance Radiation in High Pressure Metal Halide Arcs - HAROLD L. ROTHWELL and WILLIAM M. KEEFFE, GTE Sylvania Lighting Center--A systematic analysis of the spectral line shape of the resonance transitions of sodium and scandium is used to study high pressure metal halide arcs. The spectral line shapes are obtained for a wall stabilized 60Hz arc containing mercury and the iodides of sodium and scandium operating at 3 amp. Typical densities are: 4×10^{18} cm^{-3} for Hg, $\sim 4 \times 10^{15}$ cm^{-3} for Na and Sc and 10^{14}-10^{15} for electrons. Both the blue and red wing shapes for the resonance lines are analyzed in terms of resonance and impurity broadening mechanisms and a simple model is employed to reduce the intensity measurements to number densities of metal additives. This method has an advantage over the usual optically thin emission approach(1) for arc sources in which the high operating pressures cause many atomic transitions to be optically thick. The dependence of the broadening on the temporal, radial and axial properties of the arc is used as a diagnostic for studying basic arc source properties.

1. W. M. Keeffe et al, Bull. Am, Phys. Soc. 21, 846 (1976).

AA-5 Chemical Reaction Studies by Plasma Diagnostics and Modeling of a Scandium Iodide Arc W. D. PARTLOW, R. W. LIEBERMANN, R. J. ZOLLWEG, and L. N. YANNOPOULOS Westinghouse R&D Center--We have modeled the equilibrium composition of a metal halide arc containing mercury, scandium, iodine, and argon, and have compared the calculations to spectroscopic measurements on experimental lamps. Free energy minimization calculations were used to determine the vapor-condensed phase equilibria at the quartz wall, and the vapor compositions thus obtained were used as input data to radial demixing calculations of the composition throughout the arc profile using LTE assumptions. The calculated compositions were then compared to optically thin spectroscopic measurements at the arc core where all important species densities could be accurately determined. The best agreement of calculations with measurements was found when the influence of reactions of the iodide salts with the quartz arc tube and electrode materials were taken into account. Such reactions dramatically alter the arc vapor composition near the wall. On the whole, we found that quasi-equilibrium modeling of the complicated chemical system gave a consistent representation of our experimental observations.

AA-6 Effect of Low Energy Electron Impact on the Radiation Conversion Efficiency of High Power Cesium-Neon Arc Lamps*.- C.S. CHANG†, K.G. WHITNEY, Naval Research Laboratory.-- The role of low energy electron collisions with Cs and Ne atoms in high power Cs-Ne flashlamps is described. The effects of electron interactions include both elastic and inelastic collisions with Cs and elastic collisions with Ne. The energy dependence of low energy electrons on the diffusion coefficient in high pressure Cs-Ne gas mixtures was investigated. Also, an analysis was performed for electron excitations and ionizations of Cs atoms near threshold to determine the Cs excitation rate coefficients. These excitation and ionization coefficients were then used to calculate the excited state populations and the internal energy of the discharge plasmas, which in turn can be utilized to predict the spectra of optically thick radiation output.[1] This theory will be applied to analyze some aspects of the experiments by Hug et al.[2]

*Work supported by the U.S. Naval Air Systems Command
†Beers Associates, Inc., Reston, VA
1. K.G. Whitney, J. Davis, and J.P. Apruzese, Phys Rev A 22, 2196 (1980).
2. W.F. Hug, J.F.Shaw, and R.D. Buhler, Appl. Opt. 12, 1331 (1973).

AA-7 Investigation and Model Calculation of the Inital Arc in a High-Pressure Mercury-Vapour Lamp - H. GROSSE-WILDE Siemens AG, Erlangen, Germany. -- The starting period of an AC-discharge with - initially - cold electrodes and low pressure was investigated. The tungsten electrodes were coated with an emission material (ThO_2, Y_2O_3, Dy_2O_3). In each current cycle the discharge may appear in the glow mode (voltage drop: some hundred volts) or in the arc spot mode (voltage drop: some ten volts) or in both modes with a glow to arc transition and (under certain conditions) an arc to glow transition. The "trigger current" of the transition from one mode to the other depends on the emission material of the electrodes.

With experimental values of lamp voltages and "trigger currents" the electrical circuit of the starting phase of an mercury-vapour lamp with inductive ballast was simulated. The results together with the energy balance of the electrodes give the time necessary for heating up the electrodes. The starting period ends with the onset of thermoemission of electrons at a mean electrode temperature of about 1 000 K.

AA-8 Saturation of the Acoustic Waves Produced by Pulsed Arcs - F. NADEAU, IGM, Montréal and M.G. DROUET, IREQ, Varennes, Canada.-- Rapid simultaneous measurements of the arc current and voltage and the emitted acoustic wave were made on a small 20-A DC arc in open air, which was subjected to current pulses ranging in amplitude from 0.4 kA to 40 kA and in rise time from 10^{-4}s to 10^{-7}s. The results show that for a rise time $\Delta t < 10^{-5}$s, the amplitude of the pressure wave generated by the arc no longer varies with Δt but remains constant for a given amplitude of the current pulse.

An additional study shows that this saturation is accompanied by a modification in the electrical behavior of the arc, which suggests that the observed saturation is due to the arc itself and not to absorption of the pressure wave in the surrounding air.

AA-9 Hot Cathodes in High Pressure Discharge Lamps - JOHN F. WAYMOUTH, GTE Lighting Products, Danvers, Mass. -- The operation of hot cathodes in high pressure discharge lamps has been investigated in a manner similar to that described by Ecker.[1] The formalism of Dyke and Dolan[2] has been used to calculate emission of electrons from the cathode as a function of temperature and electric field. The electric field at the cathode surface is calculated from ion current and cathode fall, the largest contribution to that field being developed in the free-fall sheath less than one mean free path in thickness at the cathode surface. Two solutions to the coupled system of equations are found: a low-field, diffuse-mode solution in which electron emission is by the Schottky amplified thermionic process, cathode fall increases with increasing current density, and the cathode spot tends to expand to fill the entire extent of the cathode tip; and a high field, hot-spot mode in which electrons are emitted as a result of the temperature-field mechanism. The lowest cathode fall in the latter mode occurs when the potential drop across the free fall sheath equals the cathode fall required by the cathode energy balance. The operating mode of the discharge in a given lamp depends on which of the two modes has the lowest cathode fall. Examples of each occur in various lamps and can be accounted for with reasonable values of material constants.

1. Gunter Ecker, Zeits. Naturf. 28 417 (1973).
2. W. P. Dyke and W. W. Dolan "Field Emission" in Adv. in Electronics & Electron Physics, L. Marton Ed., Vol. VIII Acad. Press (1958).

SESSION AB

9:00 A.M., TUESDAY, OCTOBER 20, 1981

ROOM B

GLOW DISCHARGES I

CHAIRPERSON: A.J. CUNNINGHAM
UNIVERSITY OF TEXAS

AB-1 Discharge Characteristics of Externally Ionized Methane. P. BLETZINGER, USAF/AFWAL, WPAFB -- Due to its high electron drift velocity, methane is an attractive gas for possible application in electron beam switched discharges. Similar to argon, its I-V characteristics display 3 distinct regions: at low sustainer voltages the current rises very slowly then at a certain sustainer voltage transition to a high conductance region occurs and finally at a high current has a saturation-like region with smaller current rise vs. sustainer voltage. Measurements of the electric field distribution in the discharge show the cathode fall voltage to be from 2 to 6 times the discharge voltage drop per cm, indicating that ionization in the cathode sheath is likely. Also the discharge voltage in the high conductance region is smaller at lower pressure (higher E/N), indicating the effect of ionization. The comparison between experimental and theoretical characteristics is not entirely satisfactory, even though the methane materials functions were corrected using experimental data. A further discrepancy is the increased conductivity when argon is added in contrast to recent drift velocity measurements in Ar-CH_4 mixtures. The characteristics measured at the relatively small ($< 1.5 mA/cm^2$) available e-beam current densities can be extrapolated to values achievable with current e-beam technology.

AB-2 Discharge Characteristics, Optical Emission and Concentration of Species in Cl_2 Plasmas: Their Significance for Plasma Etching, D. L. FLAMM and V. M. DONNELLY, Bell Laboratories, Murray Hill, NJ--Time resolved V, I, and power were measured in Cl_2 plasmas at 0.3 Torr (10KHz-28MHz), with spatial and time resolved emission spectra from Cl, Cl^+ and Cl_2^+, and Si, GaAs and InP etching vs. temperature. He and Ar additions sampled excitation to determine relative chlorine species concentrations. Cl_2^+ was measured by laser induced fluorescence. Chemical etching of GaAs is dominant. As frequency decreases from ~5MHz to ~800KHz at constant power, Cl^+ ions appear, and sheath thickness, applied voltage and Si and InP etch rates increase. This is consistant with an ion-enhanced etch rate increasing linearly with energy. In the low frequency regime, optical emissions were 100% modulated. Emission from the momentary negative sheath lagged the voltage, most likely due to ions crossing the sheath in less than a half period and excitation by secondaries. At 13MHz, $^4S^o$ Cl emission from the glow is ~25% modulated, but $^2\Pi_i$ Cl_2^+ emission is unmodulated due to a 0.11μs fluorescence lifetime.

AB-3 Properties of the Positive Column of a Glow Discharge in Flowing Hydrogen (*) - H. BRUNET, J. ROCCA SERRA and M. MABRU, Lab. Marcoussis, France.-- Results of a theoretical model for predicting the effects of gas flow on the properties of the positive column in a glow discharge are presented. A cylindrical discharge at low pressure ($\leqslant$ 30 Torr) in a hydrogen flow is considered. The two-dimensional model couples electric, vibrational and chemical properties of the discharge through E/N, the ratio of electric field to neutral gas density. It predicts the electric field, the discharge voltage and the number densities of vibrationally excited H_2 molecules and H atoms as a function of pressure, flow velocity, diameter and length of the discharge and current. Molar flow rates of H_2 (v = 1 and 2) molecules and H atoms are presented. Comparison with available experimental data is made.

(*)Supported by DRET, Paris, France.

AB-4 Effects of Excitation Mechanism on Linewidth Parameters of Conventional VUV Discharge Line Sources.* L.G. PIPER and W.T. RAWLINS, Physical Sciences, Inc., Woburn, MA. -- Doppler broadening is often the primary line-broadening mechanism in conventional VUV resonance lamps, and thus determines the utility of these lamps for resonance fluorescence/absorption diagnostics. Doppler broadening is a complex function of the lamp excitation processes. The excitation mechanisms may either leave the radiating species with a considerable excess energy, such as in dissociative excitation by metastable rare gas atoms, or, as in electron impact excitation, the excess energy may be negligible. We review the kinetics of these processes as they relate to various VUV atomic line sources, and present absorption measurements on atomic nitrogen metastables, $N(^2D)$ and $N(^2P)$, which show markedly different behavior between microwave-excited He/N_2 and Ar/N_2 lamps. The implications of these effects for design application of resonance absorption/fluorescence diagnostics are illustrated.

*Supported by U.S. Air Force #19628-80-C-0174

AB-5 Metastable Ne (^{3}Po,2) Production in a Neon Gas Discharge,* J.W. SHELDON and K.A. HARDY, Florida International Univ. An experimental study of metastable Ne production in a hot cathode discharge is reported. The metastables which effuse from an anode slit are collimated into a beam and their velocity distributions are determined by time-of-flight. Discharge pressures from .05 to 1.2 Torr are explored. Metastable atom temperatures are found to increase with increasing pressure for a constant input power and an optimum pressure is identified for maximum metastable production at each current. Results are compared with the theory and measurements of Ichikawa and Teii.[1]

*Supported by the Research Corporation

[1]Y. Ichikawa and S. Teii, J. Phys. D 13, 2031 (1980).

SESSION BA

10:45 A.M., TUESDAY, OCTOBER 20, 1981

ROOM A

ARCS II

CHAIRPERSON: E. PFENDER

UNIVERSITY OF MINNESOTA

BA-1 Discharge Spectroscopy by the Optogalvanic Effect. - R. SHUKER, A. BEN-AMAR and G. EREZ, Ben-Gurion University, Beer-Sheva, Israel.-- Several spectroscopic applications of the optogalvanic effect in plasma discharges are discussed. This effect is utilized by us in investigating population inversion detection, optical double resonance and Penning ionization spectroscopy. We use neon to demonstrate the spectroscopic uses of the optogalvanic effect. A phenomenological model of the resulting optogalvanic signal is described which deals, in details, with the time development of the signal. The model deals with the various cases encountered in the optogalvanic effect due to transitions in neon. We have particularly investigated single step laser excitation of the 3s→3p and from the 3p manifold to higher levels in neon.

We will demonstrate experimental results of measurement of inverted population on the 3p→3p transitions.

The signal relevant to uninverted population will also be shown. The results of the model are in good agreement with the experiments.

BA-2 Arc-Gas Flow Interactions Using Differential Interferometry-N.BRATES, M.H. SANWARWALLA, S.M. MAHAJAN, and D.M. BENENSON, State University of New York at Buffalo*--The region adjacent to the arc column in such gases as air, nitrogen, and sulfur hexafluoride absorbs radiation from the plasma, forming the thermal boundary layer or arc mantle - a region that plays an important role in extinction and reignition processes. Experiments have been carried out upon a 7 bar air plasma operated in single flow configuration with a 12.5mm diameter orifice nozzle (electrode is 7.5mm upstream of the nozzle face). Peak current during the sinusoidal loop is 2kA, with $dI/dt = 15A/\mu s$ near current zero. Differential interferometry is employed, utilizing a Wollaston prism arrangement. The observed fringe shifts in both cold and hot flows are related to temperature changes in the test section or in the region surrounding the plasma. Turbulence, or fluctuations, in the flow affects strongly (and adversely) the viability of the fringe pattern. Radial distributions of temperature are determined using Abel inversion methods.

*Research supported by Electric Power Research Institute Contract RP 246-2.

BA-3 Arc Temperatures in High Speed Flow-T.F.BERNECKI, Y.C.LAU, and D.M.BENENSON, State University of New York at Buffalo*--Experiments are being conducted upon 14 bar dynamic argon plasmas immersed in a shock free converging-diverging nozzle of 10mm throat diameter. The maximum value of the sinusoidal loop is 1kA; $dI/dt = 15A/\mu s$ near current zero. Arc radiation is obtained using a high speed data acquisition system having a scan speed of 3mm/μs. Near current zero the centerline temperature decays at 200K/μs, with a value of 15,000K at 20μs before current zero. The observed centerline temperatures are substantially below the calculations of Bhansali[1] (with conditions similar to those for the experiment except for (1) $dI/dt = 50A/\mu s$ and (2) neglect of radiation). Additional calculations, using one-dimensional models, are in progress. Arc diameter remains nearly constant, at 3.6mm, during the current zero period, in good agreement with Bhansali's analysis.

*Research supported by National Science Foundation Grants ENG 76 17009 and CPE 800-7187 and by Electric Power Research Institute Contract RP 246-2.

[1]C.H. Bhansali, "Analysis of Static and Dynamic Electric Arcs in Supersonic Nozzle Flow," Ph.D. Dissertation, State University of New York at Buffalo, 1980.

BA-4
Hydrodynamic Transient in a Tip-Plane Arc Configuration. J. CONVERTI and W. UNKEL, M.I.T.* The transient response of an arc to a rapid increase or decrease in current has been studied. The transient was produced by a transistor current regulator with a rise time of $\lesssim$ 15 μsec. The time response of the light emitted from the arc was measured at several distances from the tip electrode and at several distances from the axis of the arc. For a step increase the light intensity records showed a discontinuity in slope. The delay time between the step change in current and the discontinuity varied with distance from the tip, however the delay was constant over the entire arc width. No discontinuity was observed for a step decrease in current. This suggests a flat wave front propagating away from the tip. The propagation speed was proportional to the average current associated with the step. In analogy to a starting jet, it was inferred that the step increase in current leads to a shear instability in the tip region and that a vortex structure propagates through the jet. Analytical estimates of the vortex speed were comparable to the speed measured in the experiments.

*Supported by U.S. D.O.E. Contract DE-AC02-79ER10474.

BA-5 Thermal Conductivity of O_2 in the Dissociation Regime - A. KURTZ and J. MENTEL, Ruhr-Universität Bochum FRG[+]-- Gases of diatomic molecules exhibit a pronounced maximum of the thermal conductivity in the temperature range of dissociation. This increased conductivity is caused by transport of dissociation energy by diffusion of atoms and molecules driven by temperature gradients in the region of thermal dissociation. In a cylindrical water cooled quartz tube with a low current arc the radial profile n(r) of the index of refraction of oxygen is measured by holographic interferometry. The resulting thermal conductivity is in good agreement with kinetic theory calculations[1].

[+]Supported by the DFG

[1]J. YOS, Theoretical and Experimental Studies of High Gas Transportproperties, AVCO RAD-TR-65-7

BA-6 Approximate Non-LTE State Diagrams for Atomic Plasmas - T. L. EDDY, Georgia Institue of Technology.-- A method for relating electron excitation and heavy particle temperatures to electron, atom and ion densities, as well as pressure in atomic or elemental plasmas is described. On a plot of the ion/atom density ratio versus electron density, curves of constant pressure can be placed using the ideal gas equation of state. Isotherms are placed using the Saha ionization equation assuming thermodynamic equilibrium. The non-LTE isobars and isotherms are located similarly as families of the non-LTE parameters (T_e/T_{exc}) and T_e/T_g). The approximate calculation allows the isobars and isotherms to be calculated separately, thus reducing the preparation of the diagram to a few hours. The state diagram can be used for consistency checks of experimental data, to quickly determine values of unknown properties, and to indicate type and extent of non-LTE in a plasma.

BA-7 Thermal Considerations for an Electric Arc - T.-M. FANG*, University of California, Lawrence Livermore National Laboratory†--Some basic arc properties including the radius and the E-I (Current-Field) characteristics have been obtained through the thermal considerations. The Joule heating of the current-carrying column is supposedly first conducted out from the arc center and eventually convected or radiated away from the arc boundary. The heat balance equations have been solved analytically and the results can be put in an extremely simple and workable form. By obtaining first the profile of the electrical conductivity as a function of the arc radius, a general form of E-I characteristics can be obtained through the thermal considerations. This current-field property will result in the same conventional MHD arc characteristics, i.e., $E \sim I^{0.5385}$ and $R \sim I^{-0.7693}$ in limiting cases.

* Permanent Address: Dept. of Aerospace and Mechanical Engineering, Boston University, Boston, MA 02215.

† Work performed under the auspices of the U.S. Dept. of Energy by the Lawrence Livermore National Laboratory under contract number W-7405-ENG-48.

SESSION BB

10:45 A.M., TUESDAY, OCTOBER 20, 1981

ROOM B

GLOW DISCHARGES II

CHAIRPERSON: R. ANDERSON

UNIVERSITY OF ARKANSAS

BB-1 Population of $N_2(A^3\Sigma_u^+,v)$ and $N(^4S_o)$ in Nitrogen DC Glow Discharges - G. CERNOGORA, C.M. FERREIRA*, L. HOCHARD and M. TOUZEAU, Lab. Phys. Plasmas, Paris-Sud U.-- The population of $N_2(A,0\leq v\leq 5)$ metastable states, of $N(^4S)$ atoms and of the electron density are measured in a glow discharge as a function of current and pressure from 0.1 to 2 torr. The $N_2(A,v)$ density is determined from the absorption of the 1+ system bands and that of $N(^4S)$ by NO titration. The maximum of absorption is about 2% for the v=o level which correspond to a density of $1.4\times10^{12}cm^{-3}$. The density of the different vibrational levels increases first with current and then saturates above a given limit which depends on pressure. In the experimental conditions the N_2 dissociation degree reaches 3%. A kinetic model is derived in which reported electron impact excitation coefficients of the A,B and C states vs. E/N and the continuity equation for charged particles are used to calculate the rate of excitation of $N_2(A)$ from ground state as a function of pressure. The model yields results in fair agreement with measurements and it shows that the $N_2(A,v)$ species are mainly lost by diffusion and by the reaction $N_2(A)+N(^4S)\rightarrow N_2(X)+N(^2P)$.

*Centro Electrodinâmica, Lisbon Tech U.

BB-2 Electron Distribution Functions and Characteristics of Argon Glow Discharges in 10^{-2}-1 Torr Pressure Range - C.M. FERREIRA, Centro Electrodinamica, Lisbon Tech. U.-- Electron distribution functions (EDF), transport parameters and inelastic rate coefficients have been calculated in Argon glow discharges, in the range $10^{-16}<E/N<2.10^{-15}Vcm^2$, solving the Boltzmann equation by analytical methods and using appropriate models to describe the experimental cross section data. The calculated values of the first Townsend coefficient and of the electron drift velocity were found to be very sensitive functions of the excitation cross section and a good agreement with measurements has been obtained making adjustments in the cross section data reported by different authors. Moreover, a steady-state theory of the discharge column has been derived using a modified version of common two-moment theories to account for the non-Maxwellian character of the EDF. The theory yields radial profiles of charged particle density and velocities as a function of pR, and similarity laws E/p and $n_e(0)/J$ vs. pR which are in better agreement with measurements than reported theories where a Maxwellian EDF is assumed.

BB-3 Mass Spectra from Silane Discharges,* H. CHATHAM, R. ROBERTSON and A. GALLAGHER,† JILA, U. of Colorado and NBS -- Hydrogenerated amorphous silicon films deposited from glow discharges have useful semiconductor properties that depend critically on discharge parameters. We have measured the neutral and ion mass spectra arriving at various surfaces of dc and rf discharges in 0.01 - 0.1 Torr of SiH_4. We observe primarily light ions at the cathode of a dc discharge, and many heavier ions (due to ion-molecule reactions) at the sides of dc or rf discharges or the electrodes of rf discharges. This is believed to result from different reaction times, a characteristic that should apply to many types of discharge chemistry. Qualitative models for the discharge characteristics and the ion-molecule and radical chemistry will be compared to the data.

*Work supported in part by the Solar Energy Research Institute.

†Staff Member, Quantum Physics Division, National Bureau of Standards.

BB-4 Effect of Hydrogen on Deionization Processes in Ne-Ar Mixtures A. K. BHATTACHARYA, GE, Lighting Business Group, Nela Park, Cleveland, OH 44112. The effect of small amount of H_2 (0.005-1.0%) on the deionization processes in Ne-Ar discharges was measured by microwave cavity techniques. At low charged particle densities the deionization of discharges produced in Ne-Ar mixtures is determined by the ambipolar diffusion of electrons and molecular argon ions (Ar_2^+). The charged particle density in the deionization period following a pulsed discharge decays exponentially with time. For a discharge tube of 7mm i.d. filled with Ne-Ar mixtures at a pressure of 20 Torr, the deionization of the plasma occurs with a time constant of 1.3 ms. The presence of a small amount of H_2 (0.003%) enhances the deionization process drastically. The charged particle density decreases much more rapidly (time constant of 0.61 ms) than in the pure mixture. A similar increase in the deionization rate was measured in pure Ar. At low charged particle densities the deionization rate is determined by the ambipolar diffusion of a highly mobile hydrogen ion, possibly H_3^+, compared to relatively less mobile argon ions.

BB-5 Effects of Water Vapour Concentration on Plasma Parameters of Rare Gas Positive Column Plasmas - Y. ICHIKAWA, R.M. HOBSON, York University, T. KANEDA and JEN-SHIH CHANG, McMaster University, Canada -- A numerical study of small concentrations of water vapour in the rare gas glow discharge positive column plasmas was conducted. Coupled density equations of the rare gas ions (X^+, X_2^+), the water vapour ions ($H^+(H_2O)_{n=1,2,3}, H_2O^+$, OH^+, H^+) and metastable atoms (X^*) were solved to determine the electron temperature T_e, the number densities of the charged and metastable particles. The results show that (1) the major ions in the plasma are H_2O^+ and H_3O^+ at a gas pressure $p \gtrsim 1$ Torr when the partial pressure of water $p(H_2O) \gtrsim 10^{-4}$ Torr; (2) electron temperature is affected by a small concentration of water vapour through the Penning ionization by metastables, and the dissociative recombination of $H^+(H_2O)_n$ and H_2O^+, e.g., T_e decreases by $\sim 20\%$ in a He plasma at $p = 1$ torr, $p(H_2O) = 10^{-3}$ Torr; (3) the number density of the metastables decreases rapidly due to Penning ionization even if a small amount of water vapour exists in the discharge system.

BB-6 Glow Discharges in Helium-Neon Laser Mixtures - J. A. REES, V. K. LAKDAWALLA, S. HUNTER and J. L. MORUZZI, Liverpool U., England* - - Factors limiting the life-time of low power helium-neon laser tubes have been investigated in a number of test cells for discharge lifetimes of up to 3000 hours. The cells were operated at currents of between 2 and 10 mA using 3 torr of He^4 and Ne in various proportions between 3:1 and 10:1. Variations in the operating voltage and total pressure were correlated with changes in the gas composition and were attributable to differential pumping of the helium and neon. The influence of oxygen released from the oxide-coated cathodes of the discharge cells is being studied through mass-spectrometric studies of the ion population of the glow discharge.

*Supported by the Ministry of Defence.

SESSION CA

1:30 P.M., TUESDAY, OCTOBER 20, 1981

ROOM A

ELECTRON COLLISIONS

CHAIRPERSON: P. DAVIDOVITS
BOSTON COLLEGE

CA-1 Use of Laser-Induced Fluorescence to Study Electron Excitation and Collisional Excitation Transfer of Atoms*-M.H. PHILLIPS, J.E. GASTINEAU, R.E. MIERS, L.W. ANDERSON, and C.C. LIN, U. of Wisconsin, Madison -- The use of laser-induced fluorescence to measure the electron excitation cross sections of metastable levels[1] has been extended to the two resonant levels of Ne, $1s_2$ and $1s_4$ ($2p^53s$, J=1). Electron excitation produces and radiation trapping maintains a population of atoms in the $1s_2$ and $1s_4$ levels as though these levels were metastable. Laser-induced fluorescence is used to measure the excitation cross sections of the levels in a manner similar to Ref. 1. For studying collisional excitation transfer, the $2p_i$ level is selectively populated by $1s_5 \rightarrow 2p_i$ laser absorption. Collisional transfer from $2p_i$ to $2p_j$ is monitored using the emission from the $2p_i$ and $2p_j$ levels. We have measured the rate constants for the $2p_2 \rightarrow 2p_3$, $2p_2 \rightarrow 2p_4$, $2p_4 \rightarrow 2p_3$, $2p_5 \rightarrow 2p_3$, $2p_5 \rightarrow 2p_4$ collisional transfer.

*Supported by the AFOSR.

1. M.H. Phillips et al., Phys. Rev. A23, 2751 (1981); Phys. Lett. 82A, 404 (1981).

CA-2 Emission of Free-free Radiation from Electrons in Argon,* C. YAMABE and A.V. PHELPS, JILA, U. of Colorado and NBS --Emission coefficients have been measured for the production of free-free radiation by moderate energy electrons in argon using a drift tube. Independent measurements were made at 0.5, 0.7 and 1.3 μm for $5\times10^{-22} < E/N < 5\times10^{-21}$ V m^2, i.e., mean electron energies between 1.7 and 5 eV. The argon density was 3 to 15×10^{24} m^{-3} and the electron current was 1 to 4×10^{-8} A. The measured coefficients average 15% higher than calculations using cross section formulas of Firsov and Chibisov[1] and 20% higher than theoretical and experimental values of Rutscher and Pfau[2] for a diffuse positive column. The variations of the emission coefficients with argon density and E/N are in very good agreement with calculations for $E/N < 3\times10^{-21}$ V m^2. At higher E/N line emission interferes.

*Work supported in part by Air Force Wright Aeronautical Laboratories.

[1]O.B. Firsov and M.I. Chibisov, Zh. Eksp. Teor. Fiz. 39, 1770 (1960).

[2]A. Rutscher and S. Pfau, Physica 81C, 395 (1976).

CA-3 Electron-Impact Excitation of H_2, D_2 and HD Resulting in Vacuum Ultraviolet Emission - P.W. ERDMAN and E.C. ZIPF, Univ. of Pittsburgh. -- We have studied the excitation of Lα, the Werner and Lyman bands, and the triplet dissociation continuum by electron impact on H_2, HD, and D_2. For Lα radiation, we find the emission cross sections at 300 eV are in the ratio 1:1.7:0.7 for H_2, HD, and D_2, respectively. For the Q_1 rotational lines of the Werner bands of H_2, our results agree with the emission cross sections published by Stone and Zipf[1] in contrast to recent measurements by Yung, et al.[2] The total emission cross sections for the Werner and Lyman bands for H_2, HD, and D_2 exhibit a variation in magnitude similar to that for Lα. Departures from the rotational intensity distribution predicted by the Honl-London factors are observed. The differences in D_2 and HD spectra are particularly striking, indicating pronounced vibrational-rotational coupling resulting in Franck-Condon factors that are not constant over a band. Noticeable differences also exist between the isotopes in the intensity and shape of the continuum radiation.

[1]Stone, E.J. and E.C. Zipf, J.Chem.Phys., 56,4646,1972.
[2]Yung, Y.L., G.R. Gladstone, K.M. Chang, J.M. Ajello, and S.K. Srivastave, Ap. J. Lett. (in press), 1981.

CA-4 Excitation of the CO($a^3\pi \rightarrow X^1\Sigma^+$) Cameron Bands by Electron Impact on CO and CO_2 - P. W. ERDMAN and E. C. ZIPF, Univ. of Pittsburgh.--We have studied the excitation of the Cameron bands ($a^3\pi \rightarrow X^1\Sigma_u^+$) of carbon monoxide by electron impact on CO and CO_2. For CO, we find that the a-X (1, 4) feature at 2389 Å which was used by Ajello[1] to normalize the entire Cameron band cross section is significantly contaminated by the (6,16) fourth positive band. Similarly, the anomalous intensity noted by Ajello for the a-X (0,4) band is due to contamination by the (6,17) fourth positive band. Correction for the contamination reduces Ajello's total emission cross by a factor of eight to 1.4×10^{-17} cm^2 at 11 eV. The corrected value is now compatible with CO($a^3\pi$) time-of-flight data and more recent measurements of the radiative lifetime of the $a^3\pi$ state. For CO_2, no significant contamination of the (0,1) Cameron band is observed. If the longer $a^3\pi$ lifetime (∿7 ms) now consistent with the measurements on CO is adopted, then Ajello's emission cross section for the excitation of the Cameron bands by electron impact on CO_2 must be increased by nearly a factor of seven to ∿7×10^{-17} cm^2 at 80 eV.

[1]J. M. Ajello, J. Chem. Phys., 55, 3158, 1971.

CA-5 Electron Excitation of the Xenon and Krypton Atoms* - FRANCIS A. SHARPTON,† JOHN E. GASTINEAU, L. W. ANDERSON, and CHUN C. LIN, Univ. of Wisconsin-Madison.--Electron excitation functions for the levels of the $5p^5ns$, $5p^5np$, $5p^5nd$, and $5p^5nf$ configurations of xenon and of similar groups of krypton have been measured from threshold to 200 eV. For the ns and nd families of xenon the excitation functions exhibit a broad maximum at about 60 eV for most of the J=1 levels whereas a sharp peak near the threshold is found for levels with J=0, 2, 3, 4. In the case of the np group, the J=0 levels show a peak of intermediate width and all the other levels (J=1, 2, 3) show narrow peaks of varying degree. The nf levels have much smaller cross sections; the shape of the excitation functions is, however, qualitatively similar to that of the np levels. The peak cross sections for the $5p^56p$ group of levels of xenon are in the range of 2×10^{-18} to 50×10^{-18} cm^2 and are much larger than those of the $2p^53p$ levels of neon.

*Supported in part by the Air Force Office of Scientific Research.

†Present Address: Northwest Nazarene College, Nampa, ID.

CA-6 Ionization and Dissociative Excitation of N_2 by Electron Impact on the Metastable $N_2(A^3\Sigma_u^+)$ State - M. R. GORMAN and E. C. ZIPF, Univ. of Pittsburgh.--Evidence is presented which shows that the processes

$$e + N_2(A^3\Sigma_u^+) \rightarrow N_2^+(B^2\Sigma_u^+) + 2e \qquad (1)$$

and

$$e + N_2(A^3\Sigma_u^+) \rightarrow N(^3P) + N + e \qquad (2)$$

are highly efficient at low electron-bombardment energies (<20 eV). Because metastable $N_2(A^3\Sigma_u^+)$ molecules are formed copiously by electron impact on N_2 at these energies, processes (1) and (2) provide an important mechanism for dissociating and ionizing nitrogen by electrons with energies well below the "normal" threshold. Preliminary data suggest that the cross sections for processes (1) and (2) at 20 eV are $>5 \times 10^{-17}$ cm^2. These results imply that the total cross section for the ionization and dissociation of the $N_2(A^3\Sigma_u^+)$ state by electron impact could be more than an order of magnitude larger than the above lower limit. Thus, the metastable $N_2(A^3\Sigma_u^+)$ state may play a pivotal role in the ionization and dissociation balance in ordinary gaseous discharge in N_2 while the family of processes typified by (1) and (2) may represent a serious loss mechanism for electron-pumped lasers using the $N_2(A^3\Sigma_u^+)$ as an energy intermediary.

CA-7 Kinetics of NH Created Vibrationally Excited in Electron-Irradiated N_2/H_2 Mixtures - B.D. GREEN and G.E. CALEDONIA, Physical Sciences Inc.*--Infrared radiation centered near 3 μm is observed when mixtures of nitrogen/trace hydrogen are irradiated with 40 keV electrons. This radiation arises from the fundamental vibration band of NH ($\Delta v=1$). Fluoresence from vibrational levels up to v=3 are observed; the individual rotation levels of each vibrational transition are clearly resolved, permitting a definitive species identification. Candidate formation mechanisms for NH under these conditions will be discussed in light of both symmetry and energy constraints. The spectrally resolved relaxation history of the NH fluorescence was monitored utilizing the technique of time resolved Fourier spectroscopy. The results of these observations will be presented.

*Supported by the Air Force Geophysics Laboratory through USAFOSR Project 2310G409 and DNA sub-task I25BAXHX 632.

SESSION CB

1:30 P.M., TUESDAY, OCTOBER 20, 1981

ROOM B

XENON HALIDE LASERS

CHAIRPERSON: S.F. FULGHUM

AVCO EVERETT RESEARCH LAB., INC.

CB-1 Influence of the Pulse-Forming-Network upon XeCl Laser Discharge Kinetics* - D. F. GROSJEAN, Systems Research Laboratories, Inc.,--A strong interaction exists between the pulse-forming-network and the kinetics of rare-gas-halide discharge-excited laser mixtures. Computer analysis employing a Boltzmann code for kinetic rates and an electrical-circuit code with particle-conservation equations pertinent to a He/Xe/HCl gas mixture is used to demonstrate the effects of voltage-fed, current-fed, and constant-impedance-fed discharges upon charged-particle production and losses. Although a short voltage rise time is necessary for the prevention of an ionization instability, the current rate-of-rise is most critical in determining the discharge characteristics. The mixture-weighted ionization-rate coefficient during the steady-state discharge phase, and thus the steady-state E/N, is determined by the density of easily ionizable metastables created during the electron-number-density (n_e) growth period at elevated values of E/N. On the other hand, the two-step mixture-weighted attachment-rate coefficient in the steady state is approximately independent of the growth rate of n_e.

*Work supported by AFWAL/AFAPL, Wright-Patterson AFB, OH.

CB-2 Vibrational Excitation of HCl in Ar/HCl, Ar/Xe/HCl and Ne/Xe/HCl Mixtures under Electron Beam Irradiation.* R.E.CENTER**, J.H.JACOB***, M.ROKNI and Z.ROZENBERG, Hebrew University of Jerusalem -- Recent measurements of the electron attachment rate coefficient to HCl have suggested that the e-beam pumped XeCl laser may not be attachment dominated contrary to the interpretation of current kinetic models. These measurements imply a small contribution of vibrational excitation of the HCl to the net attachment rate. In order to independently investigate this, experiments have been performed to directly measure the concentration of $HCl^{\dagger}$ in gas mixtures under e-beam excitation conditions similar to those in e-beam pumped XeCl lasers. The results indicate at most 6% excitation to the first vibrational level, a value too low to lead to the tenfold enhancement predicted by existing XeCl kinetic models. This implies the need to modify the laser models to allow for lower negative ion densities while maintaining the same excimer production rate.

* Supported by US-Israel Binational Science Foundation

** Lady Davis Fellow on leave of absence from M.S.N.W.

*** On leave of absence from AERL

CB-3 Ion Chemistry in XeCl Laser Mixtures - J. B. LAUDENSLAGER and V. G. ANICICH, Jet Prop. Lab., Caltech - The XeCl laser is produced primarily by the recombination reaction of Xe^+ with Cl^-. In an electron-beam excited XeCl laser with Ne buffer, the initial excitation produces Ne^+ which is rapidly converted to Ne_2^+. The bimolecular reactions of Ne^+ and Ne_2^+ with Xe are too slow to produce Xe^+ efficiently, but the termolecular charge transfer of Ne_2^+ with Xe has been identified as a rapid reaction loss mechanism for Ne_2^+.[1] In this paper, we report on the thermal energy bimolecular ion reactions occurring in Ne/Xe/HCl mixtures studied using an ion cyclotron resonance mass spectrometer. From these studies an efficient reaction channel for Ne_2^+ and Ne^+ with HCl followed by charge transfer of HCl^+ to Xe has been identified and the reaction rate coefficients measured. This kinetic pathway not only can convert Ne_2^+ and Ne^+ to Xe^+ efficiently, but may also provide a source of vibrationally excited HCl which is a precursor for Cl^-.[2]

[1] C. B. Collins and F. W. Lee, J. Chem. Phys. 72, 5381 (1980).

[2] M. Allan and S. F. Wong, J. Chem. Phys. 74, 1687 (1981).

CB-4 $XeCl^*$- and Xe_2Cl^*-Laser Kinetics - G. MAROWSKY, MPI biophys. Chemie, Göttingen, FRG; F.K. TITTEL, W.L. WILSON, G.P. GLASS, E.E. Dept., Rice Univ., Houston, TX*--Processes leading to the decay of the diatomic excimer $XeCl^*$ and production and removal of the triatomic excimer Xe_2Cl^* subsequent to short duration electron beam excitation of $Ar/Xe/CCl_4$ mixtures have been investigated. The radiative lifetimes of $XeCl^*$ and Xe_2Cl^* have been measured to be 41 and 135 ns respectively. Collisional decay of $XeCl^*$ occurs with a rate constant $k_1(Ar,Xe) \approx 10^{-30}$ $cm^6 s^{-1}$ due to an unidentified intermediate product. Formation of Xe_2Cl^* is also characterized by a termolecular reaction involving $XeCl^*$. Rate constants for collisional quenching of $XeCl^*$ and Xe_2Cl^* by CCl_4 and the rare gases have been determined.

*This work was supported by the Office of Naval Research, The Robert Welch Foundation, and The National Science Foundation.

CB-5 Transient Absorption of Picosecond Pulses in a 5 J UV-Preionized XeCl Laser - R. S. TAYLOR, P.B. CORKUM and A.J. ALCOCK, National Research Council -- Approximately 2ps duration UV laser pulses were used to measure the transient absorption (at ~311nm) and gain in a wide aperture 5J UV-preionized XeCl laser. Absorption measurements were performed with optimized lasing mixes using both He and Ne buffer gases as well as for many of the component gases. For certain measurements the time dependence of the absorption was correlated with the discharge voltage and current waveforms as well as with the temporal gain profile obtained at 308nm. For He based gas mixes the absorption progressively increased throughout the discharge to a value of ~0.5%/cm at the peak of the gain and to ~2%/cm near the termination of power deposition. Neon based mixes showed a similar trend to increased absorption throughout the discharge however, the absorption coefficient was four times smaller than for He. The implications of these measurements on ps energy extraction experiments and on experiments to produce high output energy, long optical pulse duration ($\geq$ 100 ns) XeCl laser operation will be discussed.

CB-6 Self-Sustained XeF Laser Discharge Characteristics- L. J. DENES and L. E. KLINE, Westinghouse R&D* -- We have studied U. V. preionized self-sustained discharges in NF_3:Xe:He mixtures at 1000 Torr. The 300 ns discharges are homogeneous and quasi-steady so we can measure E/N, the electric field-to-gas density ratio. E/N increases by a factor of 4 as the NF_3 content, $[NF_3]$ increases from 0.001 to 0.3% and is insensitive to [Xe]. E/N decreases by 15% when the current density, j increases from 5 to 160 A/cm^2 and is constant for j<5 A/cm^2. The measured E/N values agree well with the predictions of a rate equation model which balances electron production by one-step, two-step and Penning ionization against electron loss by attachment and recombination. The electron collisional rates are calculated by solving the Boltzmann equation. The calculations include momentum transfer, electronic excitation and ionization for all three species and attachment to NF_3. Agreement with experiment is obtained only by including a large cross section (10^{-16} cm^2 at 10eV increasing to 10^{-15} cm^2 at 15eV) for the electronic excitation of NF_3. The decrease in E/N vs. j is consistent with the two-step ionization rate coefficient value $k_2=10^{-8}$ cm^3/s.

*Work supported in part by U. S. Army BMDATC.

CB-7 Kinetics of Discharge Pumped XeF* Lasers - L. E. KLINE and L. J. DENES, Westinghouse R&D* -- Discharge voltage and current waveforms, XeF* B→X and C→A fluorescence waveforms and efficiencies, and laser onset times, pulse shapes and efficiencies have been measured and predicted. The experiments used 8 cm long self sustained discharges in NF_3:Xe:He mixtures. A rate equation model which predicts the densities of 12 charged and neutral species vs. time was used for the analysis. The following quantities were determined by comparing theory and experiment. Two Xe* decay channels were identified from the XeF* fluorescence decay rates: i)reaction with NF_3 to form XeF* with a rate coefficient $k=6x10^{-10}$ cm^3/s and ii)quenching by unidentified species at a rate $6x10^6$ s^{-1}. The measured variation of the XeF* B→X/C→A fluorescence ratios with the current is consistent with XeF* quenching by electrons with a rate coefficient $k=7x10^{-8}$ cm^3/s. The measured laser onset times and efficiencies are consistent with a stimulated emission cross section (appropriate to our single line laser model) of $3x10^{-16}$ cm^2.

*Work supported in part by U. S. Army BMDATC.

CB-8 Multiline Model for XeF Laser Parameters D.A. COPELAND, J.A. BLAUER, and C. E. TURNER, JR., Rockwell Int./Rocketdyne, Canoga Park, CA 91304 - A steady-state simplification of the rate equations for a three-line XeF laser model is discussed. The model retains 6 and 3 vibrational sublevels of the X and B states, respectively. Level decay by radiation, dissociation, and collision into states of lower energy is included. The e-beam pumping reactions deposit XeF(B,v) molecules into states above v=2. The cross-sections for stimulated emission are estimated from molecular physics and spectroscopy. The temperature-dependent vibrational state mixing parameters were obtained by comparison with published gain data. The model has been used to estimate gain and saturation parameters at three principal laser wavelengths. The model clarifies the kinetics origin of the potential for improved laser performance at higher temperatures although absorption effects must be accounted for to predict observed intrinsic efficiencies (E_{Laser}/E_{Dep}). The significance of these results to the future development of this laser system is discussed.

CB-9 NF_2 Radicals as Halide Donors for XeF Lasing Experiments*- D.W. TRAINOR and J.H. JACOB, Avco Everett Res. Lab., Inc., Everett, MA. -- Experiments have been carried out using electron beam excitation of mixtures containing neon, xenon and NF_3, N_2F_4 or NF_2 to determine the relative suitability of these fluorine containing components to act as donors for xenon fluoride lasers. Fluorescence and laser output were observed at various pressures, temperatures, and current intensities for a variety of laser mixtures. From these results, one can obtain qualitative information regarding the formation and quenching kinetics of these donors.

*This work was supported by IRAD and by the Defense Research Projects Agency under Contract F33615-80-C-2060 and monitored by the Air Force Aeronautical System Division.

SESSION D

3:30 P.M., TUESDAY, OCTOBER 20, 1981

ROOM B

MERCURY BROMIDE LASERS

CHAIRPERSON: E.J. SCHIMITSCHEK
NAVAL OCEAN SYSTEMS CENTER

D-1 Kinetics of the Sustained Discharge HgBr Laser - M. McGEOCH, J. HSIA, D. KLIMEK, Avco-Everett Research Laboratory, Inc., Everett, Massachusetts -- New experimental data will be presented on the following aspects of the discharge HgBr laser system: the direct excitation process $HgBr_2+e^- \rightarrow HgBr^*(B)+Br+e^-$, including formation efficiency and dependence on E/N in different buffer gases; measurement of the laser gain; measurements of absorption of HgBr (X) and $HgBr_2^+$ species; electron quenching; lower level deactivation; discharge impedance and the dependence of discharge energy loading upon the electron beam current density. A computer model of the HgBr laser will be discussed which accurately predicts the observed laser performance.

D-2 A 1.8 Joule, X-Ray Preionized HgBr Laser - C.H. FISHER, I. SMILANSKI, T. DeHART, J.P. McDANIEL, and J.J. EWING, MSNW* --We have used x-ray preionization to uniformly excite a large volume 5 x 4.5 x 100 cm^3 electric discharge HgBr laser (λ = 502 nm). The optimum operating conditions were 4 atm Ne/10 torr $HgBr_2$ at T = 190 °C. The laser energy increased with increasing pressure or charge voltage. The maximum energy obtained was 1.8 J at 1.4 percent efficiency with respect to the energy stored on the pulse forming line. Lower charge voltages resulted in lower output energies but higher efficiencies. The best efficiency was 1.7 percent for an output energy of 1.4 J.

*Supported by DARPA Contract N00123-80-C-1136.

D-3 A Kinetic Model for Electric Discharge HgBr Lasers - A.L. PINDROH, J.J. EWING and C.H. FISHER, MSNW* --A kinetic model has been developed in order to predict the performance and to aid in scaling discharge excited HgBr lasers. The energy partitioning and electron rate constants are calculated by solving the Boltzmann electron transport equations as a function of electric field strength. A curve fit of these results is then used as input to the coupled laser kinetics and circuit code. The code was validated by comparing to the 55 cm HgBr laser reported by Schimitschek and Celto.[1] The code predictions were then compared with the experimental results obtained with the 1.8 J x-ray preionized HgBr laser described in the accompanying paper.

*Supported by DARPA contract N00123-80-C-1136.

[1]E.J. Schimitschek and J.E. Celto, Appl. Phys. Lett. 36, 176 (1980).

D-4 Electron Collision Processes in $HgBr_2$ - J. J. HINCHEN, W. J. WIEGAND AND W. L. NIGHAN - United Technologies Research Center - A pulsed electron swarm experiment has been used to measure electron drift velocity and the rate coefficients for attachment and ionization in various rare gases containing $HgBr_2$. Data were obtained for total pressures of a few tenths of an atm and over an order-of-magnitude variation in E/n. Using previously determined $HgBr_2$ cross sections for attachment and ionization, along with trial cross sections for vibrational and electronic excitation, the Boltzmann equation was solved iteratively until satisfactory agreement was obtained between the experimental and computed values of drift velocity and the ion production coefficients. The $HgBr_2$ cross sections for vibrational and electronic excitation yielding the best agreement with experiment are relatively large ($\sim 10^{-16} cm^2$). Calculations show that both processes, particularly the latter, exert a significant influence on medium characteristics for conditions typical of the HgBr(B)/$HgBr_2$ dissociation laser.
Supported in part by the Naval Ocean Systems Center and by the Office of Naval Research.

D-5 Electron Attachment and Fluorescence of $HgBr_2$ - Rare Gas Mixtures - H.L. BROOKS§, K.J. NYGAARD, L. FROST+, J. FLETCHER+, and E. WEIGOLD+, University of Missouri-Rolla.*--Electron drift velocities and production of negative and positive ions in Ne, Ar, or Xe with 0.01-0.2% $HgBr_2$ have been measured. In all buffer gases studied, the electron drift velocity increases with $HgBr_2$ concentration. Rate coefficients for total ion production have been measured for E/N = 1-100 Td with buffer gas pressures ranging from 15-200 Torr. The integrated current measurements were supplemented with side-light photon flux counting data to investigate possible attachment mechanisms.

§Present address: DePauw University, Greencastle, IN 46135.
+Address: The Flinders University of South Australia, Bedford Park, S.A. 5042.
*Supported in part by Office of Naval Research.

D-6 Bound-Bound and Bound-Free Fluorescence from $HgBr(B^2\Sigma^+)$: The $B^2\Sigma^+ - X^2\Sigma^+$ and $B^2\Sigma^+ - A^2\Pi$ Transitions - W.P. LAPATOVICH, G.R. GIBBS, and J.M. PROUD, GTE Labs--Incoherent ultraviolet light in the 200 nm region has been used to photodissociate $HgBr_2$ vapor contained in a temperature stabilized ($\pm$5°C) quartz cell (1 cm^3). Typical densities of $HgBr_2$, 1.26 x 10^{16} cm^{-3} at 398 K are maintained. The photofragment HgBr is left preferentially in the excited electronic $B^2\Sigma^+$ state when photodissociation of the parent molecule, $HgBr_2$, is accomplished by short-wavelength UV. The consequential and well known bound-bound fluorescence of the $HgBr(B^2\Sigma^+ - X^2\Sigma^+)$ transition has been seen with a resolution of 0.95 nm using an optical multichannel analyzer (PAR-OMA 2). Low level undulations approximately 100 nm to the red of the $B^2\Sigma^+ - X^2\Sigma^+$ transition at 501.8 nm have also been observed. These structures are attributed to bound-free fluorescence, $HgBr(B^2\Sigma^+ - A^2\Pi)$, since the $A^2\Pi$ state is completely repulsive. The reduced intensity of the bound-free fluorescence as compared to the bound-bound transitions ($\sim$1:1000) corroborates calculations indicating a much reduced transition matrix element for the $B^2\Sigma^+ - A^2\Pi$ system. Interpretation of the observed undulatory structures provides physical insight into the nature of the repulsive $A^2\Pi$ states.

D-7 Photodissociation of HgBr, $X\Sigma 1/2$ - M. KRAUSS and W. J. STEVENS, National Bureau of Standards.*--Transition moments and energies have been calculated for the X-A, bound to continuum, transition in HgBr. Absorption at the laser wavelength of 502 nm has been examined for two cases: 1. A thermal distribution of vibrational levels at 500°K, and 2. The terminus vibrational level of the B-X laser transition. In the first case a cross section of $7 \cdot 10^{-20}$ cm^2 is calculated. Since no fast reaction for removal of the X state is known, the number density can exceed 10^{16} cm^{-3} and a significant absorption will result in late times. In the second case the laser photon can be coherently absorbed in the X-A transition leading to photon induced predissociation of the v=0, B state. An upper bound to the predissociation rate for a 2 MW/cm^2 flux is 10^6 s^{-1}.

Electron dissociative attachment of the X state is also shown to be improbable as a means of fast removal. Energy curves of the ground state of both the neutral and negative ion of HgBr are shown not to cross in any accessible region.

*Supported in part by the Defense Advanced Research Projects Agency and monitored by the Office of Naval Research under contract No. N00014-81-F-0020.

SESSION E

8:00 P.M., TUESDAY, OCTOBER 20, 1981

ROOM B

WORKSHOP ON KINETIC PROCESSES IN BLUE-GREEN LASERS

This workshop will focus on fundamental kinetic processes occuring in the 502 nm HgBr(B)/$HgBr_2$ dissociation laser, and in the 308 nm XeCl laser, the latter a prime candidate for wavelength conversion to the visible region of the spectrum. Attention in the formal portion of the workshop will be directed toward recent advances in understanding electron dissociative attachment to vibrationally excited HCl (the Cl donor in XeCl lasers), and electron impact dissociative excitation of $HgBr_2$. Ample time has been provided for general discussion of these topics as well as other subjects relevant to these lasers.

CHAIRPERSON: W.L. NIGHAN

UNITED TECHNOLOGIES RES. CENTER

VIBRATIONAL EXCITATION AND DISSOCIATIVE ATTACHMENT OF HCl BY ELECTRON IMPACT

A. HERZENBERG

DISSOCIATIVE EXCITATION OF $HgBr_2$ BY ELECTRONS

M. MCGEOCH

GENERAL DISCUSSION

SESSION FA

9:00 A.M., WEDNESDAY, OCTOBER 21, 1981

ROOM A

ARCS III

CHAIRPERSON: D.K. DAVIES

WESTINGHOUSE R&D CENTER

FA-1 Effect of Electrode Temperature on DC Breakdown in Vacuum* - D.B. LOWE and D.T. TUMA, Carnegie-Mellon University, D.K. DAVIES, Westinghouse R&D Center -- Measurements of prebreakdown current and dc breakdown voltage between uniform-field copper electrodes in vacuum ($\sim 10^{-9}$ Torr) have been made as a function of both the initial cathode and anode bulk temperature. These measurements have been carried out for electrode separations in the range 0.1 to 0.5 cm and electrode initial temperatures from 300°K to 800°K. Estimates of the surface temperature of both the anode and cathode at the onset of breakdown have been determined from the data. The results indicate that breakdown is associated with the thermal instability of a region of the anode surface when that region attains a temperature close to the melting point. This confirms the conclusion drawn from previous measurements[1] over an extended range of experimental conditions.

*Supported in part by NSF, Grant ECS-7908417.
[1]D.K. Davies and M.A. Biondi, J. Appl. Phys. 39, 2979 (1968).

FA-2 Dependence of Dielectric Recovery Field of Vacuum Gaps on di/dt and Recovery Voltage Frequency - R. E. VOSHALL, and D. BHASAVANICH, Westinghouse R&D Center.-- The high frequency transient and the low frequency recovery voltage breakdown characteristics of a vacuum gap following low magnitude (< 2 kA) high frequency (32 kHz) reignition arcing currents were studied using vacuum interrupters. Recovery data following interruption of 32 kHz reignition currents for CuCr and CuBi electrodes were compared with those taken with a circuit that generated a recovery voltage following a 60 Hz current interruption. These measurements were performed on interrupters after being arced with 20 kA (rms) power currents. Results show that the average breakdown low frequency electric field following a 32 kHz current interruption is about the same as that following a low current (< 1 kA) 60 Hz current. The low frequency breakdown fields for arced CuCr electrodes is a factor of 3 greater than that of arced CuBi electrodes. In all cases, H.F. recovery voltages result in reduced breakdown fields due to the presence of residual plasma.

FA-3 Density Population of Zn I, Zn II Excited States in Multi-Cathode-Spot Vacuum Arcs.- S.GOLDSMITH, Y.BRESLER and R.L. BOXMAN, Tel-Aviv U.*. -- The density of excited states of ZnI and ZnII in a multi-cathode-spot vacuum arc between zinc electrodes was determined spectroscopically be measuring the absolute intensity of spectral lines. The arc was run between two cylindrical electrodes (diameter 1.4 separation 0.4 cm). The current lasted for 1.75 ms with peak current of 1.2 KA at t=0.3 ms. Excited state densities were studied as function of time and distance from the cathode. The observations presented here are (1) measured densities (2) spatial dependence of excited state densities and (3) the dependence of t-time of peak density - on the distance from cathode. For Zn I we observe peak density of excited states when the arc current is decaying. Peak density of Zn II lines occur near peak current. The density of Zn I is estimated to be few percent of Zn II.

* Supported in part by the U.S.-Israel Bi-National Science Foundation (BSF) and in part by the Israel Academy of Science.

FA-4 Retrograde Motion of Arc Spots on Copper Cathodes in Vacuum. L.P. HARRIS, General Electric Corp. R&D.--The parameters calculated in an earlier analysis[1] of the operation of stationary copper cathode spots are used together with the mechanism proposed by Longini[2] to calculate the retrograde velocities of cathode spots in the presence of small transverse magnetic fields. For large magnetic fields, the spot velocity is taken at the limit set by the requirement that the hemispherical volume under the spot surface must be heated as the spot moves. Matching of these two calculations gives a piecewise linear approximation to the velocity vs. field function that agrees qualitatively with recent measurements on several cathode materials, and quantitatively with measurements by Sherman et al.[3] for copper.

[1] L.P. Harris, 8th Int. Symp. on Disch. and Ins. in Vac., Albuquerque, NM (1978).
[2] R.L. Longini, Phys. Rev. 71,642(1947).
[3] J.C. Sherman et al., J. Phys. D: Appl. Phys. 8, 696(1975).

FA-5 Surface Melting of Vacuum Arc Cathodes in Areas Remote from Cathode Sports - P.TALARICO, R. DOLLINGER, D. DETTMAN, A.S. GILMOUR, JR., and M. NIKOLICH, St. U. of NY at Buffalo.* -- Several different metals were used as small diameter (1 cm) cathode rods which have a common axis with a large diameter, (18 cm) hollow-cylinder, anode. [1] SEM photos of different cathodes show normal cathode spot erosion at the rod edge where they are symmetrically distributed[1,2]. On the flat end of the rod, where no spots existed, only molten puddling is observed. It is estimated that the high energy ions accelerated away from the repetitive growth of the anode sheath [1] would have insufficient energy to contribute to the melting of the flat end. These high energy ions are probably the cause of the luminous zone above the cathode that were seen in the high speed movie (100-150 μs/frame) shown by Burrage [3].

*Supported in part by Electric Power Research Institute (EPRI) and Sandia Laboratories.

[1] Gilmour and Dollinger, EPRI's RP 993-1, (late 1981) and Plasma Science, PS-8, p.302 (1980).
[2] Burrage and Pedrow, EPRI's RP 1140, McGraw Edison Box 100, Franksville, WI 53126.
[3] Shown at Vacuum Arc Workshop, 31th GEC (1978).

FA-6 Electrical Discharges Along Thin Ribbons of Titanium Deuteride,* G. W. MC CLURE and J. A. WEBB, Sandia National Laboratories--In light ion beam fusion accelerators it is planned to employ magnetically insulated plasma diodes operating at megavolt potentials and having distributed plasma sources on large area anodes from which ions are extracted for acceleration to a fusion target. One version of this device requires an areal density of ions of $3 \times 10^{15}/cm^2$ developed in an interelectrode space of 1 cm. Attempts have been made to generate plasmas of this density using 40 ns, kiloampere discharges through thin ribbons of titanium deuteride deposited on an alumina ceramic substrate. Arrays of nine parallel ribbons on one-inch square substrates have been studied at total currents from 2 to 8 kA. Configurations using continuous ribbons and gap-interrupted ribbons were studied. Although their plasmas are quite different in appearance, both appear to be limited to a fluence of 3×10^{14} ions/cm^2 which does not increase significantly with drive current above 8 kA. The principal cause of the limitation is shunting of the power supply current out of the ribbon and into the surface plasma sheet at times of 10 to 20 ns thereby arresting the heating of the ribbon and stopping arc operation in the gaps.
*This work was supported by the U. S. DOE.

FA-7 Investigation of Constricted Metal Vapor Arc Columns at High Currents - D. BHASAVANICH, and Y. K. CHIEN, Westinghouse R&D Center -- Electrical and spectroscopic properties of a metal vapor arc column have been investigated at currents of 10-30kA and 10^{-6} Torr ambient pressure. The columns were formed between OFHC copper electrodes having 100mm dia. anode and 60mm dia. cathode, by electrode separation at a speed of 2mm/ms. Electrode gap was kept to <5mm to maintain the arcs in a columnar mode. Measurements were obtained on arc voltages, currents, and electrode gaps. Arc column diameters were obtained from high speed movies. Spectroscopic measurements using a gated exposure of $\sim$ 100μs were made on emission spectra for the wavelength range of 490-530nm. Using assumptions of a cylindrical arc geometry with uniform radial pressure and temperature distributions, the electrical conductivity (σ) and the self-magnetic compression (P) were estimated at 40-80 mho/cm and several atmospheres respectively. With an additional assumption of LTE, the plasma temperature was estimated to be <1eV by two methods, (1) using ratios of emission lines of CuI at 510.5, 515.3, and 521.8nm, (2) using values of σ and P to estimate T. Results on σ, P, and T form a basis for characterization of the high current metal vapor arcs in the plasma column region.

FA-8 The Anode Region in a Uniform Multi-Cathode-Spot Vacuum Arc -R.L. BOXMAN and S. GOLDSMITH, Tel-Aviv U. An analysis is performed on the anode region of a multi-cathode-spot vacuum arc using a first order approach, in which a zero-order model of the plasma flow generated by the cathode spots is utilized, together with the assumption that the influence of the anode generated plasma is small. It is noted that the space charge sheath adjacent to the anode surface is collisionless, and for realistic values of the electron temperature (T_e >0.7 eV for Cu) the anode potential ϕ_A must be negative with respect to the adjacent neutral plasma in order to insure current continuity. ϕ_A and ϕ_E, an effective anode drop for heat transfer, are calculated for various materials and electron temperatures. For a 3 eV Cu arc, they have values of -2.5 and 18.0 V respectively. A significant electric field may be present at the anode surface, having a value of 0.8×10^8 V/m for a 10^7 A/m^2, 6 eV, Cu arc. Neutral emission processes from the anode surface are considered. Evaporation may be neglected if the arcing time is short compared to a critical time having a value of 64 ms in the case of a 10^7 A/m^2, 3 eV Cu arc. Sputtering, however, yields a neutral density in the vicinity of the anode equal to 37% of the unperturbed Cu ion density.

SESSION FB

8:45 A.M., WEDNESDAY, OCTOBER 21, 1981

ROOM B

VISIBLE AND UV LASERS

CHAIRPERSON: L.J. DENES

WESTINGHOUSE R&D CENTER

FB-1 Discharge Effects on a XeCl Pumped S_2 Heat Pipe Laser - K.E. GREENBERG, K. KILLEEN, and J.T. VERDEYEN, Gaseous Electronics Laboratory, U. of Illinois, Urbana, IL 61801*--Although sulfur has a vapor pressure of a few Torr at a reasonable temperature of 200°C, most of the vapor consists of the higher order molecules, S_{3-8}, with an insignificant fraction of dimers. Using a simple electrical discharge, however, the higher order molecules can be effectively dissociated into S_2, creating the proper environment for converting XeCl pump radiation at 308 nm to laser radiation in the blue-green. The S_2 vapor is pumped by the XeCl radiation on the $v'' = 2$ to $v' = 5$ of the B-X transition and lases on the $v' = 5$ to $v'' = 19$-22 transitions in the blue-green. Using a simple 60 cycle AC discharge circuit in a sulfur heat pipe configuration, conversion efficiencies of $\geq$ 1% have been achieved.

*Work supported by Office of Naval Research.

FB-2 Kinetics and Line Tunability of the Discharge Pumped IF Laser† - M.L. DLABAL* and J.G. EDEN, U. of Illinois--Dye laser absorption spectroscopy has been used to monitor the temporal behavior of the $I^*(^4P_{5/2})$ and $F^*(^4P_{1/2,3/2,5/2})$ densities in the discharge pumped IF laser. From these measurements, it is concluded that (as was the case for e-beam excitation of IF*)[1] the $I^*(^4P)$ species is the immediate precursor of the IF upper state (D') and that the energy stored in the ^4P states of flourine is not recovered as useful output. Also, by probing the plasma at 490.7 and 484.7 nm, the rate constants for quenching of the lower laser level (A',v'') by He, CF_3I and NF_3 were found to be $(1.5 \pm 0.4) \cdot 10^{-12}$, $(7.6 \pm 1.5) \cdot 10^{-10}$ and $(6.9 \pm 3.5) \cdot 10^{11}$ cm^3-sec^{-1}, respectively. Limited line tunability of the IF laser using a Littrow prism will also be discussed.

†Work supported in part by AFOSR.
*Present address: Laser Physics Branch, Naval Research Laboratory, Washington, D.C. 20375.

[1] S.B. Hutchison, J.T. Verdeyen and J.G. Eden, J. Appl. Phys. 52 (1981).

FB-3 Long Pulse XeCℓ Laser Pumped by an Electron Beam Assisted Discharge. - B. FONTAINE, B. FORESTIER and C. PERRY, Institute of Fluid Mechanics, Aix-Marseille U. 13003 Marseille, France.* -- Long pulse (200 ns FWHM) XeCℓ excimer laser emission (λ = 308 nm) has been achieved following excitation of Ne/Xe/HCℓ mixtures by an electron-beam assisted discharge either at room temperature or at very low temperature. Most of the energy was added to the medium by means of a simple spark-gap-triggered capacitor with a relatively high circuit inductance (L# 100 nH). Stable discharge was allowed during several hundred nanoseconds for conditions where discharge energy E_D was several orders of magnitude higher than absorbed e-beam energy E_G and where the energy loading was high (> 100 j/ℓ/atm). Maximum specific laser energy was over 3 j/ℓ at room temperature for 1.5 atm pressure and a volume of 100 cm^{-3} and varied only slowly when changing the E_D/E_G ratio.

*Supported by French DRET

FB-4 Long Pulse X-ray Assisted Discharge XeCℓ Laser- B. FORESTIER, B. FONTAINE and M. SENTIS, Institute of Fluid Mechanics, Aix-Marseille University, 13003 Marseille, France.* -- Long pulse (160 nm FWHM) XeCℓ excimer laser emission (λ = 308 nm) has been achieved following excitation of Ne/Xe/HCℓ mixture by an X-ray assisted discharge. Most of the energy was added to the medium by means of a simple spark gap triggered capacitor with a relatively high circuit inductance (L# 100 nH). When firing the discharge several hundred nanoseconds even for high energy loading (>100 j/ℓ/atm). Specific laser energy was over 1.5 j/ℓ at room temperature for 800 torrs pressure and 70 cm^{-3} useful volume (30 cm gain length), and varied only slowly when changing X-ray beam intensity. X-ray assisted discharge pumping will be discussed and compared with e-beam assisted discharge pumping in the frame of high average power high repetition rate excimer lasers development.

*Supported by French DRET

FB-5 KrF* Short Pulse Studies - A. MANDL, J. H. PARKS and D. KLIMEK, Avco Everett Research Laboratory, Inc.†--A short pulse (200 nsec) high current (~50 A/cm^2) KrF* 1 m laser has been built and used to measure laser and fluorescence efficiency and sidelight suppression as a function of temperature, pressure, current, output coupling and gas composition. The measurements have been used to construct a model for the KrF* system. The measurements, with comparison to our model, will be discussed.

†Supported by U. S. Department of Energy Contract #DE AC08-80DP40130

FB-6 Vibrational Relaxation and Laser Extraction in KrF--W.L. MORGAN, N. WINTER, K. KULANDER, Lawrence Livermore Lab*-- It has been demonstrated experimentally[1] that the finite rate of vibrational relaxation in the formation of KrF affects the saturation characteristics of the KrF(B) state during extraction of laser light. We have assembled a collisional radiative model using calculated Einstein A coefficients for twenty KrF states and a collisional model for vibrational energy transfer between KrF and a buffer gas. The model describes the flow of excitation through the vibrational levels of KrF. We will present model calculations demonstrating the effects of vibrational relaxation on KrF(B) saturation and spectra. The results of these calculations agree qualitatively with the measurements of Ref. 1. In addition, we find that, due to the relaxation kinetics of KrF, Kr_2F, a major absorber is not truly saturable.

*Work supported by the University of California, Lawrence Livermore Laboratory under DOE Contract #W-7405-ENG-48.

[1]J.H. Jacob, D.W. Trainor, M. Rokni, and J.C. Hsia, Appl. Phys. Lett., 37, 522 (1980)

FB-7 Study of KrCl(B) and Kr_2Cl Excited State Kinetics Using Synchrotron Radiation Excitation, M. G. DURRETT, L. HOUSTON, and G. K. WALTERS, Rice University, Houston, Texas and K. Y. TANG, D. C. LORENTS, and D. L. HUESTIS, SRI International, Menlo Park, California 94025,--Formation and decay of $KrCl/Kr_2Cl$ excited states have been studied by following the time decay of $KrCl^*(B)$ and Kr_2Cl^* chemiluminescence. Cl_2^*, excited at 135 nm, reacts with Kr to form $KrCl^*$ and subsequently Kr_2Cl^*. The decay frequency of $KrCl^*$ B-state emission at 220 nm shows two-body dependencies on Cl_2 and Kr similar to those observed previously[1] along with a Kr^2 dependence ($\sim 4 \times 10^{-31}$ cm^6 sec^{-1}), presumably leading to Kr_2Cl^* formation. The Kr_2Cl^* emission, monitored at 340 nm, is strongly quenched by Cl_2 ($\sim 6.7 \times 10^{-10}$ cm^3 sec^{-1}), and has a long radiative lifetime (> 300 nsec).

[1]M. L. Castex, J. Le Calvé, D. Hacks, B. Jordan, and G. Zimmerer, Chem. Phys. Lett. 70, 106 (1980).

FB-8 Absorption Spectra of Ar_2F and Kr_2F - H. T. POWELL and K. S. JANCAITIS, Lawrence Livermore National Laboratory* --We have measured the electron-beam-excited absorption spectra of Ar/F_2 and $Ar/Kr/F_2$ mixtures at 2 atm pressure. The e-beam-excited gases were probed with several Stokes and anti-Stokes lines produced by stimulated Raman scattering of a KrF laser in either H_2 or D_2. We found broad absorption bands in these mixtures which peaked at 300 and 315 nm, respectively. Based on theoretical predictions[1] and our kinetic modeling, we attribute these absorptions to the excited molecules Ar_2F and Kr_2F. We are now determining the concentrations of these excimers using their fluorescence intensities. The absorption and density measurements should yield absolute cross sections for absorption by the excited trimer molecules.

*Work supported by the U. S. Department of Energy under contract number W-7405-ENG-48.

[1]W. R. Wadt and P. J. Hay, J. Chem. Phys. 68, 3850 (1978).

FB-9 Heavy Particle, Electron, and Radiative Quenching of Ar_2F and Kr_2F - K. S. JANCAITIS and H. T. POWELL, Lawrence Livermore National Laboratory* --The time dependence of fluorescence from both the rare gas halide dimer (XF) and trimer(X_2F) have been studied in electron-beam-excited Ar/F_2 and Kr/F_2 mixtures over a wide range of total pressures (500-2000 Torr), e-beam current densities (8-500 A/cm^2), and for varying fluorine concentrations. The trimer fluorescence signal exhibited changes with the current density and gas pressures not exhibited by the dimer where the quenching is dominated by its short radiative lifetime. At high current densities the trimer fluorescence approached steady state during the 50 ns current pulse with a rate greater than its decay after the pulse suggesting the importance of electron quenching for the trimer. To obtain quenching coefficients, we are fitting the trimer fluorescence to the solution of a simple differential equation with a source term proportional to the dimer fluorescence and with quenching caused by radiation, heavy particles, and electron collisions.

*Work supported by the U. S. Department of Energy under contract number W-7405-ENG-48.

SESSION GA

10:45 A.M., WEDNESDAY, OCTOBER 21, 1981

ROOM A

ARCS IV

CHAIRPERSON: R. KESSLER

AVCO EVERETT RESEARCH LAB., INC.

GA-1 The Influence of the Self-Magnetic Field on the Current Flow in Axi-symmetric Tensor Conductivity Plasma. - I.ISRAELI, R.L.BOXMAN, and S.GOLDSMITH, Tel-Aviv U.--The steady state electrical current field in a uniform conducting medium described by the tensor conductivity law was determined by the solution of the magnetic transport equation subject to imposed boundary conditions.This type of medium may model the interelectrode plasma of a vacuum arc where convection prevents material flow constriction. The equation for the bulk of the medium, including a self-consistent treatment of the local conductivity which varies with the local value of the magnetic field, was reduced to a single dimensionless scalar-nonlinear partial differential equation with the azimuthal magnetic field as the dependent variable and controlled by three parameters: R_m, the magnetic Reynolds number of the axial material flow, B_s, the magnetic Reynolds number describing the axial electron flow, and AR, the ratio of axial distance to radius. The medium is enclosed in a cylindrical insulating tube between two electrodes which were described either in terms of a given current distribution, or as an equipotential surface. For $(R_m,B_s,AR)=(-0.23,2.4,0.72)$ and a uniform current flow cathode, the axial anodic current density is 6 times the uniform value.

GA-2 Electrode Arcing Phenomena in MHD Generators - I. SADOVNIK, Avco Everett Research Lab., Inc., A. SOLBES TRW, and M. MARTINEZ-SANCHEZ, MIT*--The electrical discharge behavior of MHD electrodes in the open-cycle environment was experimentally and analytically investigated Voltage drops, heat fluxes, and high frequency behavior associated with the arcing phenomenon was studied. It was found that for slagging anodes under typical operating conditions, the characteristic MHD arc current was between 0.5 and 1 A. Cathode arcs under similar conditions are of 2 types: small and very mobile (running in the downstream direction), and large (2-3 A) and fixed at the downstream edge of the electrode. The boundary layer voltage drop of the arcing transport, increases continuously with current, but its slope decreases by a factor of 2 for large currents (>2 A). The extra heat flux due to the arcing transport for anodes increases linearly with current; while for cathodes it shows saturation at high current. Single anode arc foot electrode heat loads are around 30 W for clean wall conditions, and 60 W for slagging conditions. Optical observations show an anode arc radius between 0.1 and 1 mm. The large slagging cathode arcs can be a few mm in diameter.

*Supported by US DOE Contract EF-77-C-01-2519

GA-3 Plasmatron Simulation of MHD-Channel Conditions*-V. GOLDFARB, V. HRUBY, AND R. KESSLER, Avco Everett Res. Lab., Inc.--An arc heater was used to simulate conditions in a slagged-wall MHD-channel. Two phase (4 gs^{-1} nitrogen + 2.10^{-2} gs^{-1} ash and potassium seed), $4.10^{3}Jg^{-1}$ enthalpy flow through 2-4 cm^2 cross-section channels provided adequate heating ($\sim$150 Wcm^{-2}) and erosion rates (10-100 μgC^{-1}), slagging and conductivity (12 mho $\cdot$ m^{-1}). A transverse discharge (1-3 Acm^{-2}, 20-60 V) could be superimposed on the flow between sectioned anode and auxiliary cathode. Plasma parameters ($T=3.4\text{-}4.10^{3}K$, $N_e=3.10^{14}cm^{-3}$) were derived from emission measurements. Atomic absorption was used to measure metal concentration in situ and to monitor instantaneous erosion rates.

*This work supported by the United States Department of Energy under Contract DE-AC010-80-ET15614.

GA-4 MHD Channel Plasma Diagnostics - A.M. DEMIRJIAN, Avco Everett Research Lab., Inc.*--Average measurements of conductivities and Hall parameters in the AERL Mk VII Faraday MHD generator are presented. The sidewall of the generator is of the peg design where individual copper pegs can be used to probe the channel electrical field distributions. The channel is excited axially by a 1 kW, dc - 20 kHz variable power supply, isolated from the generator by an impedance matching transformer. No corrections are made for conductivity profiles at generator walls, an assumption fairly reasonable for small generators but questionable for large ones. Operational frequencies of 4~5 kHz were found to decouple the response to the axial current (Jx) excitation of the measured electrical quantities of Faraday current density (Jy), axial (Ex) and cross (Ey) flow fields from the gasdynamic flow velocity fluctuations. This enables the fluctuating quantities to be substituted in the two dimensional perturbed ohm's equations solving for electrical conductivity and the generator Hall parameter, which are two unknowns in the two equations. Results are in good agreement with theoretical estimates of these quantities.

*Supported by US DOE Contract DE-AC01-80-ET15614

GA-5 Arc Characteristics in a Seeded Combustion Products Plasma - E. HARMON, W. UNKEL, D.A. KIRBY and A.Y. CHANG, M.I.T.*--The characteristics of arcs from a potassium-seeded plasma to metallic anodes and cathodes have been measured using a small scale (1/8th MW) gaseous fuel combustor. The plasma conditions are representative of the conditions in a combustion-driven MHD generator and the results provide important information relevant to the corrosion/erosion of MHD electrodes. Voltage-current characteristics with and without arcs have been measured and the threshold current for formation of arcs on cold copper anodes has been determined. Close-up video records of anode and cathode arcs provide arc geometry information and show the interaction of the arcs with the fluid flow field. The frequency spectra of anode and cathode current fluctuations, with and without arcs present, have been measured. Results for stainless-steel and platinum capped electrodes and results for several electrode surface temperatures will be presented.

*Supported by U.S. D.O.E. Contract DE-ACO-79ET15518

SESSION GB

10:45 A.M., WEDNESDAY, OCTOBER 21, 1981

ROOM B

ION REACTIONS I

CHAIRPERSON: J.B. LAUDENSLAGER

JET PROPULSION LABORATORY, CALTECH

GB-1 Charge Exchange in C^{++}/Rare Gas Atom Collisions*- C.E. BURKHARDT, J.J. LEVENTHAL, U. of Missouri-St. Louis --As part of a program designed to study inelastic processes involving multiply charged ions we have performed experiments on C^{++}/rare gas atom collisions in the kinetic energy range 10-1000 eV. The experiments were performed by spectroscopically analyzing visible and vuv radiation that is emitted by excited reaction products. Although the energy partitioning among final states changes with kinetic energy and differs for each of the atomic targets, C^{+} is the preponderant radiating product. The data also suggest that a significant fraction of the C^{++} beam may be in a metastable excited state, probably the $2p\ ^3P^o$ state.

*Supported by ONR Contract No. N00014-76-C-0760.

GB-2 Emission Spectrum of the $He^+ + Ne$ Radiative Charge-Transfer and Association Reactions at Near-Thermal Energies - RAINER JOHNSEN and MANFRED A. BIONDI, U. Pittsburgh*--Photons emitted as a result of the very slow radiative charge-transfer $He^+ + Ne \rightarrow He + Ne^+ + h\nu$ and radiative association $He^+ + Ne \rightarrow HeNe^+ + h\nu$ processes have been observed using a Selected Ion Drift Apparatus (SIDA) in conjunction with spectroscopic instrumentation. At 12 Å spectral resolution, two continuous emission features were found: a stronger one increasing in intensity from 4000 to 4100 Å and a second, weaker one near 4240 Å. Evidently the two features arise from transitions to the two fine structure levels of $Ne^+(^2P)$. From the intensities of the observed product ions it is concluded that charge transfer occurs in 85% of reactive collisions, association in 15%. The total rate coefficient was found to be $(1 \pm 0.3) \times 10^{-15}$ cm^3/sec at near-thermal energies, consistent with an earlier determination.

*This work was supported, in part, by the U.S. Army Research Office under Grant No. DAAG-29-80-K-0081.

GB-3 Nitrogen Ion Association Reactions - S.R. ALGER and J.A. REES, Liverpool U., England -- There is currently renewed interest in the association of N^+ and N_2^+ ions with molecular nitrogen to form N_3^+ and N_4^+ respectively. It has been established for some time[1] that both reactions are third order processes of the form $N_2^+ + N_2 + M \underset{k_2}{\overset{k_1}{\rightleftarrows}} N_4^+ + M$, and rate constant data are available[1,2] for $M = N_2$ and He. The agreement between available thermal rate constants is not good, however, and the data for the energy-dependence of the rate constants are limited. We report drift-tube measurements of the rates k_1 and k_2 for the reaction $N_2^+ \leftrightarrow N_4^+$ over the range $20 < E/N < 140$ Td and of k_1 for the reaction $N^+ \rightarrow N_3^+$. The reaction $N_3^+ \rightarrow N^+$ was not observed.

[1]A.Good, Chem. Rev. 75, 561, 1975.

[2]D.Smith, N.E. Adams, T.M.Miller, J. Chem. Phys. 69, 308, 1978.

GB-4 Basic Microscopic Theory of Neutralization and of Chemical Reactions in Dense Gases - M. R. FLANNERY, Georgia Institute of Technology* --The first basic microscopic theory of chemical reactions between two species in a dense gas is presented. The overall rate which is a combination of the rate for transport by diffusional drift and of the rate for reaction at the reaction zone is determined as a function of gas density, of density of the reacting species and of time. The first exact analytical solution of the Debye-Smoluchowski equation which is a natural consequence of the basic theory is provided for transport/reaction of species with general interaction V. The theory is illustrated for the diffusional-drift and time decay of the rate of ion-ion recombination for initial conditions appropriate to the generation of either a Boltzmann distribution of ions or an instantaneous spherical-shell source. Many interesting features emerge.

*Supported by US AFOSR under Grant AFOSR-80-0055.

[1]M. R. Flannery, Phil. Trans. Roy. Soc. A (London) (in press).

GB-5 Molecular Dynamics Simulation of Ionic Recombination in a Plasma-W.L. MORGAN, Lawrence Livermore Lab., J.N. BARDSLEY, J. LIN, U. of Pittsburgh, B.L. WHITTEN, Rice U.*--We have used the method of molecular dynamics (MD) to simulate the interaction of 50 pairs of positive and negative ions in a unit cell with periodic boundary conditions. In this calculation the ions may collide with neutral atoms and may recombine with each other. The MD simulation allows us to study how a plasma affects the ionic recombination rate, ionic transport coefficients such as diffusion and mobility, and other properties such as the ion pair correlation function and the time dependent velocity autocorrelation function. We will present results of MD calculations for O_4^+ and O_4^- in O_2 and for Kr^+ and F^- in Ar. We will also present comparisons of these MD results with calculations made using the coupled diffusion-mobility and Poisson equations. We find, as we had previously[1], that the recombination rate coefficient decreases with increasing ion density.

*Work supported by the University of California, Lawrence Livermore Laboratory under DOE Contract #W-7405-ENG-48.

[1]W.L. Morgan, B.L. Whitten, and J.N. Bardsley, Phys. Rev. Letts.,45, 2021 (1980)

GB-6 Two and Three Body Recombination in Rare Gas Fluorides-B.L. WHITTEN, Rice U., W.L. MORGAN, Lawrence Livermore Lab., J.N. BARDSLEY, U. of Pittsburgh*--Previous work has indicated that two body recombination or mutual neutralization (MN) ($X^+ + Y^- \rightarrow X^* + Y^*$) and three body recombination ($X^+ + Y^- + Z \rightarrow XY^* + Z$) are competing processes and branching between them can significantly affect the formation rate of XY*. Estimates of the MN rate,using the Landau-Zener (LZ) model, indicate that it depends strongly on the position R_X of the pseudo-crossing between the ionic and covalent curves. Thus, for NeF ($R_X \simeq 10$ Å) MN should be large enough to reduce three body recombination; for ArF ($R_X \simeq 19$ Å) MN should be a very small effect. It has been suggested, however, that for large R_X the LZ model greatly underestimates MN. We have performed close coupling (CC) calculations of the MN cross sections for NeF and ArF. Preliminary CC calculations agree well with the LZ predictions. Using these cross sections we have also performed monte carlo calculations to determine the branching between the two and three body processes for NeF and ArF in Ne as a function of temperature and pressure.

*Work supported by the University of California, Lawrence Livermore Laboratory under DOE Contract #W-7405-ENG-48.

SESSION HA

1:30 P.M., WEDNESDAY, OCTOBER 21, 1981

ROOM A

ELECTRON CAPTURE

CHAIRPERSON: F.C. SHARPTON

UNIVERSITY OF WISCONSIN

HA-1 Electron Attachment to HCℓ and DCℓ in Excited Vibrational or Rotational States-J. N. BARDSLEY, U. Pittsburgh*--A semi-empirical model, based on the theory of configuration interaction in electron-molecule scattering, is fitted to the data of Allan and Wong[1] on the temperature dependence of dissociative attachment to HCℓ and DCℓ. The validity of the model is checked by comparison with the experimental studies of associative detachment in $Cℓ^-$-H collisions[2]. Cross sections are deduced for attachment to each rotational and vibrational state of HCℓ and DCℓ. For HCℓ with J=0 the peak cross sections for attachment to the v=0, 1, 2 states are 0.09, 1.1 and 90Å^2, respectively. Rotational excitation also leads to enhanced cross sections. The cross section near threshold is approximately 2Å^2 for v=0, J=20 and 15Å^2 for v=1, J=10. For v=2, with J≥9 the process becomes exothermic and the cross section is unbounded.

[1]M. Allan and S. F. Wong, J. Chem. Phys. 74, 1687 (1981).
[2]T. S. Zwier et al, Phys. Rev. Lett. 44, 1050 (1980).

*Research supported by the Office of Naval Research.

HA-2 Reaction Kinetics of a High Pressure Helium Fast Discharge Afterglow. J. STEVEFELT, J.M. POUVESLE, and A. BOUCHOULE, U. of Orléans, France.-- A fast pulsed discharge (4 kA, 7 nsec, 10 Hz) in atmospheric pressure high purity helium was used to create an afterglow plasma with initial electron density 10^{15} cm^{-3} as determined from H_β line broadening. The afterglow radiation was emitted in He_2 transitions in the visible and far ultraviolet (60-110 nm) regions, with time-dependence in agreement with a collisional-radiative scheme of electronic recombination of He_2^+ ions. A significant fraction of the He_2^+ recombination events resulted in helium atoms in the metastable 2^3S state, and the time-dependence of this dissociation process correlated with that of He_2 populations characterized by quantum number n = 4. The concentration of 2^3S atoms was comparable to the electron density, and their destruction rates were found to agree with the results of Deloche et al.[1] The concentration of molecular $a^3\Sigma_u^+$ metastables was two orders of magnitude lower, suggesting a collisional coupling to the radiating $A^1\Sigma_u^+$ state.

[1]R. Deloche, P. Monchicourt, M. Cheret, and F. Lambert, Phys. Rev. A 13, 1140 (1976).

HA-3 Noble-Gas Trimer Ions: Dissociative Recombination of Ne_3^+ Ions and Electrons - JEFFREY A. MACDONALD, MANFRED A. BIONDI and RAINER JOHNSEN, U. Pittsburgh.*--At the very high pressures (>1 atmosphere) of rare gases used in the new high-power visible and uv lasers, trimer ions R_3^+ are thought to be an important constituent, yet little is known concerning their atomic collision properties. We have undertaken a study of the dissociative recombination of Ne_3^+ ions and electrons, using a low-temperature microwave afterglow-mass spectrometer apparatus employing microwave electron heating. At $\sim$ 80 K and $\sim$ 6 Torr of neon, Ne_3^+ is the dominant afterglow ion. The measured electron-density decays in recombination controlled afterglows are fitted by computer solutions of the continuity equation containing recombination and ambipolar diffusion loss terms to determine the recombination coefficient $\alpha(Ne_3^+)$. We find

$$\alpha(Ne_3^+) = (1.1 \pm 0.2) \times 10^{-6}[T_e/300]^{-0.36} \text{ cm}^3/\text{sec},$$

valid over the range 80 K $\leq T_e \leq$ 4000 K. Thus, the trimer ion exhibits a dependence on electron temperature similar to that predicted and measured for diatomic ions but a larger rate coefficient.

*Supported, in part, by ARO Grant DAAG-29-80-K-0081.

HA-4 Dissociative Recombination of O_2^+ - STEVEN L. GUBERMAN, Boston College*--Ab initio calculations have been completed on the valence excited states of O_2 that can provide routes for the dissociative recombination (DR) of the ground and lowest metastable states of O_2^+ leading to neutral ground and excited O atoms. Results previously reported[1] have been extended to include high vibrational levels. The ion vibrational levels leading to excited atoms are identified and the kinetic energies of the resulting hot O atoms will be reported. It is shown that several routes can provide very hot(>5.6eV kinetic energy) ground state O atoms from DR of low lying vibrational levels of the metastable ion state. However, DR of the ground vibrational level of the metastable state leading to only ground state atoms will have a comparatively small probability.

* Supported NASA-Ames Grant No. NAG2-89 and by the Air Force Geophysics Laboratory under contract No. F19628-79-C-0139.

[1]S. L. Guberman, Int. J. Quantum Chem. S13, 531(1979)

HA-5 Dissociative Recombination of Hg_2^+ Ions and Electrons - VIDYA E. JOG and MANFRED A. BIONDI, U. Pittsburgh*--Dissociative recombination of Hg_2^+ ions with electrons,

$$Hg_2^+ + e^- \rightleftarrows (Hg_2^*)_{rep.} \rightarrow Hg^* + Hg \quad ,$$

has been studied using microwave afterglow and optical spectrometric techniques. The total rate coefficient is found to be

$$\alpha[Hg_2^+] = (4.2 \pm 0.5) \times 10^{-7} \, [T_e(K)/340]^{-1.1} \ cm^3/sec$$

over the range 340 K $\leq T_e \leq$ 5600 K and at $T_+ = T_{gas} = 340$ K. The excited states produced by the dissociative recombination have been determined at T_e = 340 K and 4900 K; in both cases the 7s and 6d states are strongly populated. Compared to Xe_2^+ ions, Hg_2^+ ions exhibit a substantially smaller and more rapidly varying coefficient. This suggests that, following the initial capture step to form $(Hg_2^*)_{rep.}$, competition between dissociation to complete the recombination and autoionization to disrupt it favors autoionization.

*Supported, in part, by the U.S. Army Research Office under Grant No. DAAG-29-80-K-0081.

HA-6 Electron Affinities of Molecules - An Empirical Correlation - P. DAVIDOVITS, Aerodyne Research, Inc. and Boston College†, and A. FREEDMAN and G.W. STEWART, Aerodyne Research, Inc.*--An empirical method for the prediction of electron affinities for sequences of atoms and inorganic molecules is presented. The electron affinity for at least one member of the sequence must be known in order to estimate the values for the rest of the sequence. This method utilizes a single parameter "vertical analysis" correlating atomic ionization potentials and electronic energy levels with both atomic and molecular electron affinities. Comparison of predictions with available experimental data shows that in most cases the predicted and measured values agree to within about 0.2 eV. In all cases where the electron affinity has been experimentally determined to be negative, the empirical formula also predicts negative values.

†Permanent address

*Supported by the Department of Energy, Office of Magnetohydrodynamics under Contract EX76-C-01-2478

HA-7 Measurements of Electron Drift Velocity and Attachment in Dry Air* - D. K. DAVIES, Westinghouse R&D Center -- Arrival-time spectra of electrons and negative ions have been measured in dry (CO_2-free) air using a pulsed drift tube. Values of electron drift velocity have been determined from these measurements over the range $0.6 \leq E/N \leq 300$ Td, and represent the first set of data covering an extended range of E/N. At the lower end of the range the present values are in excellent agreement with the recent data of Hegerberg and Reid.[1] Values of negative ion mobility and electron attachment coefficient have been determined over the range $0.6 \leq E/N \leq 7$ Td. The negative ion spectra show only one ion species having a reduced mobility of 2.27 $cm^2/sec.V$, constant to within $\pm$ 1% over the range of E/N. Electron attachment is consistent with negative ion formation via a three-body process. The values of attachment rate coefficient lie on the lower edge of the spread of previous data.

*Supported in part by AFWL, Contract F29601-79-C-0036.

[1]R. Hegerberg and I.D. Reid, Aust. J. Phys. 33, 227(1980).

SESSION HB

1:30 P.M., WEDNESDAY, OCTOBER 21, 1981

ROOM B

NON-UNIFORM GLOWS & CORONA

CHAIRPERSON: P. BLETZINGER
WRIGHT-PATTERSON

HB-1 The Glow Discharge Cathode Fall - J. H. INGOLD, General Electric Co., Cleveland, OH. Existing theories of the cathode fall are based on the assumption that the electrons are in equilibrium with the electric field. The validity of this assumption is examined by solving the moment equations for electron density, drift velocity, and energy in the cathode fall of a glow discharge in argon. It is assumed that ion motion is mobility limited, and that the electric field obeys Poisson's equation. The electron velocity distribution is assumed to be a spherical shell[1] which allows all ratios of directed energy to random energy to be investigated. It is shown that the customary assumptions about electron drift velocity and energy are weak assumptions in the cathode fall.

[1]R.S. Bergman and J. H. Ingold, Bull. Am. Phys. Soc. 23, 143 (1979) (1978 Gaseous Electronics Confer.)

HB-2 Alternating Current Cathode Fall Characteristics For Rare Gases in Cold Cathode Discharges. - J. MAYA and R. LAGUSHENKO, GTE Lighting Products, Danvers, MA -- We have measured the cathode fall characteristics of tungsten and yttrium in He, Ne, Ar and Penning mixtures in the pressure range 1 to 36 torrs. We have determined the current densities of such cathodes as a function of rare gas pressure. Results indicate it is possible to obtain up to 40 ma/cm^2 in yttrium - (Ne + 0.1% Ar) combination. Current densities obtained from yttrium are about a factor of three higher than tungsten for similar conditions. We have calculated the cathode fall characteristics using parameterized low energy (10-30 eV) experimental cross section data from literature. By fitting our calculations to the experimental results we derived full excitation cross sections of rare gases in the region of 100 eV.

HB-3 Analysis of a One-Dimensional Steady State Glow Discharge - G. L. DUKE, and A. GARSCADDEN, Aero Propulsion Lab., Air Force Wright Aeronautical Labs, WPAFB, OH Davies and Evans[1] theoretical treatment of a high-voltage low current gas discharge is expanded to include the effects of attachment. This treatment provides a smoothly varying solution for the three main regions of a glow discharge: cathode sheath, positive column, and anode sheath. For the case without attachment, a linearly decreasing electric field is shown to be an exact analytic solution in the region near the cathode. The addition of attachment results in a smaller cathode sheath distance and thus results in a non-linear electric field. The slope of the electric field in the sheath region becomes much steeper and S-shaped as the concentration of an attaching species is increased. Numerical results are presented for various concentrations of chlorine in helium.

[1]A.J. Davies and J.G. Evans, J. Phys. D 13, L161, (1980)

HB-4 Plasma Boundary Layer Over a Positive Electrode - S. T. VAN BROCKLIN, and O. BIBLARZ, Naval Postgraduate School, Monterey, CA*--An analysis of the electrode region has been carried out to establish losses and other electrode contributions to the discharge. The equations of electron and ion conservation and electrical potential have been solved numerically. A two-dimensional model with periodic active sites on a flat plate is utilized to obtain results which generate the sheath and ambipolar regions adjacent to a non-emitting electrode. The active sites are voltage sources with electron densities depressed from both the nonactive wall and the undisturbed or free-stream values. Ionization/recombination has been shown to play an important role in establishing the boundary layer behavior in the ambipolar region and in the dimensionality of the problem formulation. Application is for discharges in nitrogen gas at one amagat with a pulse duration in the order of 50μs. Results indicate that a sheath length of 38μm about a 35-volt active site and 5-20μm along the nonactive portion of the electrode are established. Joule heating is determined not to be important for common flush times in molecular gas lasers.

*Supported by the NPS Foundation Research Program.

HB-5 Stability of Self-Sustained Discharges in Attaching Gas Mixtures*, L. J. DENES, P. J. CHANTRY, R.R. MITCHELL and L. E. KLINE, Westinghouse R&D Center. Self-sustained glow discharges in attaching gas mixtures exhibit electrode-surface-related instabilities, which begin preferentially near the anode in strongly attaching mixtures. When electrode surface flaws of ~μm scale size are removed, stability improves. We have combined the predictions of a discharge instability model and an electrode sheath model to develop a semi-quantitative understanding of this observed behavior. Vacuum electrostatic field calculations indicate that the field due to a typical flaw falls as $(\text{distance})^{-1}$. Thus our one-dimensional instability model approximates the flaw as an isolated cylindrical electrode. It includes single-step ionization and attachment, and electron drift, diffusion and flux divergence. This model predicts that the anode region is stable to local perturbations in electron density only if the radius of curvature r_o of the flaw exceeds D/W. Since D/W decreases with increasing pressure, stable XeF discharges should be more easily achievable at pressures $\gtrsim$ 3 amagats. The instability model neglects the effects of sheaths, which are postulated to increase the effective value of r_o.
*Work supported in part by U. S. Army BMDATC.

HB-6 Plasma Density Profiles in Gas Discharges, J. P. HAUCK, Rockwell International, Anaheim, CA--It is commonly assumed that the electron density in gas discharges is zero at the wall. It is shown here that the density at the wall must be nonzero in order to have finite electric fields. A self consistent model of the density profile is developed which predicts the density and potential profiles in terms of the discharge parameters. We first find a relationship between discharge parameters and the ambipolar diffusion rate. Next we find a relationship between the ambipolar diffusion rate, the wall potential and the electron energy distribution function. Then we find a relationship between density and potential profiles. With these relationships we have a complete model which predicts particle and charge density and potential profiles. A comparison is made to experimentally determined density profiles in He/Ne discharges.

HB-7 Unipolar Currents in a Low-Pressure Hg-Ar Plasma. G.L. ROGOFF, J.F. LOWRY, and R.I. PINSKER, Westinghouse R&D Center--An electrically floating metal plate in contact with a plasma equipotential surface will conduct no steady current. However, if a portion of the plate emits electrons, then a unipolar[1] current can flow, with different regions of the same plate serving as cathode and anode. Measurements have been made of the unipolar currents through combinations of externally-connected disk conductors mounted flush with the wall of a dc Hg-Ar positive column (3 Torr Ar, ∿7 mTorr Hg, 1.8 cm radius). Indirectly-heated dispenser cathodes act as the emitting regions, providing external control of emission levels. Measured unipolar currents are compared with values predicted by treating the disk cathodes and anodes as independent electrostatic probes; individual experimental probe characteristics are (a) adjusted to account for plasma potential shifts associated with unipolar current flow, and (b) superimposed to obtain equal but opposite currents in the cathode and anodes at a common potential. The agreement with measured unipolar currents is good.

[1]A. E. Robson and P. C. Thonemann, Proc. Phys. Soc. London 73, 508 (1959).

HB-8 Space Charge Model for Steady Point-Plane Coronas B. L. HENSON, U. Missouri-St. Louis-A mathematical model for point to plane coronas in the steady state regime has been developed using hyperboloid geometry for the point. A constant mobility model is assumed for the transport of the charge carriers and the corona current is assumed to be space-charge-limited. The resulting differential equations prove to be tractable in prolate spheroidal coordinates. Warburg's law is derived and this derivation predicts that Warburg's law is an exact relationship. The corona current-potential relation is also predicted, but the solution indicates that the commonly accepted empirical equation for the corona current is only an approximation to the actual one.

HB-9 Coronaphoresis in He and N_2 Containing Cs.- D.H. DOUGLAS-HAMILTON and V. GOLDFARB, Avco Everett Research Laboratory, Inc.*-- The coronaphoresis effect has been used to remove cesium vapor from helium and nitrogen. In these experiments cesium was used as contaminant because of its low ionization potential and its spectroscopic detectability. A D.C. positive corona is used with a tungsten anode and glass cathode, and cesium concentration is reduced from $\sim$300 ppb to $\sim$10 ppb. The cesium is deposited on or in the glass cathode wall. Theoretical predictions will be compared with experiments in the corona. Coronaphoresis is expected to be applicable to purifying a variety of gases at ultrahigh purity in the electronic industry, at very low cost.

*Supported by Naval Electronics System Command under Contract N00039-80-C-0589.

SESSION I

3:00 P.M., WEDNESDAY, OCTOBER 21, 1981

ROOM B

WORKSHOP ON CURRENT TRANSFER TO MHD ELECTRODES

A key aspect of successful open-cycle MHD technology involves current transport from the bulk flowing plasma to the channel electrodes. Prototype open-cycle MHD generators operate primarily in an arcing mode which can result in significant electrode damage. The workshop will explore recent modeling and experimental studies which characterize both arc and diffuse discharge current transport through the electrode boundary layer and investigate the effects of this transfer on heat flux to the electrodes, electrode erosion, and electro-chemical corrosion for test electrode materials.

The workshop will begin with a series of 15 minute reviews of key issues by invited speakers. These reviews will be followed by a discussion session open to all attendees. A summary of the problem by an invited speaker will close the session.

CHAIRPERSON: C.E. KOLB

AERODYNE RESEARCH, INC.

PROBLEM DEFINITION AND OVERVIEW
M. MARTINEZ-SANCHEZ

THEORETICAL UNDERSTANDING OF ARCING
W. UNKEL

EXPERIMENTAL DATA ON ARCING PHENOMENA
I. SADOVNIK

EFFECTS OF SLAG ON CURRENT TRANSPORT
D. STICILER

ELECTRODE CORROSION PHENOMENA
B. ROSSING

WORKSHOP SUMMARY
D. OLIVER

SESSION JA

8:45 A.M., THURSDAY, OCTOBER 22, 1981

ROOM A

ION REACTIONS II

CHAIRPERSON: B.L. WHITTEN
RICE UNIVERSITY

JA-1 Theoretical Studies of the $O^+ + N_2$ Ion-Molecule Reaction - H. H. MICHELS and R. H. HOBBS, United Technologies Research Center*--The rate of the ion-molecule reaction, $O^+ + N_2 \rightarrow NO^+ + N$, has been studied in the energy region 0.1 → 10.0 eV, with reactant energy either as center-of-mass translational energy or as vibrational energy of the N_2 molecule. Our lowest energy reaction path closely follows a constant angle collision trajectory on the ground electronic state $^4A''$ hypersurface. This reaction surface exhibits a barrier of ∿0.3 eV located symmetrically between the reactant and product channels. Our calculated reaction cross-sections and rate constants are in good agreement with experimental data for this system. Calculations of the separate effects of vibrational and translational energy indicate that the energy dependence is nonspecific for this reaction, in agreement with the experimental studies of Schmeltekopf, et al.[1]

*Supported in part by AFGL.

[1]A. L. Schmeltekopf, E. E. Ferguson, and F. C. Fehsenfeld, J. Chem. Phys. 48, 2966 (1968).

JA-2 Silicon-Oxide Negative Ion Chemistry* - F. C. FEHSENFELD, D. W. FAHEY, AND E. E. FERGUSON, NOAA Aeronomy Laboratory, Boulder, CO 80303.
The silicon-oxide negative ions SiO_3^- and SiO_4^- were observed in a flowing afterglow apparatus. The ions were produced in a microwave discharge containing He, O_2, and SiH_4 and from the reactions in a plasma containing O^-, O_2^-, O_3^- and SiO. Rate constants were determined for SiO_3^- and SiO_4^- for reaction with NO, NO_2, CO, CO_2, O_3, and O with the result that the ions were found to be relatively non-reactive. Since silicon is isoelectronic with carbon, by analogy with CO_3^- and CO_4^-, these ions are expected to be quite stable. The present studies suggest that the neutral oxides of silicon will strongly influence the negative ion chemistry of the mesosphere if sufficient concentrations of these neutrals exist in the gas phase.

*Supported in part by the Defense Nuclear Agency.

JA-3 Reactions of $O_2^-(H_2O)_n$, n=0-4, Ions with O_3, NO, SO_2, and CO_2* - D. W. FAHEY, F. C. FEHSENFELD, and E. E. FERGUSON, NOAA Aeronomy Laboratory, Boulder, CO 80303. Reaction rate constants for O_2^- ions with 0-4 waters of hydration have been measured for O_3, NO, SO_2, and CO_2 in the temperature range of 176-300K. The reaction with O_3 is charge-transfer to produce O_3^- with simultaneous transfer of water ligands. The reactions with NO and SO_2 are ligand switching reactions. In all of these cases the reaction rate constants are not decreased measurably by an increase in the O_2^- hydration. CO_2 rapidly displaces one water molecule clustered to O_2^- but does not react with $O_2^-(H_2O)_{3,4}$. The rapid destruction of $O_2^-(H_2O)_4$ by O_3, NO, and SO_2 guarantees that $O_2^-(H_2O)_n$ ions cannot be dominant small air ions in the lower atmosphere.

*Supported in part by the Defense Nuclear Agency

JA-4 The Hydrated Negative Hydrogen Ion - J. F. PAULSON, AFGL, and M.J. HENCHMAN, Brandeis Univ. -- The ion H_3O^- (and its deuterated analogs) has been observed as the product of an ion-molecule reaction between $OH^-.H_2O$ and H_2 (or D_2). The experiments were performed on a longitudinal double mass spectrometer in which a mass analyzed beam of reactant ions collides with H_2 in a thin collision chamber. Reaction probability is strongly energy dependent, showing a maximim at a barycentric energy of 1.1 to 1.2 eV and being negligible below 0.7 eV and above 1.8 eV. Cross sections calculated from observed product and reactant ion count rates maximize at about $0.05 \times 10^{-16} cm^2$. Thermal target motion in this beam experiment accounts for most of the width of the reaction probability function. Both collision induced dissociation of the reactant ion and proton transfer reactions occur, in addition to production of H_3O^-. Comparison of the energy dependences for these endoergic processes indicates that the energy for dissociation of H_3O^- to $H^- + H_2O$ is approximately 0.6 eV.

JA-5 Negative Ion Reactions with Acetonitrile - J.F. PAULSON and F. DALE, AFGL--Recent measurements of the positive ion composition of the stratosphere have led to the suggestion that acetonitrile is a component of that region (Arnold et al., Geophys. Res. Lett. 5, 654 (1978). Subsequent laboratory measurements have shown that the hydronium ions, which are known to exist in the stratosphere, react rapidly with acetonitrile in solvent switching reactions, to produce several positive ion species having the same mass-to-charge ratios as those observed in the stratosphere (D. Smith, et al., Plan. Space Sci., 29, 449 (1981)). We have used a selected ion flow tube to measure the rate coefficients at 300K in the gas phase for the reactions of acetonitrile with several negative ions, including, O^-, O_2^-, $OH^-\cdot nH_2O$, CN^-, Cl^-, NO_2^-, CO_3^-, and NO_3^-, and have identified the ion products of these processes. The reactions observed include both proton transfer, producing CH_2CN^-, and solvation of the reactant ions with CH_3CN.

JA-6 Collisional Studies of High Temperature Molecular Negative Ion-Neutral Reactions* - R L.C. WU, and T.O. TIERNAN, Wright State U.*--Excitation functions for several types of negative ion-molecule reactions involving molecular negative ions such as PO^-, PO_2^-, FeO^-, and FeO_2^-, which are present in certain high temperature environments, have been investigated using an in-line tandem mass spectrometer. The projectile ions were produced by electron impact/microwave discharge on mixtures of N_2O or O_2 with selected organometallic compounds. Reactions studied included endothermic charge transfer reactions, $MO_n^- + X \rightarrow X^- + MO_n$, and collision-induced dissociation processes, $MO_n^- + Y \rightarrow O^- + MO_{n-1} + Y$, where M = P, Fe, n = 1, 2, X = molecules of known electron affinity, and Y = inert gas. The electron affinities of PO and PO_2 determined by endothermic charge transfer technique are 1.0 ± 0.1 and 3.3 ± 0.2 eV respectively. The bond dissociation energies of PO^- and PO_2^- are measured to be $D_0^0(O^-\text{-}P)$=5.6 ± 0.1 and $D_0^0(O^-\text{-}PO)$=7.4 ± 0.2 eV respectively. These and other data obtained in this study will be compared with results derived from photodetachment and flame experiments.

*Supported by U.S. DOE Contract No. DE-AC02-80ER-10668

JA-7 Fragmentation and Internal Excitation of UF_6^- Ions in Collisions with Noble Gas Atoms.* J.A.D. STOCKDALE, Chemical Physics Section, Health and Safety Research Division, Oak Ridge National Laboratory.-- Beams of UF_6 ions of controlled average internal energy ranging from 0.7 to 1.6 eV have been produced by surface electron attachment on resistively heated carbon filaments. The negative ionic products of collisions between these beams and Ne, Ar, and Xe static gas targets, at a laboratory kinetic energy of 200 eV, have been identified and their kinetic energies and angular distributions measured. Fragmentation to F^- and UF_5^- increases with angle and increases as the internal UF_6^- energy prior to collision is increased. The conversion of kinetic to internal energy to produce excited UF_6^{-*} also on the average increases with the filament temperature.

*Research sponsored by the Office of Health and Environmental Research, Department of Energy under contract W-7405-eng-26 with the Union Carbide Corporation.

SESSION JB

9:00 A.M., THURSDAY, OCTOBER 22, 1981

ROOM B

DISTRIBUTION FUNCTIONS I

CHAIRPERSON: W.L. MORGAN

LAWRENCE LIVERMORE LABORATORY

JB-1 Electron Swarms in N_2 at High E/N*-L.C.PITCHFORD, Sandia National Labs, and A. V. PHELPS, JILA and NBS. Recently developed density gradient and multiterm spherical harmonic expansion techniques are used to solve the Boltzmann equation for electrons in N_2 up to an E/N of 10^{-18} Vm^2 corresponding to mean electron energies up to 25 eV. At these high E/N values, electron production by ionization is important and electron scattering is noticeably anisotropic. The various published elastic and inelastic differential scattering cross sections are compared and used to obtain total cross sections and coefficients of Legendre components of the cross sections for energies from 0 to 10 keV. Surprisingly, the two-term spherical harmonic approximation yields transport and ionization coefficients in agreement with multiterm results. Furthermore, these coefficients are insensitive to the angular distributions of scattered electrons provided the total momentum transfer cross section is unchanged. Qualitative explanations for these results will be discussed and a comparison of measured values with our calculations of transport and ionization coefficients will be shown..

*Supported in part by WPAFB and ARO and a computing grant from NCAR.

JB-2 Diffusion of Fast Electrons in a Magnetic Field* M.S. TEKULA and J.H. JACOB, Avco Everett Res. Lab., Inc. Everett, MA 02149. The Bethe Age diffusion equation for fast electrons in a magnetic field is derived. One way to solve this equation is to look for solutions separable into diffusion along the magnetic field and across it. However this set of eigenfunctions has limited use in boundary valued problems where the beam of electrons enter the gas through a foil. A transformation of coordinates has been derived which reduces the equation to the Bethe Age diffusion equation with no magnetic field. This solution is valid in the range $\lambda/RL < (40/M)^{1/2}/10$, $\lambda/RL > 10\ (M/40)^{1/2}$ where λ, r_L are the mean free path and Larmor radius, and $2 < M < 3$. The theory will be compared with experiments.

*Work supported in part by DARPA

JB-3 Transport Properties of $CC\ell_2F_2$ from the Boltzmann Equation - J.P. NOVAK and M.M. SHOUCRI, Institut de recherche d'Hydro-Québec.-- A Boltzmann equation analysis of $CC\ell_2F_2$ was performed under steady-state homogeneous conditions. Holstein's approximation, with the attachment term added, was used with a numerical code based on Sherman's iterative method. The numerical solution was tested on several model gases; the maximum deviation observed between analytical and computer results was 4.7%. The equation was then solved for nitrogen using a complete set of collisional cross sections. Very good agreement of the calculated transport coefficients with experimental values was obtained for the first ionization coefficient and drift velocity, while the maximum deviation for D/μ ratio at $E/N \sim 100$ Td was about 20%. A series of calculations was then performed with a view to determining effective collisional cross sections of $CC\ell_2F_2$ consistent with known experimental data and measured transport coefficients. The effect of the cross sections on the electron energy distribution function is discussed and effective cross sections for elastic, vibrational, and excitational collisions obtained by the fitting of transport coefficients are presented.

JB-4 Vibrational Pumping Mechanism Influencing Dissociative Attachment of Hydrogen - J.W. ENGEL, W.F. BAILEY and A. GARSCADDEN, Aero Propulsion Laboratory, Air Force Wright Aeronautical Labs, and A.F. Institute of Technology, Wright-Patterson AFB Ohio 45433 -- Calculations have been made of the electron collision pumping rates to high vibrational quantum levels in hydrogen using a numerical solution of the collisional Boltzmann equation. Results show that direct excitation from the vibrational ground state, excitation from previously excited vibrational states and excitation of the electronic B and C states with subsequent radiative decay to high vibrational levels of the electronic ground state can all be important. Comparison of direct pumping of the vibrational level V ($V \leq 5$) with indirect pumping from other vibrational states ($\Delta V=1,2,3$) reveals that for vibrational populations corresponding to vibrational temperatures $T_V=2000^oK$ and conditions representative of a low pressure discharge, the indirect pumping is more important. At higher values of E/N the high vibrational level pumping is dominated by excitation via the electronic B and C states.

JB-5 Electron Kinetics of Silane Gas Mixtures of Semi-Conductor Plasma Reactor Interest. - A. GARSCADDEN, G.L. DUKE and W.F. BAILEY, A.F. Wright Aeronautical Labs, W.P.A.F.B., Ohio 45433 -- Results are presented of calculations of the electron drift velocity, vibrational excitation, electronic excitation, ionization (including dissociative ionization) at low E/N for various gas mixtures used in semiconductor plasma reactors. The calculations use an iterative solution of the Boltzmann equation and incorporate available experimental data to derive the electron energy distribution function (EEDF). Silane is an interesting gas in its own right as it has exceptionally large vibrational cross-sections at low energy. We have included a Ramsauer minimum in the momentum transfer cross-section from comparisons with experimental data and by analogy with methane. These properties produce a very high electron drift velocity compared to most pure gases. Diluted in other gases, even Ramsauer gases, the drift velocity is less. Relative ionization rates and energy depositions have been calculated. At high E/N, the sensitivity of the drift velocity to the mixture decreases, however the multiple ionization channels are sensitive to the EEDF and consequently to the gas mixtures.

SESSION K

10:30 A.M., THURSDAY, OCTOBER 22, 1981

ROOM B

PLENARY SESSION IN HONOR OF PROFESSOR W.P. ALLIS

The Conference will honor Professor Allis' many contributions to the field of gaseous electronics through talks given by several of his friends and colleagues.

CHAIRPERSON: A.V. PHELPS

JILA/N.B.S. & UNIV. COLORADO

K-1 The Non-Convergence of the Legendre Expansion of the Electron Velocity Distribution - W.P. ALLIS, Joint Institute for Laboratory Astrophysics, Boulder, Col.-- We consider the steady state of a gas of free electrons in a gas with an electric field but no gradients. The solutions of the Boltzmann equation with scattering-out-only (SOO functions) are easily obtained. Their Legendre transforms generally fill the entire set of Legendre transform equations, that is the components f_ℓ do not vanish as $\ell \to \infty$, in fact they generally increase. For isotropic scattering the scattering-in term enters only the ℓ=o equation and determine f_1/f_o, with this ratio increasing so that f_1 crosses f_o at an energy u_1. Above u_1 $(f_o + \mu f_1)$ is negative in the backward direction so the two-term solution, P_2 approximation, is inacceptable and f_2 must enter. This situation repeats, f_2 crossing f_1 and requiring f_3, so that a set of f_ℓ is built up which increases in magnitude with ℓ. It is shown analytically that this approaches a SOO function.

SESSION LA

1:30 P.M., THURSDAY, OCTOBER 22, 1981

ROOM A

VISIBLE & INFRARED LASERS

CHAIRPERSON: M.J. PLUMMER

NORTHROP RESEARCH & TECH. CTR.

LA-1 Excitation of ArH* Luminescence by Electron Ion Recombination During the Afterglow.- J. SHMULOVICH and S. YATSIV, The Hebrew U., Jerusalem -- The ArH* emission band at 7674 Å was excited by short, pulsed, repetitive electric discharges in Ar:H_2 mixtures at pressures up to 100 torr. The time dependence of the intensity of the emission was characterized by two consequent peaks. The first peak appeared during the current pulse. It was tentatively associated with the known ArH* production mechanisms[1]: $Ar(4p)+H_2 \rightarrow ArH^*+H$. The second peak, usually stronger and broader than the first, was observed during the afterglow. The substantial reduction in the intensity of the ArH* afterglow emission was recorded upon application of a microwave electric field. This indicates that the electron-ion recombination is an important step in the ArH* production in the afterglow. An examination of the time and intensity dependence of the band at various pressures, mixture compositions (specially upon addition of small amounts of Kr) and discharge parameters established the specific process responsible for the ArH* band afterglow excitation: $ArH^+ + 2e^- \rightarrow ArH^* + e^-$.

[1] J. Shmulovich and S. Yatsiv, Chem. Phys. Letts. 75, 319 (1980).

LA-2 Kinetics of an Ar-O_2 Nuclear Pumped Plasma for an $O_2(^1\Delta)$-I_2 Laser. M. S. ZEDIKER, T. R. DOOLING, D. BURLET, and G. H. MILEY, Fusion Studies Laboratory, Univ. of Illinois, 103 S. Goodwin Ave., Urbana, IL 61801 -- A kinetics model of an Ar-O_2 nuclear-pumped discharge has been developed to study the relative importance of atomic recombination to direct excitation by secondary electrons in the formation of $O_2(^1\Delta)$. The principal objective is to determine the optimum parameters (overall pressure, Ar, O_2 ratio, and power deposition) necessary to achieve an inversion in an $O_2(^1\Delta)$-I_2 energy transfer laser. The high pressure characteristic of a nuclear-pumped plasma (Ar > 200 Torr) plays an important role in the formation of $O_2(^1\Delta)$ through three-body atomic recombination of oxygen atoms. Indeed, with low oxygen pressure (<< 1 Torr) this mechanism is dominant. However, for oxygen pressure (> 1 Torr) direct electron excitation and electron impact deexcitation of $O_2(^1\Sigma)$ become the dominant sources of $O_2(^1\Delta)$. Thus atomic recombination can add to the efficiency of $O_2(^1\Delta)$ generation for O_2 pressures greater than 2 Torr.

LA-3 4.3 μm CO_2 Laser Parameterization. D. R. SUHRE and L. H. TAYLOR, Westinghouse R&D Center, Pittsburgh, PA--A CO_2 laser operating at 4.3 μm was studied which lased on the $[101]_I$ - $[100]_I$ transition. The laser was electrically pulsed and then irradiated by a pump pulse from a second CO_2 laser at 10 μm produced by the (002) - $[101]_I$ sequence band transition. The 4.3 μm laser operated with various mixtures of CO_2, N_2 and He at about 20 Torr, while the 10 μm laser operated at higher pressure and was constrained to the sequence band by an intracavity CO_2 hot cell. The 4.3 μm energy was experimentally parameterized with respect to gas mixture, electrical input energy and the time delay between the discharge and laser pump pulse. Modeling of the system was also conducted in order to determine the dominant influences on the performance of the laser.

LA-4 Discharge Parameters of a Multi-Atmospheric, UV-preionized TE CO_2 laser-K. MIDORIKAWA, K.NAKAMURA, K.WAKABAYASHI, M. OBARA, and T. FUJIOKA, Keio U.--A high pressure TE CO_2 laser is highly attractive for tunable pump sources of optically pumped mid-ir lasers. We made the precise measurements of the time-resolved voltage and current of a UV-preionized TE CO_2 laser operating at pressures up to 10 atm. The laser was energized with a 4-stage coaxial Marx generator. The laser and Marx generator were connected with six coaxial cables working as a PFL of about 60 nsec (FWHM) voltage pulse. Dependences of the discharge impedance and power deposition on mixture pressure and on input energy density were measured with the mixture of CO_2:N_2:He=1:1:8. The E/N giving voltage plateau decreased with the increase of pressure. Comparing the experimental values with calculated ones from the rate equation of the electron density, both avalanche and recommbination coefficients were obtained as a function of pressure. The discharge characteristics predicted by our kinetic model involving excitation circuitry were in good agreement with the experimental results.

LA-5 ZnI, CdI and CdBr Photodissociation Lasers: Quenching Kinetics and B State Radiative Lifetimes* - M.N. EDIGER, A.W. McCOWN and J.G. EDEN, U. of Illinois, Urbana, Il 61801--By recording the exponential decay of the B→X fluorescence following ArF photodissociation of ZnI_2, CdI_2 and $CdBr_2$, the radiative lifetimes of the B states of ZnI, CdI and CdBr were found to be 26 ± 4, 41 ± 5 and 44 ± 2 ns, respectively. Also, the rate constants for quenching of these radicals by ZnI_2, CdI_2 and $CdBr_2$ were determined to be $(1.7 + 0.2) \cdot 10^{-9}$, $(4.7 \pm 0.3)^2 \cdot 10^{-10}$ and $(5.1 \pm 0.2) \cdot 10^{-10}$ cm^3-sec^{-1}, respectively. From the absorption of tunable dye laser radiation by ZnI ground state molecules, the ZnI_2 and Ar quenching rate constants for the ZnI lower laser level were found to be $(1.4 \pm 0.4) \cdot 10^{-9}$ and $1.6 \cdot 10^{-11}$ cm^3-sec^{-1}, respectively, giving a lifetime of 2.0 ns for $[ZnI_2] = 3 \cdot 10^{17}$ cm^{-3} and $[Ar] = 5 \cdot 10^{18}$ cm^{-3}. Also, the small signal gain coefficient for the ZnI band was found to peak at ∿ 15% - cm^{-1} for λ = 602.4 nm and to be > 5%-cm^{-1} for $591 \leq \lambda \leq 608$ nm. With an optical cavity, lasing was observed from ZnI, CdI and CdBr and strongest emission occurred at 602, 656 and 811 nm, respectively.

*Work supported by AFOSR.

LA-6 Electron Beam Excitation of cw Ion Lasers* - J. J. ROCCA, J. MEYER, Z. YU, AND G. J. COLLINS, Colorado State University. -- We are exploring electron beam pumping of cw ion lasers such as $He - Hg^+$. The use of dc electron beams is shown theoretically to result in increased operating efficiency of cw ion lasers because of improved overlap of the electron energy distribution with the ionization and excitation cross sections of interest. Experimentally we have constructed glow discharge electron guns which produce well collimated electron beams of kilowatt power, that operate successfully at pressures between .05 and 2 torr. Our gun design allows for an optical path collinear with the electron beam, which makes this gun suitable for longitudinal laser excitation schemes. Our theoretical model of electron beam excitation will be compared to experimental results.

*Research supported by N.S.F.

SESSION LB

1:30 P.M., THURSDAY, OCTOBER 22, 1981

ROOM B

DISTRIBUTION FUNCTIONS II

CHAIRPERSON: L.C. PITCHFORD
SANDIA NATIONAL LABS

LB-1 Electron Energy Distribution and Vibrational Population in CO and He-CO Discharges - Y. KAUFMAN and YU. M. KAGAN, Hebrew U. of Jerusalem.--A method for simultaneously calculating the electron energy distribution function and the vibrational population in CO and He-CO discharges is described. The solution is self-consistent and includes the interdependence between the CO vibrational population and the electron energy distribution function. This mutual influence is accounted for by incorporating the electron-impact excitation of vibrationally excited molecules as well as superelastic collisions. The cross-sections for stepwise excitation are calculated here, using a model based on experimental data. The electron energy distribution function is given in an analytical form. The calculations are carried out for different He-CO mixtures and for several values of the electron concentration, the gas temperature and the ratio E/N. The electron energy distribution function strongly depends on both the composition of the gas mixture and the parameter E/N. The influence of the electron density and the gas temperature on the distribution function is relatively weak. The vibrational temperature decreases with the gas temperature, increases with E/N and strongly increases with the electron concentration.

LB-2 Electron Collision Cross Sections for HCl Derived from Swarm Measurements* - D. K. DAVIES, Westinghouse R&D Center -- A two-term expansion Boltzmann code[1] has been used to derive a set of electron collision cross sections for HCl by comparing predicted swarm parameters with recent measurements.[2] Previously published experimental values for the shapes of the cross sections for vibrational excitation, dissociative attachment and ionization have been used in the analysis. Adjustment of the magnitudes of these cross sections together with inclusion of cross sections for momentum transfer and electronic excitation have enabled the data[2] for electron drift velocity, attachment coefficient and ionization coefficient to be fitted to within $\pm$ 10%.

*Supported in part by Aero Propulsion Laboratory, Wright-Patterson AFB, Contract F33615-79-C-2074.

[1]P. E. Luft, JILA Information Center Report No. 14 (1975).

[2]D. K. Davies, Bull. Am. Phys. Soc. 26, 726 (1981).

LB-3 Electron Drift Velocities in CO_2 Gas Laser Mixtures-M.C. CORNELL, H.L. BROOKS*, and K.J. NYGAARD, University of Missouri-Rolla.+--Using an electron swarm apparatus in which the initial electrons are produced by light from a KrF*-laser (249 nm, 15 nsec pulse width), we have measured electron drift velocities in ternary mixtures of He, CO_2, and N_2 in density ratios of 3:1:1 and 3:1:2 and in CO_2, N_2 1:1. The range of E/N was from 2-50 Td. In the ternary mixtures, the observed values fall as much as 30% above those calculated using a Boltzmann code[1]. In the binary mixture, the difference is only 10% max.

*Present address: DePauw University, Greencastle, IN 46135.

+Supported in part by Los Alamos National Laboratory.

[1]W. T. Leland, private communication.

LB-4 Monte Carlo Simulation of Electron Swarms Using an Ideal Source. P. J. CHANTRY, Westinghouse R&D Center and G. L. BRAGLIA, University of Parma, Italy.--In a semi-infinite drift space the electrons impinging on an absorbing anode constitute an ideal planar source for Monte Carlo (MC) simulations.[1] When placed in an infinite drift space this ideal source will produce the equilibrium velocity distribution appropriate to E/N at all downstream positions. On the other hand, when it is placed within the region of influence of an absorbing anode, the resulting spatially varying distribution of electrons is nowhere the same as the equilibrium distribution. Nevertheless, one can show that such a simulation yields the equilibrium velocity distribution and the spatially varying swarm properties which would exist in the anode region if the source were far upstream. Hence, one may place the source an arbitrary, convenient distance from the anode, chosen to minimize the computational work, and derive from the resulting steady state all the swarm properties of interest. MC simulations have been performed to demonstrate these ideas. Starting with a "poor guess" at the source energy distribution, three iterations sufficed to define it adequately.

[1]P. J. Chantry, Bull. Am. Phys. Soc. 26 724 (1981).

SESSION MA

9:00 A.M., FRIDAY, OCTOBER 23, 1981

ROOM A

EXCITATION TRANSFER

CHAIRPERSON: G.L. DUKE
WRIGHT-PATTERSON

MA-1 Observation of Spontaneous Emission from Penning-like Collisions between He(2^3S) and Nitrogen. L.W. DOWNES, S.D. MARCUM, D. PETROVIC, and W.E. WELLS, Miami U., Oxford, OH.* -- Recent experimental observations[1] of spontaneous emission from radiative collisions[2] between He(2^3S) metastables and N_2 have been extended to include vibrational levels as high as $N_2^R(B,v=6)$, where R is a Rydberg state near the ionization limit of nitrogen. These transitions have been observed in both low pressure flowing afterglow and high pressure static electron beam discharge afterglow apparatus.

* Supported by U.S. Army BMDATC

1 L.W. Downes, S.D. Marcum, R.A. Tilton, and W.E. Wells, Proc. CLEO '81 Conference, June 1981, Washington, D.C.

2 L. Gudzenko and S.I. Yakovlenko. Soviet Physics JETP 35 877-81, 1972.

MA-2 Excitation Transfer Reactions in Neon Afterglows at 150°K - J. CLARK* and A. J. CUNNINGHAM, Univ. of Texas at Dallas.--Time resolved absorption spectroscopy has been exploited in a study of inelastic excitation transfer reactions involving long lived electronically excited neon atoms in their parent gas at 150°K. For the $^3P_0$ and $^3P_1$ states, two body neutral assisted deexcitation rate coefficients of 3.4×10^{-15} and $1.3 \times 10^{-14} cm^3 sec^{-1}$ respectively were determined. Mixing amongst the triplet manifold of neon excited states induced by electrons were also studied and rate data at both 150 and 300°K will be presented.

*Supported by the University of Texas at Dallas' organized research funds.

MA-3 Electronic Energy Transfer between Metastable Argon Atoms and Ground-state Oxygen Atoms.* L.G. PIPER, Physical Sciences Inc., Woburn, MA, M.A.A. CLYNE and P.B. MONKHOUSE, Queen Mary College, London, U.K. -- We have measured the rate constants for excitation of the $3p\ ^3P$ and $3s\ ^3S$ states of atomic oxygen by metastable $Ar(^3P_{2,0})$ to be (7.6±2.6) and (8.2±2.5) x 10^{-11} cm^3 molecule^{-1} s^{-1}, respectively. We have also measured the translational energy of $O(3s\ ^3S)$ using a VUV absorption technique. The coincidence of the two rate constant measurements and the results of the translational-energy measurement show that the electronic energy transfer reaction between $Ar^*(^3P_{0,2})$ and $O(2p^4\ ^3P)$ excites primarily $O(3p\ ^3P)$ and that $O(3s\ ^3S)$ is excited by radiative cascade at 845 nm. We discuss the excitation mechanisms for the Ar/O_2 laser at 845 nm and the 130.4 nm OI emission from Ar/O_2 resonance lamps in terms of the results of the present study.

*Supported by SRC

MA-4 Radial Distribution of Excited Atoms in an $Ar-O_2$ Surface Wave Produced Plasma - A. RICARD*, M. MOISAN and D. COLLOBERT**, Univ. de Montréal.--As previously reported[1], excitation processes of $O(3^3P,3^5P)$ levels in an $Ar-O_2$ sputtering plasma are not well explained. Surface wave produced plasmas can be useful in elucidating some of these processes, because the radial distribution of electrons is generally quite different from that of the metastable atoms. This difference comes from the fact that the electric field of a surface wave is radially inhomogeneous, decaying in an exponential-like fashion from the plasma tube wall to the axis[2]. We found that the radial distributions of $O(3^3P,3^5P)$ are given by the following kinetic processes :

- $Ar(^3P_2) + O_2 \rightarrow Ar + O(2^3P) + O(2^1S,2^1D)$
- $Ar(^3P_2) + O(2^3P) \rightarrow Ar + O(3^3P)$
- $e + O(2^3P) \rightarrow e + O(3^5P)$.

*Plasma Phys. Lab. Univ.Paris-Sud, 91405 ORSAY, FRANCE.
**C.N.E.T., Dept.TIC/ROC, BP 40, 22301 LANNION, FRANCE.

[1] Y. Chouan et al., G.E.C. (Oklahoma) BB-7 (1980).

[2] M. Moisan et al., Rev. Phys. Appl. 15, 1383-1397 (1980).

MA-5 Product Rotational Distributions in Electronic Energy Transfer Collisions of $Ar(^3P_{0,2})$ with N_2 - C.R. LISHAWA and E.E. MUSCHLITZ, JR., University of Florida*

--The relative population of rotational energy states in the first two vibrational levels of the $N_2(C^3\Pi_u)$ product in the collision process: $Ar(^3P_{0,2}) + N_2(X^1\Sigma_g^+; v=0; J<4) \rightarrow Ar(^1S_0) + N_2(C^3\Pi_u; v'=0,1;J')$ have been obtained by spectroscopic analysis of the $N_2(C\rightarrow B)$ fluorescence in a crossed supersonic beam apparatus[1]. The (0-0) band profile fits a Boltzmann distribution with rotational "temperatures" of 2200 ± 100, 1600 ± 100, and 1700 ± 100°K at relative beam energies of 0.161, 0.089, and 0.076 eV, respectively. The (1-0) band, however, shows a better fit to a "golden rule" calculation[2], which predicts a higher degree of rotational excitation.

*Supported by NSF

[1]E.R. Cutshall and E.E. Muschlitz, Jr., J. Chem. Phys. 40, 3171 (1979).

[2]M.J. Berry, Chem. Phys. Lett. 29, 329 (1974).

MA-6 Laser Double Resonance Determination of Rapid Vibrational and Rotational Energy Transfer Rates in CO_2. - M.D. THOMASON and B.J. FELDMEN. Los Alamos National Laboratory.*-- Rates for resonant vibrational and rotational energy transfer in $CO_2 + CO_2$ collisions have been measured. All data were obtained by double resonance spectroscopy with CO_2 lasers in a 2.5 meter absorption cell at 725°K. Results for rotational transfer include pumped level relaxation and the response of levels with ΔJ up to 18. These data are compared to four relevant collision models via a 35-level rate equation analysis. Sequence-band and hot-band lasing have been used to observe relaxation involving 001+001↔002+000 and 001+010↔011+000. A multilevel rate analysis has been utilized to determine the rate coefficients for 001 going to the 002, the 101, and the 011 levels.

*Work performed under the auspices of the US DOE.

MA-7 Excitation Transfer Between Xenon Metastable Atoms and Nitrogen Molecules - M. TOUZEAU and J. JOLLY, Lab. Physique Plasmas, Paris-Sud U. 91405 ORSAY-FRANCE.-- The excitation transfer from metastable Xe to N_2 were studied in a low pressure (0.1 torr) low temperature (80K) flowing afterglow apparatus. Xe metastables were created in a low current glow discharge in Ar-Xe mixture. A small amount of Xe ($\sim 10^{-3}$) was sufficient to quench completely Ar metastables. The vibrational distribution of $N_2(B^3\Pi_g)$ was deduced from the measurement of the $1^{st}(+)$ system. At room temperature the reaction excites mostly the $N_2(B,v=5)$ level but at low temperature this level is no more populated. These experiments show that the v=5 vibrational level is excited directly by the endoergic reaction :

$Xe(^3P_2)+N_2(X,v=o) \rightarrow N_2(B^3\Pi_g,v=5)+Xe - 475\ cm^{-1}$.

The reaction of $Xe(^3P_2)$ with vibrationaly excited nitrogen was also investigated. At room temperature a second maximum corresponding to the excitation of $N_2(B,v=8)$ was observed. This phenomena can be explained by a similar endoergic reaction :

$Xe(^3P_2)+N_2(X,v=2) \rightarrow N_2(B^3\Pi_g,v=8)+Xe - 442\ cm^{-1}$.

SESSION MB

8:45 A.M., FRIDAY, OCTOBER 23, 1981

ROOM B

BREAKDOWN & CORONA

CHAIRPERSON: P.F. WILLIAMS
UNIVERSITY OF TEXAS

MB-1 Breakdown of Helium at a Very High E/N[†] - D. BHASAVANICH, Westinghouse R&D Center, and A. B. PARKER, U. of Liverpool, U. K. -- Study of breakdown for helium has been extended both experimentally and theoretically to a high E/N ($> 10^{-16}$ Vm^2), low pressure (N $< 10^{22}$ m^{-3}) region. Apparatus was constructed which enabled measurements of prebreakdown current growth and breakdown voltages of up to 30kV on the left hand branch of the Paschen minimum. A Monte Carlo computer model was used to study this non-equilibrium discharge and simulate the motion and collision of electrons and their ionization product ions. The model calculates M, the multiplication factor of primary and anode backscattered electrons, and determines the effects of ion charge exchange processes on the secondary electron emission mechanism. Theoretical values of M are in good agreement with the experimental estimates. Incorporating M and the measured values of breakdown voltages, a generalized secondary coefficient γ is calculated. Present estimates of γ agree with those from other direct measurements, reaffirming the importance of charge exchange processes of the positive ions.

[†] Supported by U.K. Science Research Council

MB-2 Development of a Short Pulse Discharge - W. W. BYSZEWSKI, M. J. ENRIGHT, and J. M. PROUD, GTE Labs-- The electron density buildup and current development in gaseous spark gaps have been investigated in the context of fast overvoltage conditions found in transmission line pulse systems. Two alternative models have been examined, which are characterized by differing assumptions concerning the initial electron density distribution. In one case, the electron density is considered to be spatially uniform throughout the discharge development. In the second model, electrons appear initially only at the cathode surface leading to growth of an ionization front across the gap space. Numerical studies are presented for four gases: nitrogen, air, argon, and helium. Experimental observations of current waveforms are presented and compared with the theoretical results.

MB-3 The Effect of Electron Beam Induced Space Charge on Breakdown of N_2-SF_6 Mixtures.- T.TZENG, E.E.KUNHARDT, M.KRISTIANSEN, Texas Tech University, and A.H.GUENTHER, AFWL.*-- Results from an investigation into the effect of electron beam induced space charge on the breakdown of N_2-SF_6 mixtures in a spark chamber are presented. Measurements of the observational delay time and the subsequent current pulse generated in the external circuit have been made. Open shutter photographs show that the character of the discharge channel is quite varied. Dark, diffuse, and filamentary channels have been observed depending on the space charge conditions. The space charge is determined by the electron beam parameters. The behavior of the transition from insulator to conductor is shown to be dependent on the net local ionization coefficient, α-η, which in turn depends on the amount and location of the space charge introduced and on the composition of the gas. The fundamental processes leading to this transition for various experimental conditions are discussed.

*Supported by the Air Force Office of Scientific Research under contract No. AFOSR 76-3124A.

MB-4 Statistical Investigations of Overvoltage Breakdown*- E.E.KUNHARDT and S.J.LEVINSON, Texas Tech Univ.-- A statistical investigation of the observational time lag in N_2 as a function of pressure (up to 1350 torr), electrode separation (1 and 2 cm) and overvoltage (up to 2800%) has been carried out. Brass, aluminum, and amorphous graphite electrodes have been used. Our results show: 1) Graphite electrodes exhibit an emission rate that is an order of magnitude higher than the other two. 2) For graphite, the statistics associated with the formative time lag are comparable to those associated with the statistical time lag for overvoltages as high as 400%. 3) The formative time lags determined from the distribution of time lags are found to be greater than predicted by the classical "streamer theory". This indicates that the streamer propagation time cannot be neglected. A possible explanation of this observation will be discussed.

*Supported by the Naval Surface Weapons Center, Dahlgren, VA under contract No. N60921-79-C-A187.

MB-5 A Study of Electron Waves in Electrical Discharge Channels - H. JURENKA and E. BARRETO, State U. of N.Y. at Albany--The fast luminous pulses, observed to propagate in electrical discharge channels, have a significant role in electrical breakdown. They are investigated using a plasma fluid approach. The average velocities of these pulses fall in two regimes - 10^6 and 10^8 m/sec. A non-dimensional analysis is used to show that waves in the low velocity regime can be considered as longitudinal fluid waves driven by electron pressure gradients in weakly ionized plasmas. Non-linear model equations with known analytical solutions are derived considering each additional term in the momentum equation as a small but finite perturbation. Electric forces lead to Korteweg-deVries eq., viscosity to Burger's eq. and electron-neutral collisions to a damped wave eq.. The propagation and attenuation of fluid waves along pre-ionized channels is naturally associated with the formation of steps. It is suggested that thermalization must be associated with the injection of electrons from an external source.

*Supported by Office of Naval Research

MB-6 Low Frequency AC (25-70 Hz) Effects in Breakdown in the PRETEXT Tokamak.* - JAY F. BENESCH, ROGER D. BENGTSON, L. FROMMHOLD and M.E. OAKES, Physics Department, University of Texas, Austin, Texas 78712.--While doing ICRF preionization experiments,[1] we discovered that the breakdown voltage in PRETEXT is frequency dependent. Minimum breakdown voltage increased from 9V @ 27 Hz to 12V @ 50 Hz and 16V @ 71 Hz. There proved to be a linear relation between breakdown voltage V and dV/dt immediately before breakdown. A similar dependence has been seen in the tokamak JFT-2.[2] This work was done at 2×10^{-4} torr and E = 0.03V/cm. E/p = 150, in the usual regime, but both E and p are reduced by four orders from those found in linear discharges.

We will discuss our investigation of this phenomenon. The low frequencies involved and the sensitivity of f(V, dV/dt) to working gas lead us to hypothesize that ions are important in the breakdown here.

*This work was supported by DoE.

[1]J.F. Benesch, R.D. Bengtson and M.E. Oakes, Paper A5 in Proc. of the 4th Topical Conf. on RF plasma Heating, February, 1981, Austin, Texas.

[2]T. Sometani & N. Fujisawa, Plasma Phys. 20, 1101 (78).

MB-7 Influence of Molecular Ion Formation on a Continous Optical Discharge A. CYBULSKI, Inst. of Fund. Tech. Res., Warsaw, Poland - It was shown, in argon, that some atomic levels in a COD plasma, mainly in the vicinity of the plasma core and near the focus of the laser beam, are populated by the dissociative recombination of electrons and molecular ions. The plasma core is continuously maintained by the laser beam and the atomic levels are populated by direct excitation through collisions with electrons. In this vicinity, the dissociative recombination is proceeded by the processes of molecular ion formation, in this case they are Hornbeck-Molnar processes of associative ionization and of ion conversion. The different mechanisms of population of excited states in this vicinity and in the plasma core and also the transport phenomena are the reasons for the local deviation from Boltzmann equilibrium. This deviation increased when the laser beam was chopped.

* Submitted by M. Kristiansen

MB-8

Multiphoton Ionization of Xe as a Charge Source for Electrical Breakdown - S.K. DHALI, and P.F. WILLIAMS, Texas Tech*--We present the results of careful experimental studies of the magnitude and power dependence of the multiphoton ionization cross-section in Xe for excitation frequency resonant with a 3-photon transition to the 5d [2-1/2] J=3 state. For a focussed beam we find a cubic dependence on laser intensity for powers up to 4KW, the maximum power available to us. With 4KW source, we observed 1.5×10^7 charges produced. Tunable lasers with 4MW power are commercially available. Extrapolation of our results using a cubic power dependence predicts more than complete ionization of the gas in the volume of the focussed laser. We suggest that multiphoton ionization used as a source of charge should be useful in experimental studies of electrical breakdown.

MB-9 Effects of Magnetic Pressure on High Density Aℓ and C Plasmas - R. J. ANDERSON, L.G. GRAY and R.H. HUGHES, University of Arkansas* -- Studies of the effects of magnetic pressure on high density aluminum and carbon plasmas have been carried out. The plasmas are produced at electron densities of $10^{21}cm^{-3}$ by high power, (e.g. $10^{11}W/cm^2$), pulsed laser irradiation of solid targets. Subsequent plasma expansion over distances of up to $\sim$ 60 cm reduces the electron densities to $\sim 10^{11}$ to $10^{12}cm^{-3}$. Observations have been carried out at magnetic field strengths in the range $\sim$ 0.2 to 6 kG. Included in these are: (i) the change of plasma ion kinetic energy and kinetic energy flow direction under the action of magnetic fields. (ii) the transportation of a laser-produced plasma by an axial magnetic field and (iii) the influence of magnetic fields on the plasma expansion. Oscillograms of ion current versus time yield measurements of the peak ion current, total integrated charge and ion time of flight, all of which can be used to describe the spatial and temporal behavior of the plasmas.

*Supported by NSF grant PHY 7825988.

SESSION NA

10:30 A.M., FRIDAY, OCTOBER 23, 1981

ROOM A

PHOTON INTERACTIONS

CHAIRPERSON: C. DUZY

AVCO EVERETT RESEARCH LAB., INC.

NA-1 Branching Ratios in the EUV for SII and SIII - M.D.MORRISON* and A.J. CUNNINGHAM, Univ. of Texas at Dallas.--Branching ratios for several sets of extreme ultraviolet transitions in singly and doubly ionized sulfur atoms have been measured. The transitions in SII all terminate on the $^2P^0$ and $^2D^0$ metastable levels. The transitions in SIII terminate on the ^1S, ^1D and ^3P levels. The emissions were excited in a windowless hollow cathode discharge lamp and viewed by a 1/2 meter differentially pumped Seya-Namioka VUV monochromator. The present results are compared with theoretical analyses and are important in the population of levels which affect *Voyager* EUV observations.

*This work was supported by NASA grant NGL-44-004-130.

NA-2 Optical Processes Affecting Glow Discharges - MARTIN GUNDERSEN, SHEKHAR GUHA and HOWARD COLE, Univ. of So. Cal.* -- Optical quenching of metastable species in glow discharges is considered for several systems, and experimental observations for H_2 at pressures below 500 μm are presented. Optical processes affecting electron and ion densities in discharges and their application to laser control of discharges is discussed. Specifically, the generation of electrons by collisions involving the hydrogen $c^3\Pi_u$ metastable molecule and other species present after pulsed electrical excitation and the effect of these collisions on the carrier density in the gas is discussed. The metastable species can be optically quenched and the effect of such quenching on the discharge is presented.

*Supported by AFOSR, ARO and DOE

NA-3 300 nm Absorption by Xe_2^* Excimer - K. Y. TANG, J. S. DICKINSON, D. L. HUESTIS, and D. C. LORENTS, SRI International--Absorption in electron-beam (360 kV, 6 A/cm^2, ~ 300 ns) excited Xe gas has been investigated in the wavelength region 300 ± 10 nm. The time-resolved absorption consists of two distinct components: absorption during the e-beam pulse followed by increased absorption after the pulse. We attribute the after-pulse absorption to Xe_2^*. The time-history and pressure dependence of the after-pulse absorption closely follow the Xe_2^* fluorescence at 172 nm. Previous studies[1] observed increased Xe_2^* fluorescence in the after pulse, and modeling calculations suggest that Xe_2^* is the only major species whose density increases after the pulse. The absorption cross-section has been estimated based on the absorption data and Xe_2^* excimer density obtained from fluorescence measurements. Our data indicate a peak absorption near 304 nm with a cross-section $\sim 6 \times 10^{-17}$ cm^2.

[1]D.J. Eckstrom et al. Paper TuB7, Topical Meeting on Excimer Lasers, Sept. 11-13, 1979, Charleston, SC.

NA-4 Zero Core-Contribution Calculation of the Photodetachment Cross Section of NO_2^- - W.B. CLODIUS, R.M. STEHMAN, and S.B. WOO, Univ. of Del.*-- The zero core contribution model has been previously applied to atomic and diatomic negative ions.[1,2] We have extended this model to symmetric triatomic molecules using symmetry and bonding considerations to determine the molecular orbital of the "outermost" bound electron, as a linear combination of atomic orbitals. The partial cross sections are calculated, for selected vibrational transitions, along with the resulting total photodetachment cross section. The angular anisotropy factors for each transitions are also shown. Good agreement is obtained with recent experimental data.[3]

1. R.M. Stehman and S.B. Woo, Phys.Rev.A,20, 281 (1979).
2. R.M. Stehman and S.B. Woo, Phys.Rev.A,23,2866 (1980).
3. S.B. Woo, E.M. Helmy, P.H. Mauk, and A.P. Paszek, to be published in the Sept. issue of Phys. Rev. A.

*Supported in part by NSF and ARO.

NA-5 The Uniqueness of a Franck-Condon Analysis. - P. W. TOWNSEND, W.B. CLODIUS and S.B. WOO, Univ.of Del.*--The result of a Franck-Condon analysis using a harmonic oscillator approximation is non-unique, when applied to transitions involving diatomic molecules and ions. Information on the bonding or anti-bonding characteristic of the molecular orbitals is required to establish uniqueness. However, the result of a harmonic approximation Franck-Condon analysis involving polyatomic molecules is unique, if two or more progressions of transitions are used in the analysis, and if the transformation matrix relating the initial and final state has off-diagonal elements.[1] The Franck-Condon analysis of a photodetachment spectrum of NO_2^- is used as an example. Analytic and numerical proofs are given. Counter examples are provided. If only one progression of transitions is used in the analysis, or if the bond angle of the initial and final state is assumed to be identical, then the result will be non-unique.

1. R. Botter and H.M. Rosenstock, J. Res. NBS 73A (Phys. and Chem.) No. 3 313 (1969).

*Supported in part by NSF and ARO.

NA-6 Measurement of Absolute Photoionization Cross Sections for the 7p Excited States of Cesium., G. W. FOLTZ**, M.G. PAYNE, and G.S. HURST, Oak Ridge Nat'l. Lab.*--Absolute cross sections for the photoionization of the $7p\,^2P_{1/2}$ and $^2P_{3/2}$ excited states of Cs have been measured as a function of wavelength near threshold. The output of a dye laser pumped by the 3547 Å harmonic of a Nd:YAG laser is used to excite a small volume of ground state Cs atoms to either the $7p\,^2P_{1/2}$ or $^2P_{3/2}$ state (λ = 4593 Å or 4555 Å, respectively). A second dye laser pumped by the 5320 Å harmonic of the Nd:YAG laser is tuned to wavelengths shorter than the ionization limit (λ = 1.037 μm for $^2P_{1/2}$ and 1.057 μm for $^2P_{3/2}$) and is used to photoionize the excited atoms. The number of atoms initially excited by the first dye laser is determined by saturating the ionization process with the 5320 Å Nd:YAG radiation and measuring the resulting photoelectron signal. The photoionization cross section at the wavelength of interest can, therefore, be obtained from a plot of photoelectron signal vs the pulse energy density of the second dye laser.

*Operated by the Union Carbide Corp. with the U.S. Dept. of Energy.
**Postdoctoral Research Appointment through Western Ky. Univ. Subcontract No. S7640 with Union Carbide Corp.

NA-7 Electron Attachment and Charge Recombination Following Two-Photon-Ionization of Methylamines,* LONG C. LEE and WILLIAM K. BISCHEL, SRI International, Menlo Park, California 94025--Ion currents produced by two-photon ionization of methylamines were investigated. At low charge density, the ion current is proportional to the product of gas pressure and the square of laser intensity. At high gas pressure and high laser intensity, the ion current saturates. The saturation effect is well interpreted by a model including electron attachment and charge recombination processes. The two-photon-ionization coefficients were determined from the low ion current data. Among the molecules studied, trimethylamine has the highest coefficient of 3.6×10^{-26} cm^4/W at the KrF laser wavelength of 248 nm. Such a high photoionization coefficient indicates that trimethylamine could be used to produce a high density of initial electrons for laser-controlled switches. The present results could also be used to develop new techniques for investigating the electron attachment and charge recombination processes at high gas pressures.

*Supported by AFOSR under Contract No. F49620-79-C-0191.

NA-8 A Theoretical Investigation of the Photodissociation of Polyatomic Molecules - C.A. ASARO† and A. DALGARNO, Harvard-Smithsonian Center for Astrophysics -- A theoretical method for obtaining the total photodissociation cross section for molecules is presented. The method employs L^2 basis functions to discretize the continua of the initial and final electronic states. Transition energies and oscillator strengths between a specific vibrational level of the ground state and the spectrum of discretized levels in the upper state are obtained. Stieltjes imaging techniques are applied to this distribution to obtain the cross sections. Bound state vibrational energy levels, oscillator strengths and cross sections are presented for several diatomic molecules, including H_2 and LiH. Comparison is made with previous theoretical results and experiment. Preliminary results for H_2O are given.

†Also Department of Chemistry, Harvard University

NA-9 State-Selective Photolysis of CsKr and Cs_2Kr^*. - C. B. COLLINS, F. W. LEE, H. GOLNABI, F. DAVANLOO and P. VICHARELLI, Univ. of Texas at Dallas; D. POPESCU and I. POPESCU, Central Inst. of Physics of Romania--A two photon technique for the measurement of relative cross sections for the photolysis of simple molecules into particular product channels has been recently developed.[1,2] When used here to examine the dissociation of CsKr and Cs_2Kr, several general conclusions were supported. Many of the component bands of the absorption spectrum generally attributed to CsKr appeared to belong to Cs_2Kr. Most of the photolysis bands excited at visible wavelengths in either species were observed to lead to adiabatic and hence, state-selective dissociation. From the stability of product state populations, rate coefficients were estimated for mixing and quenching processes.

Conducted as part of the U.S.-Romanian Cooperative Program in Science and Technology, supported by NSF Grant INT76-18982 and NSF Grant PHY80-19525.

1. C. B. Collins and J. A. Anderson, D. Popescu, and I. Popescu, J. Chem. Phys. 74, 1053 (1981).
2. C. B. Collins, F. W. Lee, J. A. Anderson, P. Vicharelli, D. Popescu and Iovitzu Popescu, J. Chem. Phys. 74, 1067 (1981).

SESSION NB

10:45 A.M., FRIDAY, OCTOBER 23, 1981

ROOM B

EXCITATION TRANSFER II & QUENCHING

CHAIRPERSON: J. STEVEFELT

UNIVERSITY ORLEANS, FRANCE

NB-1 Collisional Relaxation of Electronically Excited Copper Atoms - HAO-LIN CHEN and GAYLEN V. ERBERT, Lawrence Livermore.*--Laser induced fluorescence was used to study the cross sections of collisional mixing and deactivation of electronically excited copper atoms ($^2P_{3/2}$, $^2P_{1/2}$, $^2D_{3/2}$, $^2D_{5/2}$) in various buffer gases. The cross sections for total deactivation of metastables ($^2D_{5/2}$, $^2D_{3/2}$) to the ground state by the buffer gases at 1450°C are less than 10^{-20} cm^2 . Cross sections for collisional mixing of the ^2P and ^2D levels are more than an order of magnitude larger.

---

*This work was performed under the auspices of the U.S. Department of Energy by the Lawrence Livermore Laboratory under contract number W-7405-ENG-48.

NB-2 Collisional Deactivation of the Pb $6p^2$ $^3P_2$ and $^3P_1$ Metastables by Ground-State Pb Atoms - C. REISER*, N. DJEU, AND R. BURNHAM, Naval Research Laboratory -- The collisional kinetics of the low-lying metastable states of Pb, which are the terminal laser levels in both the Pb-vapor laser and the XeCl-Pb Raman laser, are important for determining the route of energy flow in pulsed laser systems. Quenching of these states by inert gases is slow.[1] We have measured the self-quenching rate constants of these states by Pb atoms over a temperature range of 1200-1500°K, using single frequency tunable UV to probe transitions which terminate on each of the metastables. Transient absorption on these transitions was probed following excitation of the metastables through stimulated Raman scattering in a lead heat pipe cell using an XeCl pump laser. Rate constants were 3.2×10^{-13} cc/sec for the $^3P_2$ and 2.0×10^{-13} for the $^3P_1$ states. These rate constants are sufficiently large that self-quenching dominates energy transfer from these levels in Pb vapor Raman lasers.

*NRC-NRL Postdoctoral Fellow

[1]D.W. Trainor and J.J. Ewing, J. Chem. Phys. 64,222(1976)

NB-3 Collisional Processes in a Dense Sodium Vapor Following Resonant Excitation by Short Laser Pulses,* D.J. KREBS and L.D. SCHEARER, Univ. of Missouri-Rolla--A dense sodium vapor in a high pressure buffer of argon has been simultaneously excited by short (4 ns) laser pulses from two lasers: the first tuned to one of the D line transitions at 589 nm and the second tuned to the photoionization threshold of the 3p states near 406 nm. The temporal evolution of the system was studied with and without the photoionizing laser pulses. At early times ($\sim$ 100 nsec) excited state populations are determined by energy transfer collisions between two laser-excited 3p atoms while the ion/electron density is controlled by superelastic heating of "seed" electrons followed by electron impact ionization of excited state atoms. At late times ($\sim$ 1 μsec) excited state populations are controlled by collisional-radiative recombination processes. Excitation transfer rates into the 4d, 5d, 6d, and 6s levels are measured.

*Research supported by the Office of Naval Research.

NB-4 Associative Ionization in Laser Excited Sodium Vapor*-V.S. KUSHAWAHA, J.J. LEVENTHAL, U. of Missouri-St. Louis--We have studied the production of Na_2^+ in $Na(n\ell)/Na(n'\ell')$ collisions by irradiating a cell containing Sodium vapor at low density ($< 10^{13}$ cm^{-3}) with two cw dye lasers, each tuned to the appropriate atomic transition. We have found that the rate constants for associative ionization increase with increasing reactant energy, that is, k(4d/3s) > k(3p/3p) > k(5s/3s). The results suggest that associative ionization processes play an important role in some laser-produced plasmas.[1]

*Supported by DOE Contract No. DE-AS02-76-ER02718.

[1] M. E. Koch, K. K. Verma, and W. C. Stwalley, J. Opt. Soc. Am. 70, 627, 1977.

NB-5 Collisional Depopulation of High-Rydberg Na s States by Argon- J. BOULMER, J.-F. DELPECH, J.-C. GAUTHIER, and K.A. SAFINYA*, U. de Paris, Orsay - -

Collisional depopulation cross-sections of high Rydberg Na s states by argon have been investigated using a beam-pulsed cell technique with time-resolved selective field ionization. The total s state depopulation cross-section has a broad maximum of 130 $\mathring{A}^2$ around n = 30-35. Preliminary observations indicate that principal quantum number changes are large in such collisions. The implication of these findings on neutral-stabilized collisional recombination will be discussed.

*Permanent address: Schlumberger-Doll Research, Ridgefield, CT 06877

NB-6 Experimental Determination of 6 ^{3}P-6 ^{3}P Collisional Excitation Cross-Sections for Line Emission in the Positive Column of DC Mercury Discharges. - P.van de WEIJER, and R.M.M. CREMERS, Philips Research Labs., Eindhoven, The Netherlands. -- The absolute emission intensities of lines originating from highly excited mercury levels in the positive column of a DC mercury discharge have been determined for various discharge conditions. For the same conditions the densities in the 6 ^{3}P states have been determined with the hook method. From these experimental data the 6 ^{3}P-6 ^{3}P collisional excitation cross-sections for line emission can be derived for nine transitions. Generally, these cross-sections are much smaller than assumed so far in the literature.

NB-7 Proton-Induced Deactivation of Metastable Ions - S. BIENSTOCK, T.G. HEIL†, and A. DALGARNO, Harvard-Smithsonian Center for Astrophysics* -- In high temperature plasmas, the population of metastable impurity ions may be modified by collisions with protons. Deactivation of several metastable ions by proton impacts has been studied. The process is driven by the long range quadrupole interaction, modified by the effects at shorter distances of avoided crossings with intermediate charge transfer channels. Detailed results for the process $H^+ + C^+ (2p^2\ ^1S) \rightarrow H^+ + C^+(2p^2\ ^1D)$, obtained by distorted wave and close-coupling quantal calculations in a diabatic formulation, will be reported.

*Supported by DOE Contract DE-AC02-76ER02887
†Permanent address: University of Georgia

INDEX TO ABSTRACTS

34th ANNUAL GASEOUS ELECTRONICS CONFERENCE

BOSTON PARK PLAZA HOTEL, BOSTON, MASSACHUSETTS, OCTOBER 20–23, 1981

TUESDAY OCTOBER 20		WEDNESDAY OCTOBER 21		THURSDAY OCTOBER 22		FRIDAY OCTOBER 23	
AA 8:45–10:15 ARCS I Room A	AB 9:00–10:20 GLOW DISCHARGES I Room B	FA 9:00–10:20 ARCS III Room A	FB 8:45–10:15 VISIBLE & U.V. LASERS Room B	JA 8:45–10:10 ION REACTIONS II Room A	JB 9:00–10:05 DISTRIBUTION FUNCTIONS I Room B	MA 9:00–10:10 EXCITATION TRANSFER Room A	MB 8:45–10:15 BREAKDOWN & CORONA Room B
COFFEE 10:15 – 10:45		COFFEE 10:15 – 10:45		COFFEE 10:00 – 10:30		COFFEE 10:15 – 10:45	
BA 10:45–12:10 ARCS II Room A	BB 10:45–11:45 GLOW DISCHARGES II Room B	GA 10:45–11:35 ARCS IV Room A	GB 10:45–12:00 ION REACTIONS I Room B	K 10:30 – 11:40 PLENARY SESSION IN HONOR OF PROF. W.P. ALLIS Room B		NA 10:30–11:55 PHOTON INTERACTIONS Room A	NB 10:45–11:55 EXCITATION TRANSFER II & QUENCHING Room B
LUNCH 12:15 – 1:30		LUNCH 12:00 – 1:30		BUSINESS MEETING 11:45 – 12:15 Room B		12:00 NOON ADJOURN	
CA 1:30–2:55 ELECTRON COLLISIONS Room A	CB 1:30–3:00 XENON HALIDE LASERS Room B	HA 1:30–2:40 ELECTRON CAPTURE Room A	HB 1:30–3:00 NON-UNIFORM GLOWS & CORONA Room B	LUNCH 12:15 – 1:30			
COFFEE 3:00 – 3:30		I 3:00–5:30 WORKSHOP ON CURRENT TRANSFER TO MHD ELECTRODES Room B		LA 1:30–2:30 VISIBLE & INFRARED LASERS Room A	LB 1:30–2:25 DISTRIBUTION FUNCTIONS II Room B		
D 3:30–4:55 MERCURY BROMIDE LASERS Room B				3:00 TECHNICAL TOUR AVCO EVERETT RES. LAB. AVCO METALWORKING LASERS (BUS TRANSPORTATION)			
E 8:00–10:30 WORKSHOP ON KINETIC PROCESSES IN BLUE–GREEN LASERS & RELATED TOPICS Room B				7:00 SOCIAL HOUR Room A 8:00 BANQUET GEORGIAN ROOM Speaker: J. Herbert Holoman			